POLITECNICO
DI TORINO

UNIVERSITÀ
DEGLI STUDI
DI TORINO

Doctoral Dissertation
Doctoral Program in Pure and Applied Mathematics (30^{th}cycle)

Diffusion Processes on Networks

By

Lorenzo Zino

******

Supervisor:
Prof. Fabio Fagnani, Supervisor

Doctoral Examination Committee:
Prof. Enrico Bini, Università di Torino
Prof. Franco Pellerey, Politecnico di Torino
Prof. Sandro Zampieri, Università di Padova

Università di Torino - Politecnico di Torino
2018, October 9

Declaration

I hereby declare that, the contents and organization of this dissertation constitute my own original work and does not compromise in any way the rights of third parties, including those relating to the security of personal data.

Lorenzo Zino
2018, October 9

* This dissertation is presented in partial fulfillment of the requirements for the degree of ***Philosophiæ Diploma*** **(PhD degree)** in **Pure and Applied Mathematics**.

Acknowledgements

First and foremost, I would like to express my heartfelt gratitude to my supervisor, prof. Fabio Fagnani[1]. I thank him for his continuous guidance, support, and patience throughout these years. Our constructive discussions, his valuable suggestions and thoughtful comments have helped a lot for the successful completion of this work and for my growth as a scholar.

Besides my supervisor, I would like to thank prof. Giacomo Como[1,2], for his constant support, availability and for the constructive scientific discussions we had both during the time I spent at Lund University and at Politecnico di Torino. I would also like to express my sincere gratitude to prof. Alessandro Rizzo[3] for his scientific advice and knowledge and many insightful conversations. I am also grateful to prof. Maurizio Porfiri[4], who gave me the opportunity to work with him and join the Dynamical System Laboratory at New York University.

My sincere thanks go to prof. Kimon Drakopoulos and prof. Ayalvadi Ganesh, who have carefully read and reviewed this dissertation. I thank them for their encouraging comments and for the insightful suggestions that have allowed me to improve the quality of this work.

I am also grateful to the university staff of the Department of Mathematical Sciences "G.L. Lagrange", Politecnico di Torino; the Department of Mathematics "G. Peano", Università di Torino; the Department of Automatic Control, Lund University; and the Dynamical System Laboratory, Department of Mechanical and Aerospace Engineering, New York University Tandon School of Engineering, for the precious help and assistance during these years.

[1]Department of Mathematical Sciences "G.L. Lagrange", Politecnico di Torino, Torino, Italy
[2]Department of Automatic Control, Lund University, Lund, Sweden
[3]Department of Electronics and Telecommunications, Politecnico di Torino, Torino, Italy
[4]Department of Mechanical and Aerospace Engineering, Tandon School of Engineering, New York University, Brooklyn NY, US

I would like to express my gratitude to my mother Caterina for her encouragement, motivation and support during all these years, to my sister Ester and all my family for their everlasting love. A special thank goes to my father Elio: he will always be an example to me. Particular thanks are due to my girlfriend Sara for her support, patience and, most of all, for her inestimable love that enabled me to complete this work. Finally, I want to thank my dear friends: I am really lucky since I can always count on them!

While I am writing these final lines, Steven Tyler is singing *life's a journey, not a destination*[5] from the pub on the street right behind my the window of my room. He is absolutely right, and PhD is not an exception. Therefore, I cannot conclude these acknowledgments without thanking my fellow travelers for the sincere, priceless friendship that made pleasant even the hardest periods of these years, making this travel *amazing*.

[5] Aerosmith. *Amazing*. Get a Grip (1993)

Abstract

Diffusion processes on network systems are ubiquitous. An epidemic outbreak in an interconnected population, the adoption of a new smartphone application by the members of a social community, and the spread of a genetically modified organism in a geographic area are just three examples of real-world phenomena that can be represented through the formalism of diffusion dynamics on networks. The main goal of this dissertation is to study the evolution of these diffusion processes and predict their outcome. Specifically, we aim to investigate whether the diffusion process reaches large part of the network and how long does the spreading process lasts, unveiling the influence of *i*) the topological structure of the networked system, and *ii*) the characteristics of the diffusive dynamics. In order to address this issues, we formulate a general and flexible theory for diffusion processes which can be tailored to suit the specific features of many real-world phenomena. The main strength of our theory is that the mathematical models designed in accordance to it satisfy Markov property, enabling us to analytically treat them. The main contribution of this dissertation, besides proposing a mathematical model for general diffusion processes on networks, is thus the development of a set of analytical techniques, which are used to gain new insights into the the effect of the network topology on the evolution of diffusive real-world phenomena and to develop effective control techniques for the system.

After having introduced our general formulation and having developed the techniques mentioned above, we focus on the analysis of three relevant applications of our general theory, which exemplify different physical and social phenomena and include various distinct features into our framework. Specifically, we consider an epidemiological, a marketing, and a biological application. First, we deepen the analysis of a well established model for the diffusion of an infectious disease: the susceptible-infected-susceptible model. The techniques developed in our general theory enable us *i*) to gain new insights into the epidemic process, enhancing the

characterization of its phase transition; and *ii*) to obtain short- and medium-term predictions of the evolution of the outbreak, from few empirical data. Second, we tailor our general theory to propose a novel model for the adoption of a new technological asset. The main modeling novelty is the presence of positive externalities, i.e., the indirect effect of the adoption of the asset by a user, which boosts its diffusion. Using the techniques developed in our theory, we are able to study the system, showing a complex bi-stability phenomenon: besides the success and failure regimes — which are similar to the endemic and fast extinction regimes in epidemic models, respectively — we witness the presence of an intermediate regime, where the outcome of the system depends on the initial condition. Third, we model evolutionary dynamics using our framework, enabling us to extend the theoretical analysis of these models and to study the effect of the introduction of an external control. We apply evolutionary dynamics to model the insertion of a mutant species in a geographic area to substitute the native one, e.g., the species of mosquitoes that transmit Zika virus. Our general analysis enables us to understand the effect of the topology and of the control policy adopted on the time required to spread the mutants and on the effort needed to achieve this goal, and allows also for the definition of an effective feedback control policy to speed up the diffusion process.

Contents

List of Figures

List of Tables

Chapter 1

Introduction

1.1 Introduction and Motivation

In the last few decades, the world has become more and more deeply and globally connected. First, distances of thousands of kilometers can be physically covered in few hours, thanks to the developments in transportation systems of the last century. Then, the progresses in information technology and the diffusion of digital media has completely reshaped the world, transforming the notion of distance in our "Small World" where the information can flow all around the globe in a heartbeat.

In this framework, networks have emerged as very powerful mathematical tools to deal with the inherent complexity of networked systems in such a hyper-connected reality. For this reason, networks have been used in many different fields to represent, e.g., physical interacting particles systems [1], social systems where individuals exchange opinions and information [2–4], biochemical systems made of molecular regulators interacting with enzymes [5, 6], technological systems of connected sensors and devices [7, 8], or transportation systems made of moving vehicles [9].

The study of dynamics on networks has been absolutely effective in improving our understanding of several physical, social, and biological phenomena. Besides the theoretical contributes due to the insights into the phenomena gained through these studies, the increased awareness of the mechanisms ruling the various interacting systems allows for the development of several useful prediction and control techniques, with many benefits for the society.

A paradigmatic example is the study of epidemic spreading. The deep improvements in the understanding of their diffusion on a generic network [10–12] paved the way for the design and the analysis of an array of control policies that have direct applications to the health system in the last few years [13–17]. Another archetypal example consists in the analysis of the diffusion of opinions and ideas. In this field, the voter model was one of the first model proposed [1] and an extensive analysis in terms of long-run behavior and convergence time to consensus on lattices and regular structures is available [1, 18]. More recently, game-based opinion models have been proposed and analyzed [19, 20]. From these theoretical results, many control policies and relevant applications have been developed. Among the others, we mention an analytical study aiming to maximize the influence of an opinion depending on the position in the network it is introduced [21], and a study of the spread of hoaxes and false news [22]. These two examples help us to comprehend the wide range of possible applications in social sciences of the theoretical results on opinion dynamics on networks.

In this dissertation, we focus on diffusion processes. Diffusion processes are ubiquitous: the analysis of an epidemic outbreak in an interconnected population, as well as the study of the adoption of a new technological asset such as a smartphone application, or the control and removal of a dangerous mosquito species in a geographic area, which are the three main applications we will discuss in this dissertation, are just three of the many possible real-world dynamics that involve diffusion processes. Having already mentioned the effectiveness of networks in capturing the complexity of physical and social systems, it is very natural to embed diffusion dynamics in networked systems and study them using tools form network science.

Here, we analyze a relevant class of diffusion processes where the spreading mechanism is essentially ruled by two simple mechanisms: pairwise contacts between the components of a network (e.g., the individuals of a population) and spontaneous mutations. The rationale for these models is that simple local dynamics on complex networks give rise to interesting, and sometimes unexpected, emergence phenomena. We remark that a totally different approach to diffusion processes (and in general to network dynamics), is the one followed in many papers in the literature [19, 20, 23, 24], where the diffusion is driven by nontrivial neighbors-based dynamics, often model in a game-theoretical framework.

Specifically, we develop a general theory to model pairwise-based diffusion processes on networks. Our general formulation encompasses and generalizes several well known dynamics: epidemic models such as the Susceptible–Infected (SI) and the Susceptible–Infected–Susceptible (SIS) [25, 26], opinion dynamics as the voter model [1], and biological models as evolutionary dynamics [27]. Then, along this dissertation, we propose some relevant applications, in which the general model is tailored to the specific features of the considered diffusion phenomenon. The objective of the study of these applications is twofold. On the one hand, we want to gain novel insights on the specific phenomena analyzed, thanks to the new results we have developed in our general theory. On the other hand, through these applications, we emphasize the generality of our framework, showing how it allows to include into the system's dynamics nonstandard features, such as heterogeneity (as in the SIS model considered in Chapter 3), nontrivial indirect effects of the diffusion (as we show in Chapter 4), as well as exogenous control policies (that are considered in Chapter 5).

1.2 Organization of the Dissertation

The thesis is organized as follows. In Chapter 2 we introduce our general framework. First, in Sections 2.1 and 2.2 we recall some basic notions of graph theory and continuous time Markov processes in order to formulate and analyze our model. Then, in Section 2.3 we present our general formalism by introducing the pairwise-based mechanism that rules the spreading processes. Section 2.4 is devoted to the analysis of the stochastic process induced by these mechanisms, and in Section 2.5 we present an important technique to derive a deterministic approximation of the stochastic process useful for perform predictions and estimations on the system's evolution. The following chapters are devoted to present relevant applications of our general theory to different fields. In these applications our general model is tailored in order to fit the specificity of the considered dynamics to model and additional features are added, proving the flexibility of our theoretical framework.

In Chapter 3, we adapt our formalism to the application field of epidemics spreading. Specifically, we analyze the SIS model, already mentioned above. The chapter is divided into three parts. First, in Section 3.1, we present the epidemic model studied and we show how our general framework can be tailored to it. Then, we

revisit some important results available from the literature. Specifically, we identify two regimes depending on the epidemic strength and on the network properties: in the first regime, the epidemic quickly extinguish; in the second one, instead, it becomes endemic. In Section 3.2, leveraging tools from our general theory, we give new insights on the epidemic process by proposing an interesting refinement of the existing results, specifically concerning with the long persistence of the epidemics when it becomes endemic. Finally, in Section 3.3 we analyze a different issue related to the same model: understand how an epidemic outbreak evolves if the network of interactions is time-varying and heterogeneous. Specifically, our contribution consists in the proposal of an effective method to produce accurate short and medium time horizon predictions of the epidemic curve, both when no data are available, and when epidemics data at the population level can be sampled at fixed time windows in order to dynamically correct the predictions.

In Chapter 4, instead, we face a problem in the field of social sciences, specifically a marketing problem: to develop and analyze a model for the diffusion of a new technological asset, such as a smartphone application. This model includes a nontrivial global effect of the diffusion, known in economics as externalities: the more a product is diffused, the more likely a new potential user decides to adopt it. Section 4.1 is devoted to the design and the discussion of the model. Then, the model is studied in order to predict whether the product will be successful of not, depending on its characteristics and on the structure of the network of interactions. Specifically, the analysis is performed in three steps: i) in Section 4.2, we study the model under a fully-mixing assumption (i.e., assuming that all the individuals can communicate) and we witness the presence of a failure regime, a success regime, and an intermediate regime where the outcome depends on the initial condition, being the main novelty of this model; ii) in Section 4.3, we extend our analysis to non connected networks of interactions, and finally iii) in Section 4.4 the case of a general network of interactions is analytically studied, along with numerical simulations on relevant topologies.

In Chapter 5, a controlled evolutionary dynamics is considered, inspired by a new method to control mosquitoes-borne diseases which consists in inserting harmless genetically modified mosquitoes in a geographic region to substitute those that diffuse pathogens (e.g., Zika or Dengue) [28, 29]. The chapter is divided into three parts. In the first one, we tailor our general pairwise-based interaction diffusion process in order to model the specific features of evolutionary dynamics. In Section

5.2, we use our theoretical results to perform the analysis of the model and we discuss the possibility to control it and speed up the diffusion, depending on the topology of the geographic region and on the control policy adopted. Finally, in Section 5.3 we propose a feedback control policy for the system and we show its effectiveness through two relevant examples.

Chapter 2

Diffusion Processes on Networks: a General Formulation

This chapter is divided into two parts. In the first one, we present some mathematical preliminaries on graph theory and Markov processes and we introduce the notation used throughout this dissertation. Then, we develop a general formulation for diffusion processes on networks driven by pairwise interactions.

The rest of this chapter is organized as follows. In Section 2.1, we recall some important notions of graph theory and we present the notation used in this dissertation. In Section 2.2, we briefly present Markov jump processes focusing on the important sub-family of birth-death Markov processes. At this stage, we can finally introduce the mechanism that governs pairwise-based diffusion processes in Section 2.3. In Section 2.4, we deduce and discuss the Markov jump process induced by the mechanisms we have introduced. Finally, Section 2.5 is devoted to present a deterministic finite time-range approximation of the stochastic process presented in the previous section, which allows for the development of accurate prediction of the evolution of diffusion processes on large-scale networks.

2.1 Notions of Graph Theory

In this section we present some basic notions of graph theory and we introduce the notation and the terminology used in the rest of this dissertation. Finally, we

conclude presenting some relevant examples of graph topologies we will use in this dissertation.

A graph $G = (V,E)$ is a mathematical entity identified by an ordered pair of objects:

- a set of N *nodes*, usually labeled by positive integer numbers, gathered in the *node set* $V = \{1,\dots,N\}$; and
- a set of ordered pairs of nodes (i,j), $i,j \in V$, named *edges*, which are collected in the *edge set* $E \subseteq V \times V$.

The presence of the edge (i,j) has to be interpreted as a connection between node i and node j. Connections between nodes can be represented in a more compact way using the *adjacency matrix* $A \in \{0,1\}^{V\times V}$, which is defined as follow:

$$A_{ij} = \begin{cases} 1 & \text{if} \quad (i,j) \in E \\ 0 & \text{if} \quad (i,j) \notin E. \end{cases} \tag{2.1}$$

Therefore a graph can be defined either through the couple V and E, or through V and A.

Given a node $i \in V$, we refer to the nodes that are connected to it as *neighbors* of node i. Namely,

$$\mathcal{N}_i := \{j \in V : (i,j) \in E\}. \tag{2.2}$$

Given a node i, we define its degree as

$$d_i := \sum_{j\in V} A_{ij} = |\mathcal{N}_i|. \tag{2.3}$$

The maximum degree of a graph is denoted by Δ, wheres the average degree is denoted by $\bar{d}$. Graphs with $d_i = d$, $\forall\, i \in V$ are said to be *regular*.

A graph is said to be *undirected* if $(i,j) \in E \implies (j,i) \in E$, which implies A to be a symmetric matrix. Otherwise, we refer to it as a directed graph. For directed

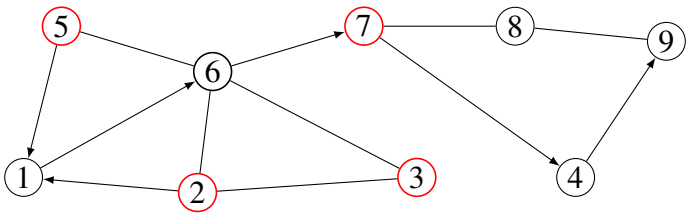

Fig. 2.1 A graph $G = (V,E)$ with $N = 9$ nodes. An arrow from i to j represents an edge from i to j, whereas a segment from i to j represents a couple of edges (i, j) and (j,i). The graph is directed, since, e.g., $(6,7) \in E$, but $(7,6) \notin E$. The set $\mathcal{N}_6 = \{2,3,5,7\}$ of the neighbors of nodes 6 is colored in red, so $d_6 = 4$.

graph, the in-degree of a node can also be defined as

$$d_i^- := \sum_{j \in V} A_{ji}, \tag{2.4}$$

and, similarly, Δ_{in} denotes the maximum in-degree. We remark that the average in-degree coincides with $\bar{d}$.

A *path* is a sequences of nodes $\gamma = (\gamma_0, \dots, \gamma_l)$, such that $(\gamma_i, \gamma_{i+1}) \in E$, $\forall i = 0, \dots, l-1$. If, for any pair of nodes i and j there is a path on the graph that goes from i to j passing only on existing edges, then we say that the graph G is *strongly connected*. In this work we will mostly consider strongly connected graphs, but for a short parenthesis in Chapter 4. Fig.2.1 depicts a graph, explaining some of the notions presented here.

Given a graph G, a positive weight $W_{ij} > 0$ can be associated to each edge $(i, j) \in E$. All the weights can be gathered in a matrix $W \in \mathbb{R}_+^{V \times V}$ named *weight matrix*. We notice that $W_{ij} > 0 \iff (i, j) \in E$ or, in other words, $W_{ij} > 0 \iff (i, j) \in A_{ij} = 1$. A graph equipped with a weight matrix $G = (V,E,W)$ is called *weighted graph*.

A weighted graph with all the weights equal, i.e., $W = \alpha A$, $\alpha > 0$, is said to be *simple* and all the information of the weight matrix can be condensed in the unique parameter α. Similar to the unweighted case, also a weighted graph is said to be *undirected* if W is a symmetric matrix. We observe that the notion of undirected weighted graph is more strict than the one for unweighted graphs. In fact, undirected weighted graphs are also undirected (unweighted) graphs, but the reverse implication is not true for nonsimple graphs, since $W_{ij} \neq W_{ji} \neq 0 \implies A_{ij} = A_{ji}$.

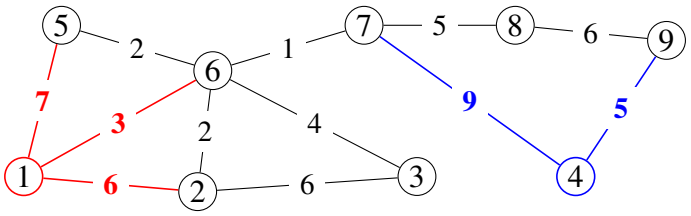

Fig. 2.2 A weighted undirected graph $G = (V, E, W)$ with $N = 9$ nodes. The weight of node 1 is $w_1 = 16$ (corresponding edges are in red), while $w_4 = 14$ (edges in blue).

Similar to the degree for unweighted graphs, given a node i of a weighted graph, we define its weight as

$$w_i := \sum_{j \in V} W_{ij}. \tag{2.5}$$

In the case of a simple graph, we observe that the weight of the nodes is proportional to their degree:

$$w_i = \sum_{j \in V} W_{ij} = \sum_{j \in V} \alpha A_{ij} = \alpha |\mathcal{N}_i| = \alpha d_i. \tag{2.6}$$

Fig.2.2 depicts an example of weighted graph, clarifying the notions presented so far.

We conclude this section by presenting some relevant examples of graphs we will use in the rest of this dissertation. In order to keep the notation and the presentation simple, when not differently specified graphs are always simple. Moreover, when dealing with simple graphs the weight matrix is omitted since all its information is condensed in a single parameter α.

Example 2.1 (Complete graph)**.** *A graph with N nodes, each one connected to itself and to all the other nodes is called* complete graph *and it is denoted by K_N. We remark that $\mathcal{N}_i = V$, $\forall i \in V$. Hence, simple complete graphs are undirected and regular with $d_i = N$, $\forall i \in V$. An example of a complete graph is presented in Fig. 2.3(a).*

Example 2.2 (Line graph)**.** *A line graph with N nodes is a graph where node i is connected to nodes $i+1$ and $i-1$, but the first node that is connected only with the second one, and the last is only connected with node $N-1$. Simple lines are thus undirected but not regular.*

Example 2.3 (Ring graph)**.** *A Ring graph, denoted by C_N is obtained from a line graph by adding the couple of edges $(1,N)$ and $(N,1)$. Simple ring graphs are thus undirected and regular with $d_i = 2$, $\forall i \in V$. An example is presented in Fig. 2.3(b).*

Example 2.4 (Star graph)**.** *A graph with $N+1$ nodes, where all the first N nodes are connected to node $N+1$ and node $N+1$ is connected to all the other nodes is named star graph and denoted by S_N. Simple stars are undirected but not regular: all nodes but $N+1$ have degree 1, instead, node $N+1$ has degree N. An example of a star graph is presented in Fig. 2.3(c).*

Example 2.5 (Barbell graph)**.** *A graph with N (even) nodes partitioned into two complete communities with $N/2$ nodes each with a symmetric edge connecting a single node of the first community to a single node of the second one is named barbell graph. Simple barbel graphs are undirected but not regular: all nodes have degree $N/2-1$, but the pair of nodes belonging to different communities that are linked: they have degree $N/2$.*

Example 2.6 (Erdős-Rényi random graph)**.** *The Erdős-Rényi (ER) model $G(N,p)$ is the first random graph model, introduced in 1959 [30]. $G(N,p)$ is a random undirected simple graph with N nodes where each couple of edges (i,j) and (j,i) is present with a probability $p \in (0,1)$, independently of the other couple of edges. Thus, the graph is undirected. The degree of each node is thus a realization of a binomial random variable with parameters $N-1$ and p. Standard concentration results [11] show that with high probability (w.h.p.) as $N \to \infty$, $\bar{d} \asymp \Delta \asymp Np$. An example of an Erdős-Rényi graph is presented in Fig. 2.3(d).*

Example 2.7 (Barábasi-Albert model)**.** *The Barábasi-Albert model is a model for a simple graph introduced in 1999 to represent social networks [31]. Starting from an initial connected graph, at each time step a node is added to the graph and it is connected to m existing nodes with a probability proportional to their degrees, until there are N nodes [31]. This algorithm constructs a graph whose degree distribution follows asymptotically a power-law [31] (in particular $\mathbb{P}[d_v = k] \propto k^{-3}$). As $N \to \infty$ it is immediate to verify that $\bar{d} = m + o(1)$ (due to construction). On the other hand, from [32], $\Delta = \sqrt{N}(1+o(1))$.*

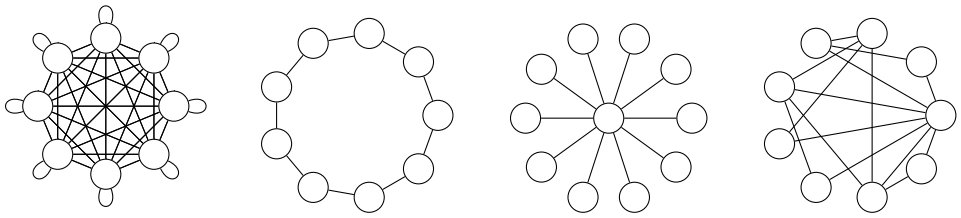

(a) Complete graph. (b) Ring Graph. (c) Star Graph. (d) ER Graph.

Fig. 2.3 Relevant graph topologies presented in the examples of this section.

2.2 Notions on Markov Processes

In this section we briefly present an important family of stochastic processes that will be used throughout this dissertation: Markov processes. The literature of Markov processes is extremely wide and they have been studied from many point of view in different fields and with different applications. In this section, we will stick to the specific case of continuous-time finite-space processes and we will present only those properties that will be useful in the rest of this dissertation. For a more complete treatment of these processes one can see [33, 34].

Definition 2.1 (Markov jump process [33])**.** *A continuous-time Markov jump process $X(t)$, $t \in \mathbb{R}^+$ is a stochastic process taking values in a finite (or countable) space $\mathcal{S}$, such that Markov property is verified, i.e.,*

$$\mathbb{P}[X(t+\Delta t) = s \,|\, \mathcal{F}_t] = \mathbb{P}[X(t+\Delta t) = a \,|\, X(t)], \quad \forall \Delta t \geq 0, \forall a \in \mathcal{S}, \tag{2.7}$$

where $\mathcal{F}_t$ is the natural filtration of the process $X(t)$ at time t.

Hence, the transitions a Markov jump process can have at time t, are only influenced by its actual state at time t. Therefore, the process is fully determined by its initial condition $X(0) = X_0 \in \mathcal{S}$, and by a nonnegative (entry-wise) matrix $\Lambda = (\lambda_{rs})_{r,s\in\mathcal{S}}$ with null diagonal entries that governs the transitions of the process, according to the following infinitesimal definition:

$$\mathbb{P}[X(t+\Delta t) = s \,|\, X(t) = r] = \lambda_{rs}\Delta t + o(\Delta t), \quad \forall s \neq r \in \mathcal{S}. \tag{2.8}$$

The elements of the matrix Λ are called *transition rates* of the process. The state space and the transitions of a Markov jump process can be represented through a weighted

graph where the node set $V = \mathcal{S}$, the weight matrix is Λ, and $(r,s) \in E \iff \lambda_{rs} > 0$. We will refer to this graph as *transition graph* of the Markov process.

A first fundamental example of Markov jump process is the Poisson process $N(t)$, having $N(0) = 0$, $\mathcal{S} = \mathbb{N}$, and all transition rates null, but $\lambda_{i,i+1} = \lambda$, $\forall i \in \mathbb{N}$. Hence, a Poisson process can only have jumps in which the state increases by 1. Throughout this dissertation, we refer to this process as a *Poisson clock* with rate λ. We say that a Poisson clock *clicks* at time t, if a transition of the process occurs at time t.

From the infinitesimal definition in (2.8), the explicit law governing the transitions can be derived [34]. When the process $X(t)$ enters in state r at time t, it spends there an exponentially distributed random time T with parameter $\sum_{s\in\mathcal{S}} \lambda_{rs}$, i.e.,

$$\mathbb{P}[T \leq t] = \begin{cases} 1 - \exp\{-\sum_{s\in\mathcal{S}} \lambda_{rs} t\} & t \geq 0 \\ 0 & t < 0. \end{cases} \tag{2.9}$$

Then, after a time T, the process $X(t)$ enters in its following state, that is selected stochastically, according to

$$\mathbb{P}[X(t+T) = s] = \frac{\lambda_{rs}}{\sum_{s\in\mathcal{S}} \lambda_{rs}}. \tag{2.10}$$

Finally, another equivalent and interesting interpretation of Markov jump processes is the one of a discrete-time Markov chain $X(k)$, $k \in \mathbb{N}$, coupled with a vector τ encapsulating the temporal features of the process [34]. Both the discrete-time process and the temporal vector are initialized at 0, i.e., $X(0) = X_0$ and $\tau_0 = 0$. We introduce a matrix $Q = (q_{rs})_{r,s\in\mathcal{S}}$, which is related to Λ as follows,

$$q_{rs} = \begin{cases} \dfrac{\lambda_{rs}}{\sum_p \lambda_{rp}} & \text{if } \displaystyle\sum_p \lambda_{rp} > 0 \\ 1 & \text{if } \displaystyle\sum_p \lambda_{rp} = 0,\ r = s \\ 0 & \text{if } \displaystyle\sum_p \lambda_{rp} = 0,\ r \neq s, \end{cases} \tag{2.11}$$

and we define the transition of the discrete-time Markov chain accodring to the following probabilistic law:

$$P[X(k+1) = s \,|\, X(k) = r] = q_{rs}. \tag{2.12}$$

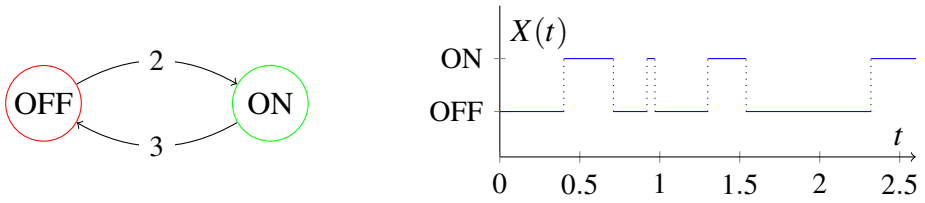

(a) Transition graph. (b) Admissible trajectory.

Fig. 2.4 Transition graph and an admissible trajectory of the Markov jump process presented in Ex. 2.8.

The vector τ is obtained recursively: given $X(k) = r$, we let

$$\tau_{k+1} = \tau_k + T_k, \tag{2.13}$$

where T_k is an exponentially distributed random variable with parameter $\sum_{s\in\mathcal{S}} \lambda_{rs}$. The information on the state reached by the Markov jump process after each transition and the time this transition occur is thus divided into two processes. Specifically, τ_k is the time the Markov jump process has its k-th jump, while $X(k)$ is the state the process enters, after the jump. This interpretation is very powerful to perform theoretical analysis of Markov jump processes as well as to perform fast numerical simulations [35].

We present now a very simple example of Markov jump process to clarify our notation.

Example 2.8. *Let us consider a system consisting in a light and its switch. The light is initially of OFF. When the light is OFF, then it is switched ON after a random time that is exponentially distributed with parameter* 2*. Then, if the light is ON, then it is switched OFF after a time that is exponentially distributed with parameter* 3*. The variable $X(t)$, denoting the state of the light at time t, is a Markov jump process with transition matrix*

$$\Lambda = \begin{bmatrix} 0 & 2 \\ 3 & 0 \end{bmatrix}, \tag{2.14}$$

where the first line is associated with the state OFF and the second one with the state ON and $X(0) = OFF$. The transition graph and an admissible realization of $X(t)$ are represented in Fig. 2.4.

From (2.11), we immediately deduce that a state $s \in \mathcal{S}$ with $\sum_r \lambda_{sr} = 0$ has the remarkable property that, if $X(t)$ ever enters in s, then it never exits. States exhibiting this property are named *absorbing states*. In this dissertation, we will mainly focus on Markov processes possessing at least one absorbing state, and we will analyze the probability that the process is absorbed into one of these states and the time needed for such event to occur.

We introduce now an important family of Markov jump processes for which many analytical results are available due to the simplicity of their transition graphs: birth-death Markov jump processes.

Definition 2.2 (Birth-death Markov jump process)**.** *A continuous-time finite-space Markov jump processes $Z(t)$ is a birth-death process if and only if its transition graph is a (possibly nonsimple) line graph (see Ex. 2.2).*

Remark 2.1. *We remark that, due to its structure, a birth-death Markov jump process $Z(t)$ admits at most two transitions from each state: the one to the previous state on the line graph, and the one to the following one. We refer to these rates as increasing and decreasing rates, respectively, and we denote them as $\lambda^{\pm}(z)$.*

In our dissertation, we focus on birth-death Markov jump process whose state space is in the form $\mathcal{S}_N := \{0, 1/N, \ldots, 1\}$, or, equivalently, $\tilde{\mathcal{S}}_N := \{0, 1, \ldots, N\}$. We remark that, due to the specific structure of the transition graph of a birth-death process, its state space can always be mapped into $\mathcal{S}_N$, where $N = |\mathcal{S}| - 1$. Therefore, from now on, without any loss in generality we stick our analysis to processes on $\mathcal{S}_N$

The notion of birth-death process can be naturally generalized to non-Markov processes, where the transition graph of the process representing the admissible transitions is a line, but (2.8) is not verified because, typically, it is not possible to define the transition rates. We generally refer to such processes as birth-death processes. In order to deal with these processes, ancillary Markov processes acting as estimations and bounds on the original process are defined, using the important notion of stochastic dominance, presented in the following.

Definition 2.3. *Let $Z(t)$ and $\tilde{Z}(t)$ be two stochastic processes on the same state space $\mathcal{S}$. We say that $Z(t)$* stochastically dominates *$\tilde{Z}(t)$, denoted as $Z(t) \succeq \tilde{Z}(t)$, if*

$$\mathbb{P}[\tilde{Z}(t) \leq s] \leq \mathbb{P}[Z(t) \leq s], \quad \forall t \geq 0, \forall s \in \mathcal{S}. \tag{2.15}$$

A simple method to prove stochastic domination between two processes consists in defining a bi-dimensional process $(Y(t), \tilde{Y}(t))$, in which i) the marginal distribution $Y(t)$ coincides with the distribution of $Z(t)$; ii) the marginal distribution $\tilde{Y}(t)$ coincides with the distribution of $\tilde{Z}(t)$; and iii) $Y(t) \geq \tilde{Y}(t), \forall t \geq 0$ [11].

Using stochastic domination, we are able to reduce the analysis of many non-Markov stochastic processes, to the analysis of some Markov bounds on them. In order to perform these analysis, besides the standard results known from the literature [33, 34], we often leverage a couple of technical results, which are extensively presented and proven in Appendix A.

2.3 Pairwise-Based Diffusion Mechanism

Let us consider a system made of a set of N interconnected components (agents). Each one can be identified with a node of a graph $G = (V, E)$, where the presence of the edge $(i, j) \in E$ has to be interpreted that agent i can be influenced by agent j. In order to model the evolution of the diffusion process, each node is given a *state* $X_i(t)$ which is equal to 1 if node i has been reached by the diffusion process at time $t \in \mathbb{R}^+$ or 0 otherwise. States can be assembled in a N-dimensional vector $X(t) \in \{0,1\}^V$, called *configuration* of the system, which is the state variable of the system.

We introduce two dynamics: *mutations* and *pairwise interactions*. The former consists in spontaneous state updates, whereas in the second dynamics, an agent updates its state after an interaction with another agent in its neighborhood.

Mutations are modeled as follows: each node $i \in V$ is equipped with a Poisson clock with rate λ_i. All Poisson clocks are one independent of the others. When the clock associated with agent i clicks, if the state of agent i is 0, then it updates its state to 1 with probability m_{01}. Otherwise, if its state is 1, it change its state from 1 to 0 with probability m_{10}. The probabilities m_{01} and m_{10} are called *mutation probabilities*.

Similarly, pairwise interaction acts as follows. Each edge $(i, j) \in V$ is equipped with a Poisson clock with rate W_{ij}, independent of the others. When the clock associated with edge (i, j) clicks, then agent i is allowed to update its state depending on the state of agent j. Specifically, if agent i has state 0 and agent j has state 1, then agent i change its state to 1 with probability p_{01}. On the contrary, if agent i has state

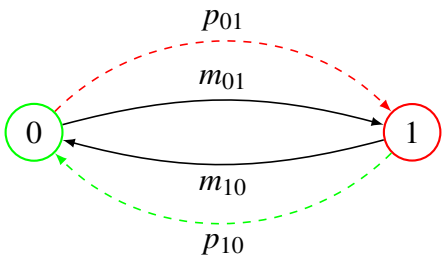

Fig. 2.5 State transitions characterizing the pairwise-based mechanism. Black solid lines are spontaneous mutation, colored dashed lines are transitions taking place after a pairwise interaction with a node with the other state.

1 and agent j has state 0, then agent i updates to 0 with probability p_{10}. Otherwise, nothing happens. These transitions are represented in Fig. 2.5, which will be used in the following chapters to depict the specificity of the several models analyzed. The probabilities p_{01} and p_{10} are called *copying probabilities*.

The rates of the Poisson clocks associated with the edges can be gathered into a matrix W, whose nonnull entries correspond to positions W_{ij} with $(i,j) \in E$. Thus, we can model the network of interactions between the agents using a weighted graph $G = (V,E,W)$. We refer to a homogeneous pairwise-based diffusion process when all the rates $W_{ij} = \lambda_e$ are equal, which means that W is simple. In this case, the network of interactions between agents can be modeled using an unweighted graph and the parameter λ_e.

This formulation is very general and allows for the inclusion of several features depending on the phenomenon to model. In fact, the probabilities m_{01}, m_{10}, p_{01}, and p_{10} can be constant or, more in general, they can be functions of the state of the system and/or can depend on external parameters and quantities. In this dissertation we consider different scenarios: cases in which all these probabilities are fixed (as in the case of the SIS epidemic model studied in Chapter 3, cases in which are functions of the state of the system (as in Chapter 4), and cases in which they are function of an exogenous control (as in the evolutionary dynamics analyzed in Chapter 5.

2.4 Markov Process and its Analysis

Mutations and pairwise interactions yield state transitions that depend only on the state of the system at the specific time the transition happens, without any memory

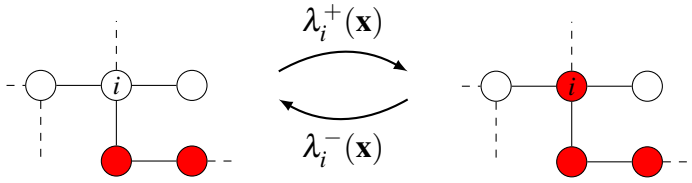

Fig. 2.6 Transition graph of the jump Markov process $X(t)$ induced by the pairwise-based diffusion mechanism.

of the past. Therefore, they induce a Markov jump process $X(t)$ on the configuration space $\{0,1\}^V$ [34]. The Poisson clocks involved in the dynamics are all independent of the others. Hence, no concurrent clicks can occur [34]. Therefore, the only transitions that can take place from a generic state $X(t) = \mathbf{x} = (x_1, \ldots, x_n)$ are the ones to states that differ from $\mathbf{x}$ in a single entry, represented in the transition graph in Fig. 2.6. The corresponding transition rates are denoted as $\lambda_i^{\pm}(\mathbf{x})$ for the transition rate from $\mathbf{x}$ to $\mathbf{x} \pm \delta^{(i)}$. These rates are

$$\begin{cases} \lambda_i^+(\mathbf{x}) &= (1-x_i)\left[\lambda_i m_{01} + \sum_{j\in\mathcal{N}_i} W_{ij}x_j p_{01}\right] \\ \lambda_i^-(\mathbf{x}) &= x_i\left[\lambda_i m_{10} + \sum_{j\in\mathcal{N}_i} W_{ij}(1-x_j) p_{10}\right]. \end{cases} \tag{2.16}$$

We observe that, if $m_{01} = 0$, then an agent with state 0 will never update its state unless it contacts an agent with state 1. Therefore, the pure configuration where all the agents have state 0, denoted as $0\mathbb{1}$, is an absorbing state. Similarly, if $m_{10} = 0$, the pure configuration where all agents have state 1, denoted as $\mathbb{1}$, is an absorbing state. In all the models we consider in this dissertation, and in many other diffusion models, at least one of the two mutation probabilities is set equal to 0. Under this assumption, the Markov process $X(t)$ admits at least an absorbing state, being one of the two pure configurations. Moreover, ifthe copying probability $p_{01} > 0$ ($p_{10} > 0$) and the graph is strongly connected, then i) no other absorbing states can be present; ii) the pure configurations $\mathbb{1}$ ($0\mathbb{1}$) can be reached with non null probability from each configuration that is not absorbing. Therefore, we conclude that, under the hypothesis that at least one mutation probability is null and that at least one of the copying probability is nonnull, then the process eventually enters (in finite time) in one of the absorbing states with probability equal to 1, due to Borel-Cantelli lemma [34].

The main issues for these models consist thus in understanding how the initial condition, the topology of the network of interactions, and the model parameters influence i) the absorbing state reached, where more than one absorbing states is present; and ii) the time needed for the process to enter an absorbing state. In the literature, several works are focused on tackling the first problem in situation with multiple absorbing states [36, 19, 20]. In this work, instead, we focus our analysis on dynamics possessing only one absorbing state and we deepen the study of the second issue: estimating the absorbing time and predicting the evolution of the spreading process.

The size of the system is one of the main limitations for the analysis of the process. In fact, the size of the state space of $X(t)$ grows exponentially with the number of agents N, and also the number of possible transitions from a configuration increases as N grows. Hence, for large scale graphs, the analysis of the process $X(t)$ becomes almost unfeasible. This issue can be approached by defining and analyzing the following one dimensional projection of $X(t)$:

$$Z(t) = z(X(t)) := \frac{1}{N}\sum_{i=1}^{N} X_i(t), \tag{2.17}$$

which counts the fraction of agents having state equal to 1.

The process $Z(t)$ is a stochastic process on the state space $\mathcal{S}_N = \{0, 1/N, \ldots, 1\}$ whose transition graph is a line, as represented in its transition Fig. 2.7, therefore it is a birth-death process. Analogously, we can define the birth-death process as

$$\tilde{Z}(t) := \sum_{i=1}^{N} X_i(t) = NZ(t), \tag{2.18}$$

which counts the number of agents having state equal to 1 and is also a birth-death process. In this dissertation, for the sake of simplicity, depending on the specificity of the model we consider, we will decide either to analyze $Z(t)$ or $\tilde{Z}(t)$ that are equivalent but for a scaling factor.

The study of $Z(t)$ makes intuitively the analysis of the system more tractable. In fact, the size of the state space of this process grows only linearly with N, and the possible transitions from each state are, at most, two. However, an important property is lost in the projection from $X(t)$ to $Z(t)$: the birth-death process could in general be non-Markov. This has a simple explanation: the distribution of 1's in a

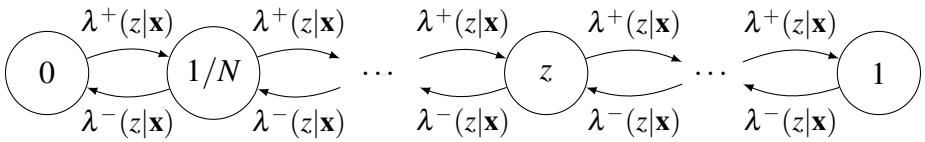

Fig. 2.7 Transition graph of the birth-death Markov jump process.

neighborhood of a node is in general different from the global distribution of 1's in the population, hence, the transition rates $\lambda^{\pm}$ depend on the whole process $X(t)$ and not just on $Z(t)$. To stress this dependence, we denote them as $\lambda^{\pm}(z|\mathbf{x})$.

We assume all the agents activation to be homogeneous, so that all the clocks associated with their activation have the same rate $\lambda_i = \lambda, \forall i \in V$. This homogeneity assumption will be kept throughout this dissertation, but for a specific case considered in Chapter 3, when we will analyze a heterogeneous epidemic model, and in Chapter 5, where the rates are time-varying and ruled by exogenous control policies. Then, we introduce the notion of *active boundaries* of the process. An edge (i, j) belongs to the active boundary $B_{01}(t)$ at time t if $X_i(t) = 0$ and $X_j(t) = 1$. Similarly, if $X_i(t) = 1$ and $X_j(t) = 0$, the edge (i, j) belongs to the active boundary $B_{10}(t)$. We define the size of an active boundary at time t as the sum of the weights of the edges belonging to the boundary, namely

$$\xi_{01}(t) := \sum_{(i,j)\in B_{01}(t)} W_{ij} = \sum_{i\in V} (1 - X_i(t)) \sum_{j\in V} W_{ij} X_j(t) \tag{2.19}$$

and

$$\xi_{10}(t) := \sum_{(i,j)\in B_{10}(t)} W_{ij} = \sum_{i\in V} X_i(t) \sum_{j\in V} W_{ij} \left(1 - X_j(t)\right) \tag{2.20}$$

We notice that, when the graph G is undirected, it holds $B_{01}(t) = B_{10}(t)$, $\forall t \geq 0$. Therefore, we have $\xi_{01}(t) = \xi_{10}(t)$ and the notation can be simplified by dropping the indexes.

At this stage, we can analyze the process $Z(t)$ and notice that, even if Markov property is lost due to the one-dimensional projection, when conditioned to $\xi_{01}(t)$ and $\xi_{10}(t)$, the process is Markov. Notably, when conditioned to $\xi_{01}(t) = \xi_{01}$ and $\xi_{10}(t) = \xi_{10}$, $Z(t)$ is a birth and death jump Markov process whose transition rates

from the state z to $z+1/N$ and $z-1/N$ are, respectively

$$\begin{cases} \lambda^+(z|\xi_{01}) &= N(1-z)\lambda m_{01} + \xi_{01} p_{01} \\ \lambda^-(z|\xi_{10}) &= Nz\lambda m_{10} + \xi_{10} p_{10}, \end{cases} \tag{2.21}$$

In fact, fixed $X(t) = \mathbf{x}$, the quantities $B_{01}(t) = B_{01}$, $\xi_{01}(t) = \xi_{01}$, and $Z(t) = z$ are given. Hence, we compute

$$\begin{aligned} \lambda^+(z|\mathbf{x}) &= \sum_{i\in V} \lambda_i^+(\mathbf{x}) \\ &= \sum_{i\in V} (1-x_i) \left[\lambda m_{01} + \sum_{j\in\mathcal{N}_i} W_{ij} x_j p_{01} \right] \\ &= N(1-z)\lambda m_{01} + \sum_{i,j\in V} (1-x_i) x_j W_{ij} p_{01} \\ &= N(1-z)\lambda m_{01} + \sum_{(i,j)\in B_{01}} W_{ij} p_{01} \\ &= N(1-z)\lambda m_{01} + \xi_{01} p_{01} = \lambda^+(z|\xi_{01}). \end{aligned} \tag{2.22}$$

A similar computation allows to derive the decreasing rate $\lambda^-(z|\mathbf{x})$ as a function of the only ξ_{10}.

However, the difficulties arise from the fact that the processes $\xi_{01}(t)$ and $\xi_{10}(t)$ are, in general, not explicitly known. There is a single case in which $\xi_{01}(t)$ and $\xi_{10}(t)$ are deterministic functions of $Z(t)$: when G is a simple complete graph. Since complete graphs are undirected, we can drop the indexes and we write $\xi(t) = \xi_{01}(t) = \xi_{10}(t)$. Being the graph simple, all the weights are equal, thus, we set $W_{ij} = \lambda_e$, $\forall i, j \in V$. Therefore, the active boundary is a deterministic function of the process $Z(t)$ that is so Markov itself, namely $\xi(t) = N^2 \lambda_e Z(t)(1-Z(t))$. To sum up, the transition rates (2.21) read

$$\begin{cases} \lambda^+(z) &= N(1-z)\left[\lambda m_{01} + N\lambda_e z p_{01}\right] \\ \lambda^-(z) &= Nz\left[\lambda m_{10} + N\lambda_e (1-z) p_{10}\right]. \end{cases} \tag{2.23}$$

The assumption of homogeneity (i.e., $\lambda_i = \lambda$) and fully-mixed network of interaction (i.e., G simple complete graph) go under the name of *mean field* assumptions for the model.

2.5 Hydrodynamic Limit

Another important tool that is used along this dissertation is the hydrodynamic limit of the model. Under mean field assumption, we can consider the limit case in which $N \to \infty$. In this limit case, the evolution of the stochastic birth-death Markov jump process $Z(t)$ can be approximated arbitrarily well with a deterministic function $\zeta(t)$ for fixed (finite) time-windows. Figure 2.8 depicts this approximation, which is more accurate, the larger is N. The detherministic function $\zeta(t)$ is defined in the following theorem.

Theorem 2.1 (Kurtz Theorem [37, 38])**.** *Let us suppose there exist two Lipschitz continuous functions $\tilde{\lambda}^+ : [0,1] \to \mathbb{R}^+$ and $\tilde{\lambda}^- : [0,1] \to \mathbb{R}^+$ such that*

$$\frac{\lambda^+(z)}{N} \to \tilde{\lambda}^+(z), \quad \textit{and} \quad \frac{\lambda^-(z)}{N} \to \tilde{\lambda}^-(z), \tag{2.24}$$

uniformly as $N \to \infty$. Let $Z(0) \to \zeta_0$ as $N \to \infty$ and let $\zeta(t)$ be the solution of the following Cauchy problem:

$$\begin{cases} \zeta'(t) = F(\zeta) := \tilde{\lambda}^+(\zeta) - \tilde{\lambda}^-(\zeta) \\ \zeta(0) = \zeta_0. \end{cases} \tag{2.25}$$

For every $T > 0$ $\exists\, C_T > 0$, the following exponential decay holds

$$\mathbb{P}\left(\sup_{0 \le t \le T} |Z(t) - \zeta(t)| > \varepsilon \right) \le 4 \exp\left(-C_T N \varepsilon^2\right), \tag{2.26}$$

where C_T only depends on T and on the sup norm of the right-hand-side of equation (2.25) *and is bounded away from* 0 *when the two quantities are both bounded.*

Remark 2.2. *A typical choice that is often made to guarantee the two functions $\tilde{\lambda}^\pm$ to be Lipschitz-continuous consist in setting the weight of each edge proportional to the inverse of the average degree of the graph. In the case of the complete graph the average degree is equal to the size of the graph, therefore, it is set $W_{ij} = \lambda_e / N$, $\forall\, i, j \in V$. In this case* (2.25) *reduces to*

$$\dot{\zeta} = F(\zeta) = (1-\zeta)\left(\lambda m_{01} + \lambda_e \zeta p_{01}\right) - \zeta\left(\lambda m_{10} + \lambda_e (1-\zeta) p_{10}\right). \tag{2.27}$$

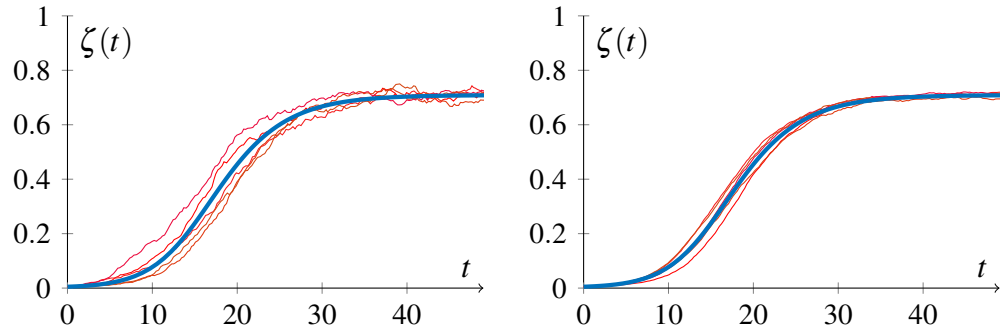

(a) $N = 1000$. (b) $N = 10000$.

Fig. 2.8 Comparison between the stochastic process (red) and the solution of the Cauchy problem (2.25) (blue) for increasing values on N for the SIS model, presented in Chapter 3. As the size of the system grows, the deterministic approximation becomes more accurate.

We conclude this section by presenting an useful generalization of Kurtz's Theorem for k-dimensional stochastic processes $Z(t) = (Z_1(t), \dots, Z_k(t))$ taking values in $\mathcal{S}_{N_1} \times \cdots \times \mathcal{S}_{N_k}$, where the component Z_j takes values in $\mathcal{S}_{N_k}$ and can only increase or decrease by $1/N_j$ at each transition. The transition graph of $Z(t)$ is thus a $N_1 \times \cdots \times N_k$ lattice. We name $\lambda_j^{\pm}$, the transition rates of the j-th component of process $Z(t)$, i.e., $\lambda_j^+(z)$ represents the transition probability from z to $z + N_j^{-1}\delta^{(j)}$. Let $N = \sum_j N_j$. This result allows to deal with heterogeneous dynamics, as we will see in Chapter 3.

Theorem 2.2 (Generalized Kurtz Theorem [37, 38])**.** *Let us suppose $N_j/n \to \eta_j > 0$, $\forall j = 1, \dots, k$ as $N \to \infty$ and that there exist $2k$ Lipschitz continuous k-dimensional functions $\tilde{\lambda}_j^+ : [0,1]^k \to \mathbb{R}^+$ and $\tilde{\lambda}_j^- : [0,1]^k \to \mathbb{R}^+$, $j = 1, \dots, k$, such that*

$$\frac{\lambda_j^+(z)}{N} \to \tilde{\lambda}_j^+(z), \qquad \text{and} \qquad \frac{\lambda_j^-(z)}{N} \to \tilde{\lambda}_j^-(z), \tag{2.28}$$

uniformly as $N \to \infty$, for $j = 1, \dots, k$. Let $Z(0) \to \zeta_0$ as $N \to \infty$. Let $\zeta(t) = (\zeta_1(t), \dots, \zeta_k(t))$ be the solution of the following k-dimensional Cauchy problem:

$$\begin{cases} \zeta_j'(t) = F(\zeta) := \tilde{\lambda}_{(j)}^+(\zeta) - \tilde{\lambda}_{(j)}^-(\zeta) & j = 1, \dots, k \\ \zeta_j(0) = Z_j(0) & j = 1, \dots, k. \end{cases} \tag{2.29}$$

Then, for every $T > 0$ $\exists\, C_T > 0$, the following exponential decay holds:

$$\mathbb{P}\left(\sup_{0 \le t \le T} |Z(t) - \zeta(t)| > \varepsilon \right) \le 2^{k+1} \exp\left(-C_T N \varepsilon^2\right), \tag{2.30}$$

where C_T only depends on T and on the sup norm of the right-hand-side of equation (2.29) *and is bounded away from* 0 *when the two quantities are both bounded.*

2.6 Conclusion

In this Chapter, first, we have presented the preliminaries and tools that will be used in this dissertation. Then, we have formalized our general model for diffusion processes. In Section 2.1, we have started by recalling some important notions on graph theory and by presenting the notation used throughout this work. We have also proposed and analyzed a bunch of network topologies, which will be used in the following chapters as examples for the considered dynamics. Then, in Section 2.2, we have revisited some relevant notions on continuous-time Markov jump process, useful in our further results.

Chapter 3

Susceptible–Infected–Susceptible Epidemic Model

In this chapter, we consider and study the SIS epidemic model. The SIS model, introduced in 1927 [25], is one of the most popular and extensively analyzed mathematical models for epidemics and it describes the evolution of an outbreak of a contagious disease transmitted by contacts for which recovered individuals do not acquire immunity and can contract the disease again.

In Section 3.1, we formally define the SIS model within the general framework developed in Chapter 2. Then, we present some important results available in the literature. Specifically, we show that the SIS model exhibits a phase transition between two regimes, depending on the model parameters and on the network structure: in the first regime the epidemic is circumscribed to a small subset of individuals, and quickly vanishes; in the other one the epidemic becomes endemic, spreading all over the network for (typically) a long time. In the literature, this characterization has been analyzed in terms of expected duration of the dynamics before reaching the disease-free equilibrium.

In Section 3.2, we improve the characterization of the second regime. We analyze the time needed for the epidemics to extinguish, proving that, if the strength of the epidemics is sufficiently high, i.e., larger than a threshold which depends on the topology of the network and on the initial condition, the time to extinction grows exponentially in the size of the population, with probability converging to 1 as the size of the population grows large. This provides new insights with respect

to the results from the literature, which are mainly focused on the expected time to extinction, as already mentioned. In particular, new insights into the epidemic process are gained through our improved characterization of the phase transition, yielding a better understanding of the properties of the model in the regime above this threshold, depending on the topology of the network of interactions and on the initial condition.

Then, in Section 3.3, we study the SIS model from a different point of view. Specifically, we study an epidemic outbreak spreading on a heterogeneous time-varying network of interaction and we develop an array of techniques to predict its evolution for short and medium time horizons. Finally, we test our framework against two real-world case studies, which exemplify different physical phenomena and time scales. Part of the work described in this chapter has been previously published in [39–41].

3.1 Model and Mean Field Analysis

The SIS model [25, 26] can be formalized within our general theory for diffusion processes. We naturally set $X_i(t) = 1$ if and only if agent i is *infected* at time t and $X_i(t) = 0$ else, if the agent i is *susceptible* to the disease. Two mechanisms characterize the SIS model: i) the *spread*, through which infection spreads along the edges connecting a susceptible agent to an infected one; and ii) the *recovery*, through which infected agents can spontaneously recover from infection and return to the susceptible state. Coherently, we set the mutation probability m_{10} and the copying probability p_{01}, associated with the two admissible transitions (spontaneous mutation from 1 to 0 and update from 0 to 1 after an interaction) to be strictly positive, whereas the other two probabilities are set to zero, i.e., $m_{01} = p_{10} = 0$. Admissible transitions are represented in Fig. 3.1.

Hence, the transition rates (2.16) for the SIS model read

$$\begin{cases} \lambda_i^+(\mathbf{x}) = (1-x_i)p_{01} \sum_{j \in \mathcal{N}_i} W_{ij} x_j \\ \lambda_i^-(\mathbf{x}) = \lambda m_{10} x_i. \end{cases} \tag{3.1}$$

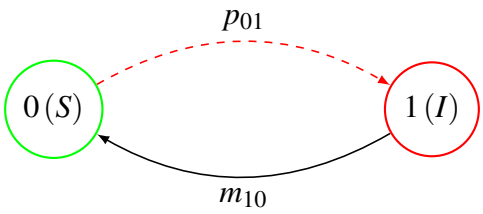

Fig. 3.1 State transitions characterizing the SIS epidemic model. Black solid lines are spontaneous mutation, colored dashed lines are transitions taking place after a pairwise interaction with a node with the other state.

The process $X(t)$ has a unique absorbing state $0\mathbb{1}$ that corresponds to the disease-free configuration. As already observed, since there exists a path of non zero probability transitions from every state to the absorbing state, then, almost surely, there exists a t for which $X(t) = 0\mathbb{1}$ [34]. We can thus define the absorbing time of the process as the following random variable:

$$\tau = \min\{t \in \mathbb{R}^+ : X(t) = 0\mathbb{1}\}. \tag{3.2}$$

In the homogeneous mean field case, we set $W_{ij} = \lambda_e/N$, according to Remark 2.2. This case have been extensively studied, both using finite-horizon predictions obtained through Theorem 2.1, and by directly analyzing the absorbing time τ, enabling the technical community to define a phase transition in correspondence of $\lambda_e p_{01}/\lambda m_{10} = 1$.

In order to present these important results, we focus on the process $Z(t)$. Its transition rates read

$$\begin{cases} \lambda^+(z) &= N(1-z)z\lambda_e p_{01} \\ \lambda^-(z) &= Nz\lambda m_{10}. \end{cases} \tag{3.3}$$

Hence, the ODE described by Theorem 2.1 is simply

$$\dot{\zeta} = \zeta\left[(1-\zeta)\lambda_e p_{01} - \lambda m_{10}\right]. \tag{3.4}$$

We define the *effective infection rate* as $\beta = \lambda_e p_{01}/\lambda m_{10}$. The results of the analysis of (3.4) can be summarized in the following Proposition.

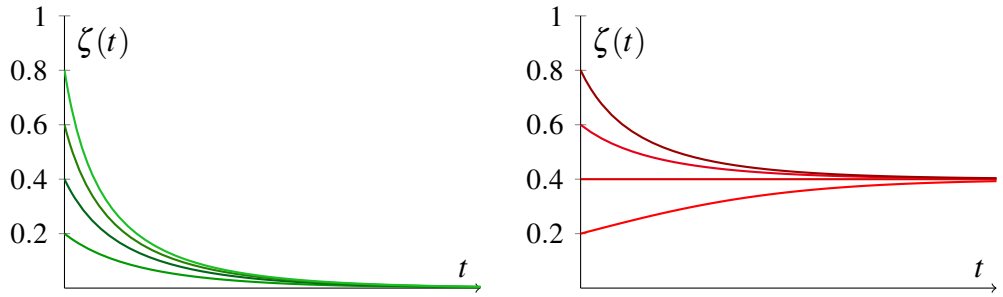

(a) $\lambda_e = \lambda = 1$, $p_{01} = 0.5$, $p_{10} = 0.7$. (b) $\lambda_e = \lambda = 1$, $p_{01} = 0.5$, $p_{10} = 0.3$.

Fig. 3.2 Solutions of the Cauchy problem (3.4) for different values of the parameter show the presence of the two regimes, depending on β.

Proposition 3.1. *If $\beta < 1$, the disease-free equilibrium is the only stable point of* (3.4)*. Otherwise, if $\beta > 1$, the disease-free state is unstable and $\bar{\zeta} = 1 - \beta^{-1}$ is the only stable equilibria of the system.*

Figure 3.2 depicts this phase transition phenomenon.

Hence, for finite time horizons, the trajectories of the process converge close to 0, if $\beta < 1$, and close to $\bar{\zeta}$, else. As the stochastic process is considered, the phase transition of the deterministic approximation reflects into a bifurcation in the expected absorbing time τ. The following proposition is a well known result from the literature [11].

Proposition 3.2. *Let $X(t)$ be an SIS model on a complete graph with transition rates* (3.1)*, and let $\tilde{Z}_0 = \sum_i X_i(0) > 0$. Then,*

1. *if $\beta < 1$, it holds*
$$\mathbb{E}[\tau] \leq \frac{2}{1-\beta}\left[1 + \ln\left(\tilde{Z}_0\right)\right]; \tag{3.5}$$
2. *if $\beta > 1$, it exists $C > 0$ such that*
$$\mathbb{E}[\tau] \geq \exp\{CN\}. \tag{3.6}$$

3.2 Analysis of the Absorbing Time

Here, we study the absorbing time τ for general graphs, specifically focusing on its tail probabilities, in order to deepen the understanding of the phase transition

phenomenon analyzed above under mean field assumptions. Without any loss in generality, we can assume $\lambda = p_{01} = m_{10} = 1$ and $\lambda_e = \beta$, since, as mentioned above, the discriminating parameter is the effective infection rate, i.e. $\lambda_e p_{01}/\lambda m_{10}$. Our benchmark are the results in [11], briefly summarized in the following, that extend the bounds in Proposition 3.2, which proves the presence of a phase transition, far beyond the fully connected graph. In that work, the absorbing time τ has been studied in terms of its expected value, i.e., $\mathbb{E}[\tau]$, for large-scale networks, analyzing its asymptotic behavior as a function of the number of nodes N. For the sake of simplicity, we stick our analysis to the homogeneous case, where the graph G is a simple graph.

Remark 3.1. *In order to keep consistency with the results in [11], here we set $A = W$ and we re-scale the effective infection rate β, differently from our standard homogeneous settings, where we re-scale the adjacency matrix as $A = W/\bar{d}$. We remark that the systems obtained according to the two different re-scaling methods are equivalent.*

Definition 3.1. *Given a subset of nodes $S \subset V$, its* cut*, denoted by $c[S]$, is the cardinality of the set of out-going edges from S to $V \setminus S$, in formula:*

$$c[S] := |\{(i,j) \in E : i \in S, j \notin S\}| = \sum_{i \in S, j \notin S} A_{ij}. \tag{3.7}$$

We remark that this definition can be naturally extended to the case of weighted graph summing the terms of the weight matrix W instead of the adjacency matrix in (3.7). This generalized definition will be used in Chapter 5, when dealing with dynamics on a weighted graph.

Definition 3.2. *The* isoperimetric constants *of the graph [11] are a set of N constants, defined as follows:*

$$\eta(m) = \min_{S \subseteq V : |S| = m} \frac{c[S]}{m}, \qquad \forall m \in \{1, \dots, m\}. \tag{3.8}$$

Remark 3.2. *Since $\eta(n) = 0$, only $N-1$ of the isoperimetric constants actually have a non trivial value. The notion of isoperimetric constants is related to the Cheeger constant for directed graphs [42], that is $\gamma = \min_m \eta(m)$. Cheeger constant will be used later in this dissertation, in Chapter 4. Note that while γ gives only a global measure of the presence of bottlenecks and isolated subsets in the graph, the*

isoperimetric constants point out the presence of isolated subsets of nodes of any fixed dimension.

The following two Theorems are the two main theoretical results, which characterize the phase transition of the SIS model on a general network of interactions.

Theorem 3.1 (Corollary 8.2.1 from [11])**.** *Let G be a graph with by N nodes and let us consider an SIS model on G with effective infection rate β. Let ρ be the spectral radius of the adjacency matrix of G. Then, if $\beta\rho < 1$, it holds that*

$$\mathbb{E}[\tau] \leq \frac{\ln(N)+1}{1-\beta\rho}. \tag{3.9}$$

Theorem 3.2 (Corollary 8.4.1 from [11])**.** *Let G be a graph with N nodes and let us consider an SIS model on G with effective infection rate β and initial condition $X(0) \neq 0\mathbb{1}$. If $\exists m > 0$ such that $\beta\eta(m) > 1+\varepsilon$, for some $\varepsilon > 0$. Then*

$$\mathbb{E}[\tau] \geq \exp(b_\varepsilon m), \tag{3.10}$$

where b_ε is a positive constant only depending on ε.

If we consider a sequence of graphs for which $\beta\rho$ is below and kept bounded away from 1, Theorem 3.1 says that the expected time to extinction grows at most logarithmically in N. Using Markov inequality, we can actually assert that such behavior holds for τ, with probability converging to 1 as N grows. Indeed, for every $\forall\,\alpha > 1$,

$$\mathbb{P}[\tau \geq (\ln N)^\alpha] \leq \frac{\ln N + 1}{(1-\beta\rho)(\ln N)^\alpha}. \tag{3.11}$$

On the other hand, Theorem 3.2 does not enable us to analogously conclude that τ will undertake an exponential growth with high probability, even in the case when the parameter m grows linearly in N. Indeed, the behavior of the expected value could be determined by events of small or even negligible probability. This situation could arise, e.g., when an SIS model satisfies the hypothesis of Theorem 3.2, but starts from a single node i infected at time $t = 0$. In this case, even if (3.10) holds true, node i recovers before any other gets infected with probability $1/\beta|\mathcal{N}_i| > 0$, implying that with nonzero probability the disease immediately extinguishes. We remark that situations with few nodes initially infected are not the only relevant cases in which a huge discrepancy between $\mathbb{E}[\tau]$ and the tail probabilities of τ is present. In

fact, also the topology of the network of interaction may cause analogous phenomena. As an example, we consider a line of infected individuals connected with a complete graph made of susceptible nodes. In situations like these, the analysis of $\mathbb{E}[\tau]$ is not sufficient to understand and predict the behavior of the epidemic process.

3.2.1 New Bounds on the Tail Probabilities

Here, we provide a direct (lower bound) estimation of the tail probabilities of τ. This will show that, for β above a certain threshold (depending on the model parameters and on the isoperimetric constants of the graph), the time to extinction τ indeed grows exponentially in N asymptotically almost surely.

In order to develop our estimate, we start by defining a new measure of connectivity based on the isoperimetric constants of the graph, which will play a central role in our estimation.

Definition 3.3. *Given constants α and s with $0 < \alpha \leq s$, we define the (α, s)-bottleneck of a graph G as*

$$\gamma_{\alpha,s} = \max_{k \in \{\lceil \alpha N \rceil, \ldots, \lceil sN \rceil\}} \min_{m \in \{k - \lceil \alpha N \rceil, \ldots, k\}} \eta(m), \tag{3.12}$$

where $\eta(m)$ is the set of isoperimetric constants.

The quantities we have just introduced give information regarding the existence of sequences of subsets of nodes poorly connected to the rest of the graph. More precisely, a small value of the (α, s)-bottleneck points out the presence of a sequence of αN subsets of nodes of consecutive increasing cardinality below sN. Intuitively, the presence of such a sequence creates an obstacle to the diffusion of the epidemics when its size is still below sN.

The following is the main technical result of this section: it gives an estimate of the tail probabilities of the time to extinction in terms of the $\gamma_{\alpha,s}$-bottlenecks.

Theorem 3.3. *Let G be a graph with N nodes and let us consider a SIS model $X(t)$ with effective infection rate β on G. Assume that $X(0)$ is deterministic and that $X(0) \neq 0\mathbb{1}$. Let $\xi_0 = N^{-1} \sum_i X_i(0)$ be the initial fraction of infected nodes and put*

$$a = \max_{\alpha \in (0, \xi_0] : \beta \gamma_{\alpha, \xi_0} > 1} \alpha \frac{(\beta \gamma_{\alpha,\xi_0} - 1)^2}{8\beta(\beta \gamma_{\alpha,\xi_0} + 1)^2}. \tag{3.13}$$

(conventionally $a = -\infty$ if $\beta\gamma_{\alpha,\xi_0} \leq 1$ for every α). Then, $\forall\,\varepsilon > 0$, the time to extinction of $X(t)$ satisfies the inequality

$$\mathbb{P}\left[\tau < e^{(a-\varepsilon)N}\right] \leq 9(\beta N^2 + N)e^{-2\varepsilon N} + e^{-(a-\varepsilon)N}. \tag{3.14}$$

Proof. We consider the process $\tilde{Z}(t) = \sum_i X_i(t)$, counting the number of infected agents in the population. According to (2.21), its transition rates from $\tilde{Z}(t) = z$, when the boundary is such that $\xi(t) = \xi$, are

$$\begin{cases} \lambda^+(z|\xi) = \beta\xi \\ \lambda^-(z) = z. \end{cases} \tag{3.15}$$

We observe that (3.8) yields the following implication: $\tilde{Z}(t) = z \implies \xi(t) \geq z\eta(z)$. Hence, standard arguments [11] show that $\tilde{Z}(t)$ stochastically dominates [34] a birth and death process $\bar{Z}(t)$ with the same initial condition $\bar{Z}(0) = \tilde{Z}(0)$ and transition rates

$$\begin{cases} \bar{\lambda}^+(z) = \beta z\eta(z) \\ \bar{\lambda}^-(z) = z. \end{cases} \tag{3.16}$$

Hence, observed that also $\bar{Z}(0)$ admits the disease-free state 0 as unique absorbing state, we name

$$\bar{\tau} = \min\{t \geq 0 : \bar{Z}(t) = 0\}. \tag{3.17}$$

The stochastic domination between processes $\tilde{Z}(t)$ and $\bar{Z}(t)$ implies that also the time to extinction τ of $\tilde{Z}(t)$ stochastically dominates $\bar{\tau}$ of $\bar{Z}(t)$. In fact, stochastic domination means that $\forall t \in \mathbb{R}^+$ and $\forall z \in \{0,\ldots,N\}$,

$$\mathbb{P}[\tilde{Z}(t) > z] \geq \mathbb{P}[\bar{Z}(t) > z]. \tag{3.18}$$

In particular, by setting $z = 0$, this yields

$$\mathbb{P}[\tau > t] \geq \mathbb{P}[\bar{\tau} > t], \tag{3.19}$$

which the stochastic domination between τ and $\bar{\tau}$.

From now on, we focus on the process $\bar{Z}(t)$ and on the estimation of $\bar{\tau}$. We fix α to be a maximum point of the expression (3.13). Let M^* be an element in the argmax of (3.12) for the $(\alpha - \xi_0)$-bottleneck of G, $m^* = M^* - \lceil \alpha N \rceil$ and $I = \{m^*, m^* + 1, \ldots, M^*\}$. Then, if the process $\bar{Z}(t)$ never goes beyond m^* in a time

range T, then it is surely not absorbed in the disease-free equilibrium in that time range, which implies

$$\mathbb{P}[\tilde{\tau} < T] \leq \mathbb{P}\left[\inf_{t\in[0,T]} \bar{Z}(t) \leq m^*\right]. \tag{3.20}$$

Considering that $\bar{Z}(0) \geq M^*$, for $\bar{Z}(t)$ to be absorbed in the disease-free configuration $0\mathbb{1}$, necessarily $\bar{Z}(t)$ has to cross completely the interval I from top (i.e., M^*) to bottom (i.e., m^*). This remark will now be used in order to estimate the right hand side of (3.20) using Lemma A.1, considering that i) being $\eta(z) \leq N$,

$$\mu := \max_{z\in\{0,\dots,N\}} (\beta z\eta(z) + z) \leq \beta N^2 + N; \tag{3.21}$$

ii) (A.1) is verified by $\delta = \beta\gamma_{\alpha,\xi_0} - 1$; and iii) (A.10) can be re-written as

$$\mathbb{P}(E_l) = \sum_{h=0}^{\frac{l}{2}-\frac{\varepsilon N}{2}} \binom{l}{h} p^h (1-p)^{l-h} \leq \exp\left\{-\frac{(2p-1)^2 l}{8p}\right\} \leq \exp\left\{-\frac{(2p-1)^2 l}{8}\right\}. \tag{3.22}$$

Finally, from the last passage of the proof of Lemma A.1, by fixing $\varepsilon > 0$ and putting $T = e^{(a-\varepsilon)N}$, we conclude that (A.14) reduces to

$$\mathbb{P}\left[\inf_{t\in[0,T]} \bar{Z}(t) \leq m^*\right] \leq 9(\beta N^2 + N)e^{-2\varepsilon N} + e^{-(a-\varepsilon)N}. \tag{3.23}$$

This together with (3.20) and the stochastic domination between τ and $\bar{\tau}$, yields the thesis.

□

Notice first that if $\beta\gamma_{\alpha,\xi_0} > 1$ for some $\alpha \leq \xi_0$, then $a > 0$. In this case, inequality (3.14) can be written in a more compact way, as follows.

Corollary 3.1. *Let G be a graph with N nodes and let us consider a SIS model $X(t)$ with effective infection rate β on G. Assume that $X(0)$ is deterministic and that $X(0) \neq 0\mathbb{1}$. Let $\xi_0 = N^{-1}\sum_i X_i(0)$ be the initial fraction of infected nodes and let $\beta\gamma_{\alpha,\xi_0} > 1$. Then, defined a according to* (3.13)*, for any $0 < \varepsilon < a/2$ and N sufficiently large,*

$$\mathbb{P}[\tau < \exp\{(a-\varepsilon)N\}] \leq e^{-\varepsilon N}. \tag{3.24}$$

The typical application of Corollary 3.1 consists in considering a family of graphs $G^{(N)}$ made by N nodes such that the quantity a defined in (3.13) is lower bounded by a strictly positive constant. In this way, it is ensured the presence of a long lasting diffusion regime in which the epidemic becomes endemic and it lasts for a time that grows at least exponentially in N almost surely when $N \to \infty$.

We remark that, on the one hand, inequality (3.24) is a stronger result than the estimation in Theorem 3.2). On the other hand, the hypothesis of Corollary 3.1 are more restrictive. In fact, $\beta\gamma_{\alpha,\xi_0} > 1$ for some $\alpha \leq \xi_0$, implies $\beta\eta(m) > 1$ for some $m \leq N\xi_0$, but the reverse implication is not always verified. Therefore, in principle, our result is stronger in the probability estimation but identifies a higher epidemic threshold. However, in the examples presented in the following section, we will show that the epidemic thresholds identified by Corollary 3.1 and the one from Theorem 3.2 for the expected time to extinction actually coincide for many relevant graph topologies.

3.2.2 Application on Specific Topologies

In this section, we apply our new analytical bound on some relevant graph topologies. Specifically, we analyzed several expander graphs (such as complete, ER graphs, star graphs), and an interesting example of nonexpander graph for which our result can be applied, giving condition for having an exponentially long absorbing time.

Example 3.1 (Complete graph)**.** *Let us consider a complete graph with N nodes, as described in Ex. 2.1. With the natural parametrization $\beta = c/N$, from to [11] it is known that the expected time to extinction grows exponentially in N if $c > 1$. Theorem 3.3 allows us to refine this result proving that the time to extinction grows exponentially in N a.a.s. as $N \to \infty$. In particular, for any choice of $\varepsilon > 0$, formula (3.14) holds true with*

$$a = \begin{cases} \xi_0 \dfrac{(c(1-\xi_0)-1)^2}{8(c(1-\xi_0)+1)^2} & \text{if } \xi_0 \leq 1 - \frac{\sqrt{4c+5}-2}{c} \\ \dfrac{1}{8} - \dfrac{\sqrt{(4c+5)^3} - 12c - 11}{16c(c+1)} & \text{else.} \end{cases} \tag{3.25}$$

Proof. In the case of a complete graph, the isoperimetric constant is $\eta(m) = N - m$. Due to its monotonicity in m we can immediately obtain that $\gamma_{\alpha,\xi_0} = (1-\alpha)N$. Thus,

the maximization problem (3.13) becomes

$$\max_{\alpha\in[0,\min\{\xi_0,\frac{c-1}{c}\}]} \phi(\alpha) := \alpha\frac{(c(1-\alpha)-1)^2}{8(c(1-\alpha)+1)^2}. \tag{3.26}$$

The domain $\alpha \in [0, \min\{\xi_0, \frac{c-1}{c}\})$ is a consequence of having $\alpha \leq \xi_0$ and $\beta\gamma_{\alpha,\xi_0} > 1 \iff \alpha < \frac{c-1}{c}$.

We first solve the maximization problem in the relaxed domain $\alpha \in [0, \frac{c-1}{c})$. Through standard computations we claim that the function $\phi(\alpha)$ has a maximum in the relaxed domain for

$$\alpha^* = 1 - \frac{\sqrt{4c+5}-2}{c}, \tag{3.27}$$

while it is monotonically increasing from 0 to α^* and then monotonically decreasing to $\frac{c-1}{c}$. Therefore if $\xi_0 > \alpha^*$, then α^* is in the original domain, so $a = \phi(\alpha^*)$. Otherwise, if $\xi_0 \leq \alpha^*$, $\phi(\alpha)$ is monotonically increasing in the whole original domain of the maximization problem, therefore its maximum is attained at the extreme $\alpha = \xi_0$, that is $a = \phi(\xi_0)$. Formulae in (3.25) come from explicit computations of $\phi(\alpha)$ in this two cases. □

We remark that, a more precise result for the parameter of the exponential in the case of the complete graph is available in [43]. This result has been obtained through the direct analysis of the process $Z(t)$, that in the specific case of a complete graph is a Markov birth and death process. The result therein can be rewritten according to our formulation in Corollary 3.1. Then, $\forall\,\varepsilon > 0$,

$$\mathbb{P}(\tau < e^{(b-\varepsilon)N}) \leq Ce^{-\varepsilon N}, \tag{3.28}$$

for some $C > 0$, where $b = \log c - 1 + 1/c$, which is always greater then or equal to the value of a from (3.25).

Even though the result in [43] yields a better estimate, the strength of our computation is that it can be immediately applied to many interesting network topologies, not comprised in the work cited above, such as Erdős-Rényi random graphs.

Example 3.2 (Erdős-Rényi random graphs)**.** *Let G be an Erdős-Rényi random graph, as presented in Ex. 2.6. The same result for a computed for complete graphs can*

also be applied to ER graphs with $p >> \ln N/N$ with the parametrization $\beta = c/Np$, when $c > 1$.

Proof. It is known that $p = \ln N/N$ is the connectivity threshold function of an ER random graph [44, 45]. This means that, if $p >> \ln N/N$, the graph is connected w.h.p.. As the isoperimetric constant is considered, from [11] we claim that w.h.p. $\eta(m) = (1+o(1))(N-m)p$. As in the complete graph case, due to the monotonicity of $\eta(m)$, we can conclude that $\gamma_{\alpha,\xi_0} = (1+o(1))(1-\alpha)Np$. Therefore, the maximization problem (3.13) for an ER graph reads exactly as the one for the complete case:

$$\max_{\alpha\in[0,\min\{\xi_0,\frac{c-1}{c}\}]} \alpha\frac{(\beta(1-\alpha)Np-1)^2}{8(\beta(1-\alpha)Np+1)^2} = \max_{\alpha\in[0,\min\{\xi_0,\frac{c-1}{c}\}]} \alpha\frac{(c(1-\alpha)-1)^2}{8(c(1-\alpha)+1)^2}. \tag{3.29}$$

□

This means that in an ER graph over the connectivity threshold, for any choice of $\varepsilon > 0$, formula (3.14) holds with the exponential rate a given by (3.25). However, because of the different parametrization, c represent a different parameter with respect to the complete case.

Example 3.3 (Star graph)**.** *Let G be a star graph, presented in Ex. 2.4. We prove that, if $\beta > 1$, then formula (3.14) holds with the following exponent*

$$a = \begin{cases} \dfrac{(\beta-1)^2}{8(\beta+1)^2}\xi_0 & \text{if } \xi_0 \le \dfrac{1}{2} \\ \max\left\{\dfrac{\xi_0(\beta(1-\xi_0)-\xi_0)^2}{8(\beta(1-\xi_0)+\xi_0)^2}, \dfrac{(\beta-1)^2}{16(\beta+1)^2}\right\} & \text{if } \xi_0 \in A \\ \dfrac{(\beta-1)^2}{16(\beta+1)^2} & \text{if } \xi_0 > \bar{\xi},\ \beta \le \beta^* \\ \dfrac{2\beta^3+14\beta^2+11\beta-\beta\sqrt{(4\beta+5)^3}}{16(\beta-1)^3} & \text{if } \xi_0 > \bar{\xi},\ \beta > \beta^*, \end{cases} \tag{3.30}$$

where β^* is the second real solution of

$$x^7 - 11x^6 - 3x^5 - 29x^4 + 131x^3 + 59x^2 - x - 19 = 0, \tag{3.31}$$

i.e., $\beta^* \approx 2.10165$*,*

$$\bar{\xi} = 1 - \frac{\beta\sqrt{4\beta+5} - 2\beta - 1}{\beta^2 - 1}. \quad \textit{and} \quad A = \left(\frac{1}{2}, \bar{\xi}\right]. \tag{3.32}$$

The regime in which the time to extinction grows at least exponentially in N w.h.p. is, therefore, when $\beta > 1$*. On the other hand, in [46], it have been prove that if* $\beta > \alpha/\sqrt{N}$*, for some constant* α*, then* $\mathbb{E}[\tau]$ *grows exponentially with N. This paves the way for further research in order to clarify the behavior of the system in the regime with* $\alpha/\sqrt{N} < \beta < 1$*, by studying the probability distribution of* τ *in that regime.*

Proof. The isoperimetric constant of a star can be obtained considering two different situations: if $m \leq N/2$, then we have $\eta(m) = 1$. Otherwise, if $m > N/2$, $\eta(m) = (N-m)/m$. For this reason γ_{α,ξ_0} can be written in the following piece-wise form:

$$\gamma_{\alpha,\xi_0} = \begin{cases} 1 & \text{if } \alpha \leq 1/2 \\ (1-\alpha)/\alpha & \text{if } \alpha > 1/2. \end{cases} \tag{3.33}$$

If $\xi_0 \leq 1/2$, then (since $\alpha \leq \xi_0$) only the first expression is present and the maximization problem (3.13) yields

$$a = \max_{\alpha \in [0,\xi_0]} \alpha \frac{(\beta-1)^2}{8(\beta+1)^2} = \xi_0 \frac{(\beta-1)^2}{8(\beta+1)^2}. \tag{3.34}$$

A more complex situation occurs when $\xi_0 > 1/2$. In this case we can partition the domain of the maximization problem in two parts according to the piece-wise definition of γ_{α,ξ_0}, solve the maximization problem in each one of the two domains and then compare the two results (called a' and a'', respectively) and find the global maximum.

As the first domain is considered, i.e. $[0, 1/2]$, the problem is trivial since the function is monotonically increasing, so we have the first candidate

$$a' = \frac{(\beta-1)^2}{8(\beta+1)^2}. \tag{3.35}$$

In the second part of the domain we have the following maximization problem

$$\max_{\alpha\in(\frac{1}{2},\min\{\xi_0,\frac{\beta}{\beta+1}\}]} \phi(\alpha) := \alpha\frac{\left(\frac{\beta(1-\alpha)}{\alpha}-1\right)^2}{8\left(\frac{\beta(1-\alpha)}{\alpha}+1\right)^2}. \tag{3.36}$$

The domain $\alpha \in (\frac{1}{2}, \min\{\xi_0, \beta/(\beta+1)\})$ is a consequence of having $\alpha \leq \xi_0$ and $\beta\gamma_{\alpha,\xi_0} > 1 \iff \alpha < \beta/(\beta+1)$. Thus we consider the maximization problem on the relaxed domain $\alpha \in [0, \min\{\xi_0, \beta/(\beta+1)\})$, noticing that if the maximum is attained for some $\alpha < 1/2$, then it is trivial that $a' > a''$, so this extension does not influence the final result.

We find out that $\phi(\alpha)$ is monotonically increasing from 0 to

$$\alpha^* = 1 - \frac{\beta\sqrt{4\beta+5}-2\beta-1}{\beta^2-1}, \tag{3.37}$$

and then decreasing till $\beta/(\beta+1)$. Hence if $\xi_0 > \alpha^*$, $a'' = \phi(\alpha^*)$; otherwise $a'' = \phi(\xi_0)$.

After some computations we obtain the results in (3.30). Unfortunately, the maximum in the second expression depends both on β and ξ_0, so it is not possible to give simple conditions under which the maximum is attained by the first term or by the second one. On the contrary, this is possible in the case $\xi_0 > \alpha^*$ (since $\phi(\alpha^*)$ does not depend on ξ_0), giving the third and the fourth expressions. □

These expander graphs (complete, ER graphs, star graphs), characterized by the presence of a large isoperimetrical constants for almost every level m, present very similar behavior. We present now a relevant example of the application of our result to a nonexpander graph possessing a bottleneck, on which our result can be applied.

Example 3.4 (Barbell graph)**.** *Let G be a barbell graph, presented in Ex. 2.5. Similar to the complete graph, we parametrize $\beta = c/N$, from [11] we can deduce that the expected time to extinction grows exponentially in N when $c > 2$. Theorem 3.3 ensures that formula (3.14) holds with*

$$a = \begin{cases} \xi_0\dfrac{(c(1/2-\xi_0)-1)^2}{8(c(1/2-\xi_0)+1)^2} & \text{if } \xi_0 \leq \frac{1}{2} - \dfrac{\sqrt{2c+5}-2}{c} \\ \dfrac{1}{16} - \dfrac{\sqrt{(2c+5)^3}-6c-11}{8c(c+2)} & \text{else.} \end{cases} \tag{3.38}$$

Proof. Taking advantage of the structure of the graph, the isoperimetric constant of a barbell graph can be easily computed and it is

$$\eta(m) = \begin{cases} N/2 - m + 1/m & \text{if } m \leq N/2 \\ (m - N/2)(N-m)/m & \text{if } m > N/2, \end{cases}$$

that immediately implies that, for large N, $\forall\, \alpha \geq 1/2$, $\gamma_{\alpha,\xi_0} \to 0$, since $\eta(N/2) = 2/N \to 0$. Therefore choosing $\alpha < 1/2$, we obtain $\gamma_{\alpha,\xi_0} = (1/2 - \alpha)N$. Hence, the maximization problem (3.13) reads

$$\max_{\alpha \in [0, \min\left\{\xi_0, \frac{c-2}{2c}\right\}]} \alpha \frac{(c(1/2-\alpha)-1)^2}{8(c(1/2-\alpha)+1)^2}. \tag{3.39}$$

The domain $\alpha \in [0, \min\{\xi_0, (c-2)/2c\}]$ is a consequence of having $\alpha \leq \xi_0$ and $\beta\gamma_{\alpha,\xi_0} > 1 \iff \alpha < (c-2)/2c$.

This problem can be reduced to a maximization problem very close to the one solved in the case of a complete graph by defining $\alpha' = 2\alpha$ and $c' = c/2$:

$$\max_{\alpha' \in [0, \min\{2\xi_0, \frac{c-2}{c}\}]} \phi(\alpha') := \alpha' \frac{(c'(1-\alpha')-1)^2}{16(c'(1-\alpha')+1)^2}. \tag{3.40}$$

Hence, relaxing the domain to $\alpha \in [0, (c'-2)/c']$, $\phi(\alpha')$ is monotonically increasing from 0 to its maximum in

$$\alpha'^* = 1 - \frac{\sqrt{4c'+5}-2}{c'} \implies \alpha^* = \frac{1}{2} - \frac{\sqrt{2c+5}-2}{c}, \tag{3.41}$$

and decreasing then until $(c'-2)/c'$. The same argument used for the complete graph leads to the result. □

3.3 Predictions for Time-Varying Networks

Here, we analyze the spread of a disease on time-varying heterogeneous networks and we seek to establish an analytical framework to study the entire dynamics at the population level (from the zero-infected condition to the endemic equilibrium). In the last few years, activity driven networks (ADN) [47, 48] have emerged as a powerful paradigm to analyze time varying networks. In this work, differently from

the original ADN formulation, where a discrete-time epidemic model is implemented with a continuous probability distribution for the nodes' activities, we formulate a continuous-time model with a discrete distribution, which can be modeled within our framework. This change of perspective leads to a rigorous analytical treatment, without the need of extensive Monte Carlo simulations that have constituted the primary tool for the study of ADNs. Our approach is not prone to the confounds associated with the selection of the time step, which has been proven to influence the dynamics of the discrete-time dynamical process [49]. Our theory relies on a reduced number of parameters with respect to traditional ADNs. This is critical for robust parameter identification from real-world data.

We consider a (large) population of N individuals, each associated with an agent of an undirected weighted graph. Each agent $i \in \mathcal{V}$ is assigned a time-invariant activity rate a_i which represents the expected number of contacts that node i generates in a unit time interval. Contacts are generated uniformly at random among all the individuals of the population. Hence, the weight of the edge (i, j) is given by $W_{ij} = (a_i + a_j)/N$. The relationship with discrete-time ADN models [47] is straightforward. In a time step Δt, the continuous-time model establishes as many edges as in a realization of the discrete-time model. Therefore, the time-varying graph obtained in the discrete-time model can be retrieved by integrating the edges created by the continuous-time model over Δt. The activity rate of a node in continuous-time corresponds to the product of its activity potential and the number of contacts it can establish in the time step. The probability that an infected node recovers in a discrete-time step is $1 - e^{-\lambda m_{10} \Delta t}$. The per-contact infection probability does not change between continuous- and discrete-time.

The proposed discrete activity distribution follows a power-law with k equidistant activation classes, characterized by an activity rate a_h ($a_1 < \cdots < a_k$). For the generic h-th class, we denote with n_h its number of nodes and we let $N_h \propto a_h^{-\gamma}$. The parameter γ controls the heterogeneity among individuals, similar to the classical ADN paradigm with a continuous distribution of activity potentials. The original formulation of ADNs posits a continuous power-law distribution with $2 \leq \gamma \leq 3$.

We indicate by $Z(t)$ the k-dimensional stochastic process $Z(t)$, encapsulating the fraction of infected nodes in each activation class. In the hydrodynamic limit $N \to \infty$, the fraction of nodes $(N_1/N, \ldots, N_k/N)$ in each of the activation classes converges to $(\eta_1, \ldots, \eta_k)$, independent of N. Then, Theorem 2.2 ensures that for every finite

time horizon, the stochastic process $Z(t)$ is close to $\zeta(t)$, solution of

$$\dot{\zeta}_h = -\lambda m_{10}\zeta_h + p_{01}(1-\zeta_h)(a_h x_1 + x_2), \tag{3.42}$$

with $h = 1,\ldots,k$ and $\zeta_h(0) = Z_i(0)$. Here, the macroscopic variable $x_1 = \sum \eta_h \zeta_h$ represents the fraction of infected individuals across all classes, which is the main observable in the study of epidemic spreading. The macroscopic variable $x_2 = \sum \eta_h a_h \zeta_h$ takes into consideration the fraction of infected nodes weighted by their individual activity rates. In general, we define $x_j = \sum \eta_h a_h^{j-1} \zeta_h$.

From (3.42), we appreciate that the drift in the fraction of infected nodes in each class is determined by three effects: the recovery of infected nodes ($-\lambda m_{10}\zeta_h$); the spreading associated with active nodes in the h-th class generating contacts toward infected nodes ($p_{01}(1-\zeta_h)a_h x_1$); and the spreading related to active infected nodes generating contacts with the nodes of the h-th class ($p_{01}(1-\zeta_h)x_2$). The k-dimensional Cauchy problem (3.42) has a unique solution due to Picard-Lindelöf theorem. Moreover, $[0,1]^k$ is a positive invariant set, since $\dot{\zeta}_i$ is positive when $\zeta_i = 0$ and negative when $\zeta_i = 1$. Therefore, trajectories with initial conditions within the set do not escape from it. This, along with the monotonicity of the system [50], guarantees that all trajectories converge to a constant solution, that is, an equilibrium.

The elegant form of the system dynamics (3.42) in terms of the variables $\zeta_1,\ldots,\zeta_k$ lends itself into rigorous and revealing schemes to gain insight into the physics of the epidemic spreading. Here, we focus on two complementary strategies that could be systematically utilized for short- and long- term predictions. First, we propose the use of differential inclusions to establish rigorous bounds for the transient and endemic equilibrium of the system. Second, we explore the integration of estimation techniques to accurately predict the population of infected individuals from sporadic data which could be collected in real-world scenarios.

Integrating (3.42) allows to closely simulate the epidemic spreading without the need of Monte Carlo simulations. To verify this claim and demonstrate the correspondence between continuous- and discrete-time epidemic models, we consider two different dynamics on real-world phenomena, modeled through ADNs: flu spreading in a university campus and trend diffusion on Twitter. System parameters are obtained from case studies, as detailed in the Supplemental Material of [40], and are summarized in Table 3.1. We compare the outcome of Monte Carlo simulations averaged over 200 trials for both the continuous- and the discrete-time processes,

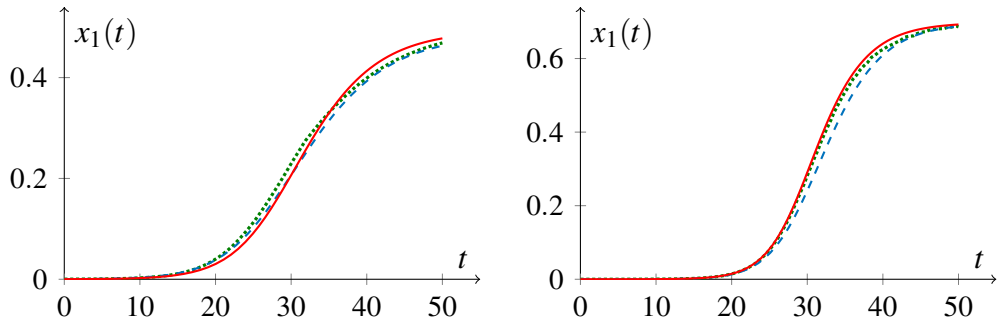

(a) Flu case study (b) Twitter case study

Fig. 3.3 Time evolution of the fraction of infected nodes for the case studies. Comparison between discrete-time continuous-distribution ADN process (blue, dashed), our continuous-time discrete-distribution approach (green, dotted) model, and theoretical predictions (red, solid) from (3.42).

along with the integration of the deterministic system (3.42). In both examples, the activity distribution is discretized over $k = 59$ equidistant activation classes. Fig. 3.3 demonstrates the equivalence of our approach with respect to traditional ADNs in Monte Carlo simulations, along with the validity of equation (3.42) to exactly predict the epidemic spreading.

3.3.1 System of Macroscopic Variables

To facilitate the mathematical treatment of the k-dimensional system (3.42), we rewrite the system dynamics in terms of the first k macroscopic variables, $x_1, \ldots, x_k$, using the following proposition.

Table 3.1 Parameters of real-world case studies based on ADNs

Parameter	flu	Twitter
N	30896	531788
k	59	59
γ	2.09	2.10
p_{01}	0.430	0.332
λm_{10}	0.138	0.0997
α_1	0.317	0.536
α_2	0.381	0.781
time unit	day	minute

Proposition 3.3. *System (3.42) is equivalent to the following:*

$$\begin{cases} \dot{x}_1 = (p_{01}\alpha_1 - \lambda m_{10})x_1 + p_{01}x_2 - 2p_{01}x_1x_2, \\ \dot{x}_2 = p_{01}\alpha_2 x_1 + (p_{01}\alpha_1 - \lambda m_{10})x_2 - p_{01}x_1x_3 - p_{01}x_2^2, \\ \dot{x}_3 = p_{01}\alpha_3 x_1 + p_{01}\alpha_2 x_2 - \lambda m_{10}x_3 - p_{01}x_1x_4 - p_{01}x_2x_3, \\ \dots \\ \dot{x}_k = p_{01}\alpha_k x_1 + p_{01}\alpha_{k-1}x_2 - \lambda m_{10}x_k - p_{01}x_1\sum \eta_h a_h^k \zeta_h - p_{01}x_2x_k, \end{cases} \tag{3.43}$$

where $\alpha_j = \sum \eta_h a_h^j$ are the moments of the activity rates distribution, whose first two values are also reported in Table 3.1 for completeness. This system is well-posed since the term $\sum \eta_h a_h^k \zeta_h$ in the k-th equation is a linear combination of the linearly independent variables $x_1, \dots, x_k$.

Proof. Recalling that $x_j = \sum \eta_h a_h^{j-1} \zeta_h$, we compute the right-hand-side determining the evolution of x_1 in the ODE system (3.43):

$$\begin{aligned} \dot{x}_1 &= \sum \eta_h \dot{\zeta}_h \\ &= -\lambda m_{10}\sum \eta_h \zeta_h + p_{01}x_1\sum \eta_h a_h + p_{01}x_2\sum \eta_h - p_{01}x_1\sum \eta_h a_h \zeta_h \\ &\quad - p_{01}x_2\sum \eta_h \zeta_h \\ &= -\lambda m_{10}x_1 + p_{01}x_1\alpha_1 + p_{01}x_2 - p_{01}x_1x_2 - p_{01}x_2x_1. \end{aligned} \tag{3.44}$$

A similar computation can be carried out for x_2, yielding

$$\begin{aligned} \dot{x}_2 &= \sum \eta_h a_h \dot{\zeta}_h \\ &= -\lambda m_{10}\sum \eta_h a_h \zeta_h + p_{01}x_1\sum \eta_h a_h^2 + p_{01}x_2\sum \eta_h a_h - p_{01}x_1\sum \eta_h a_h^2 \zeta_h \\ &\quad - p_{01}x_2\sum \eta_h a_h \zeta_h \\ &= -\lambda m_{10}x_2 + p_{01}x_1\alpha_2 + p_{01}x_2\alpha_1 - p_{01}x_1x_3 - p_{01}x_2^2. \end{aligned} \tag{3.45}$$

For a generic $j = 3, \dots, k-1$, we obtain

$$\begin{aligned} \dot{x}_j &= \sum \eta_h a_h^{j-1} \dot{\zeta}_h \\ &= -\lambda m_{10}\sum \eta_h a_h^{j-1} \zeta_h + p_{01}x_1\sum \eta_h a_h^j + p_{01}x_2\sum \eta_h a_h^{j-1} - p_{01}x_1\sum \eta_h a_h^j \zeta_h \\ &\quad - p_{01}x_2\sum \eta_h a_h^{j-1} \zeta_h \\ &= -\lambda m_{10}x_j + p_{01}x_1\alpha_j + p_{01}x_2\alpha_{j-1} - p_{01}x_1x_{j+1} - p_{01}x_2x_j. \end{aligned} \tag{3.46}$$

When considering the last macroscopic variable x_k, the previous formula reads

$$\dot{x}_k = -\lambda m_{10}x_k + p_{01}x_1\alpha_k + p_{01}x_2\alpha_{k-1} - p_{01}x_1\sum \eta_h a^k \zeta_h - p_{01}x_2x_k, \tag{3.47}$$

where the term $\sum \eta_h a^k \zeta_h$ is not linearly independent of $x_1, \dots, x_k$. In fact, the first k macroscopic quantities are linearly independent due to the nonsingularity of the Vandermonde matrix and the system has exactly k degrees of freedom. Hence, $\sum \eta_h a^k \zeta_h$ can be written as a linear combination of the first k macroscopic quantities.

Finally, notice that (3.43) is obtained from the k equations in (3.42 with a change of variables. Hence, the existence and uniqueness of a solution along with the convergence of any trajectory toward an equilibrium are automatically inherited. □

The study of (3.43) offers important insight on the epidemic spreading, beyond the mere computation of the epidemic threshold $(\alpha_1 + \sqrt{\alpha_2})^{-1}$ from linear stability analysis [47, 48]; details are presented in the Supplemental Material of [40]. However, numerical instabilities may emerge when considering power-laws with $\gamma \in [2,3]$, where all statistical moments from the second onwards may blow up. Moreover, prescribing initial conditions for higher order macroscopic variables beyond x_1 may be not feasible when dealing with experimental data.

3.3.2 Low-dimensional System of Differential Inclusions

A possible approach to address these issues is to project the k-dimensional dynamics to a lower dimensional space consisting of only $k^* \ll k$ equations. We approximate the term x_{k^*+1} using two elementary bounds: $a_1 x_{k^*} \leq x_{k^*+1} \leq a_k x_{k^*}$ and $x_{k^*+1} \leq \alpha_{k^*}$. Using these bounds, we can reduce system of k ODEs in (3.43) to a system of k^* ordinary differential inclusions (ODIs) [51], consisting of one inclusion and $k^* - 1$ equations.

If $k^* = 1$, we bound $a_1 x_1 \leq x_2 \leq \min\{\alpha_1, a_k x_1\}$, reducing (3.43) to

$$\dot{x}_1 \in (p_{01}\alpha_1 - \lambda m_{10}) x_1 + p_{01}(1 - 2x_1)\,[a_1 x_1, \min\{\alpha_1, a_k x_1\}]\,. \tag{3.48}$$

This one-dimensional system should not be contemplated to accurately predict the evolution of the process during the transient, between the zero-infected condition and the endemic equilibrium, due to the conservativeness of the bounds during such a transient phase. However, it can be effectively used to analytically determine an interval $\mathcal{I}$ for the endemic equilibrium $\bar{x}_1$, as follows.

Proposition 3.4. *It holds $\bar{x}_1 \in \mathcal{I}$, where*

$$\mathcal{I} = \left[\max\left\{ \frac{p_{01}\alpha_1}{p_{01}\alpha_1 + \lambda m_{10}}, \frac{p_{01}(a_k + \alpha_1) - \lambda m_{10}}{2p_{01}a_k} \right\}, \frac{p_{01}(a_1 + \alpha_1) - \lambda m_{10}}{2p_{01}a_1} \right], \tag{3.49a}$$

if $p_{01}\alpha_1 > \lambda m_{10}$, and

$$\mathcal{I} = \left[\frac{p_{01}(a_1 + \alpha_1) - \lambda m_{10}}{2p_{01}a_1}, \min\left\{ \frac{p_{01}\alpha_1}{p_{01}\alpha_1 + \lambda m_{10}}, \frac{p_{01}(a_k + \alpha_1) - \lambda m_{10}}{2p_{01}a_1} \right\} \right], \tag{3.49b}$$

if $p_{01}\alpha_1 < \lambda m_{10}$. If $p_{01}\alpha_1 = \lambda m_{10}$, we analytically compute $\bar{x}_1 = 1/2$.

Proof. The computation can be split depending on the sign of the term $(p_{01}\alpha_1 - \lambda m_{10})$. If $p_{01}\alpha_1 < \lambda m_{10}$, then the first term on the right-hand-side of (3.48) is negative, such that the second one should be positive to sum up to zero. Thus, the endemic state $\bar{x}_1$ lies in the interval between the solution x_l of

$$p_{01}\alpha_1 - \lambda m_{10} + p_{01}(1 - 2x_l)a_1 = 0, \tag{3.50}$$

and the solution x_u of

$$(p_{01}\alpha_1 - \lambda m_{10})x_u + p_{01}(1 - 2x_u)\min\{\alpha_1, a_k x_u\} = 0. \tag{3.51}$$

Solving for x_l and x_u, we establish the bounds (3.49b). Following a similar line of arguments, we obtain the other bounds in the case $p_{01}\alpha_1 > \lambda m_{10}$. Since $\bar{x}_1 \in [0,1]$, the bounds for the endemic state can be trivially tighten as $[x_l, x_u] \cap [0,1]$. □

To demonstrate the use of these bounds we refer, here and henceforth, to the two real-world case studies on flu spreading and trend diffusion on Twitter. From simulations in Fig. 3.4, we evince that the accuracy of the bounds depends on the system parameters. Specifically, our results suggest that the closer is the endemic state to $\bar{x}_1 = 1/2$ (that is, $\alpha_1 p_{01} = \lambda m_{10}$), the more precise the bounds are.

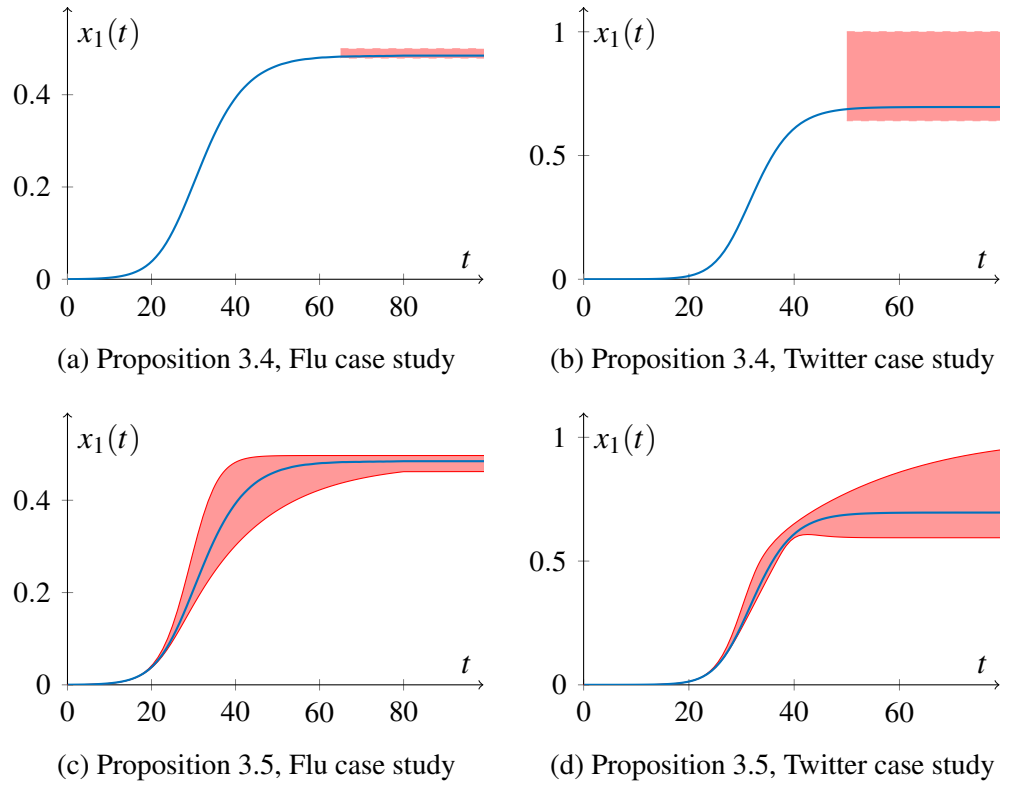

(a) Proposition 3.4, Flu case study

(b) Proposition 3.4, Twitter case study

(c) Proposition 3.5, Flu case study

(d) Proposition 3.5, Twitter case study

Fig. 3.4 Averaged Monte Carlo simulations of a discrete-time continuous-distribution ADN process (blue) and theoretical bounds (red) from Propositions 3.4 and 3.5 (with $\varepsilon = 10^{-3}$).

An improved prediction of the transient phase is obtained with $k^* = 2$, which leads to the following ODI for the evolution of x_2:

$$\dot{x}_2 \in p_{01}\alpha_2 x_1 + (p_{01}\alpha_1 - \lambda m_{10})x_2 - p_{01}x_2^2 + p_{01}x_1[-\min\{a_k x_2, \alpha_2\}, -a_1 x_2], \tag{3.52}$$

coupled to the first ODE in (3.43).

Proposition 3.5. *We establish the two following ancillary ODEs:*

$$\dot{x}_2 = p_{01}(\alpha_2 - \phi_{\varepsilon,x_2}(x_1))x_1 + (p_{01}\alpha_1 - \lambda m_{10})x_2 - p_{01}x_2^2, \tag{3.53a}$$

$$\dot{x}_2 = p_{01}(\alpha_2 - \phi_{\varepsilon,x_2}(1-x_1))x_1 + (p_{01}\alpha_1 - \lambda m_{10})x_2 - p_{01}x_2^2, \tag{3.53b}$$

where $\phi_{\varepsilon,x_2}(x_1)$, is a continuous function that, in the limit $\varepsilon \to 0$,

$$\phi_{\varepsilon,x_2}(x_1) \to \begin{cases} a_1 x_2 & \text{if } x_1 < 1/2, \\ \min\{a_k x_2, \alpha_2\} & \text{if } x_1 > 1/2. \end{cases} \tag{3.54}$$

Upper- and lower-bounds for x_1 are obtained by coupling the first ODE in (3.43) with (3.53a) and (3.53b), respectively, and integrating in the limit as $\varepsilon \to 0$.

Proof. The two ODEs are obtained as follows. To upper-bound the evolution of x_1, we select among all possible right-hand-sides for $\dot{x}_2$ in (3.52) those that yield the largest $\dot{x}_1$. From (3.43), in the right-hand-side of $\dot{x}_1$, the only term that depends on x_2 is multiplied by $(1-2x_1)$. Therefore, when $x_1 < 1/2$, the derivative $\dot{x}_1$ increases as x_2 increases; whereas, when $x_1 > 1/2$, it decreases as x_2 increases. We encapsulate this relationship through the continuous function $\phi_{\varepsilon,x_2}(x_1)$.

From (3.52) and (3.54), we establish the ancillary ODE (3.53a). We obtain the sought upper-bound by coupling the first ODE in (3.43) with (3.53a), and integrating for small values of ε. We comment that $\phi_{\varepsilon,x_2}(x_1)$ is introduced to provide regularity to the right-hand-side of the ancillary ODE (3.53a). In fact, Lipschitz-continuity of $\phi_{\varepsilon,x_2}(x_1)$ guarantees existence and uniqueness of the solution of the system, which would be hindered by the use of a Heaviside function. The lower-bound is obtained by following a similar argument, thereby considering, among all the possible right-hand-sides of $\dot{x}_2$ in (3.52), those that yield the smallest $\dot{x}_1$. □

Simulation results in Fig. 3.4 demonstrate the accuracy of the bounds in capturing the transient response. Higher endemic equilibria seem manifest into tighter prediction bounds during the transient, albeit the upper bound becomes conservative as time progresses. In general, the predictions of the endemic state from $k^* = 2$ are less precise than the simpler closed-form results for $k^* = 1$. This is related to the solutions of the ancillary ODEs (3.53a) and (3.53b) leaving the bounds for $k^* = 1$. With this in mind, the overall prediction accuracy could be improved combining the two bounds in Figs. 3.4.

3.3.3 Online Prediction Technique

An alternative strategy for the analysis of system (3.43) entails the use of epidemic data, sampled at the population level at a time period T, to drive the reduction of the dynamics on a lower dimensional space. Given the accuracy of (3.53) in estimating the transient response of the system, we focus on a two-dimensional dynamics in terms of x_1 and x_2. With reference to (3.43), we consider only the first two ODEs and we hypothesize that x_3 is linear in x_1 with a proportionality constant

C that is estimated from epidemic data. Specifically, we propose the following two-dimensional dynamics:

$$\begin{cases} \dot{x}_1 = -\lambda m_{10} x_1 + p_{01}\alpha_1 x_1 + p_{01} x_2 - 2p_{01} x_1 x_2, \\ \dot{x}_2 = p_{01}\alpha_2 x_1 + (p_{01}\alpha_1 - \lambda m_{10}) x_2 - p_{01} C x_1^2 - p_{01} x_2^2. \end{cases} \tag{3.55}$$

As a first approximation, we hypothesize that C is constant throughout the entire epidemic spreading and set to $C = \alpha_2$, which corresponds to a homogeneous distribution of infected individuals over all the activation classes. Our prediction of the infected population is defined piece-wise in time. In particular, we denote the piece-wise predictions with $x_1^{(h)}(t)$ and $x_2^{(h)}(t)$, in the interval $t \in [hT, hT+T)$, where $h \in \mathbb{Z}^+$. These predictions are informed by the knowledge of the overall infected fraction of population X_{hT} at the sampling times hT. We initialize the algorithm at time $t = 0$ by setting $x_1^{(0)}(0) = X_0$ and $x_2^{(0)}(0) = X_0\alpha_1$. The algorithm loops through the following steps:

i) system (3.55) is integrated from hT to $(h+1)T$, producing the solutions $x_1^{(h)}(t)$ and $x_2^{(h)}(t)$;

ii) at $t = (h+1)T$, the initial conditions for marching in time are set as $x_1^{(h+1)}(t) = X_{(h+1)T}$ and $x_2^{(h+1)}(t) = x_2^{(h)}(t)$; and

iii) h is incremented by 1 and the process resumes to step i).

We remark that this algorithm is only based on few data: the fraction of infected nodes at the inception of each time window of duration T, which is central for real-world applications. For example, it may be possible to periodically estimate the number of individuals affected by flu or the number of mentions and re-tweets of a specific trend. The knowledge of the detailed state of all the network nodes is not required by the algorithm, which dispenses with information about higher order microscopic variables. In Fig. 3.5, we demonstrate the use of the prediction algorithm against a simulation for the flu case study, by using a time window of a day or a week. Short-term forecasts (daily) are very close to the real dynamics (the average error is less than 1%), while forecasts on longer horizons (weekly) tend to be less accurate (with an average error around 10%).

To improve on the finite horizon forecast algorithm, we may treat C as piece-wise constant in time and adaptively update it during each prediction window. We initiate

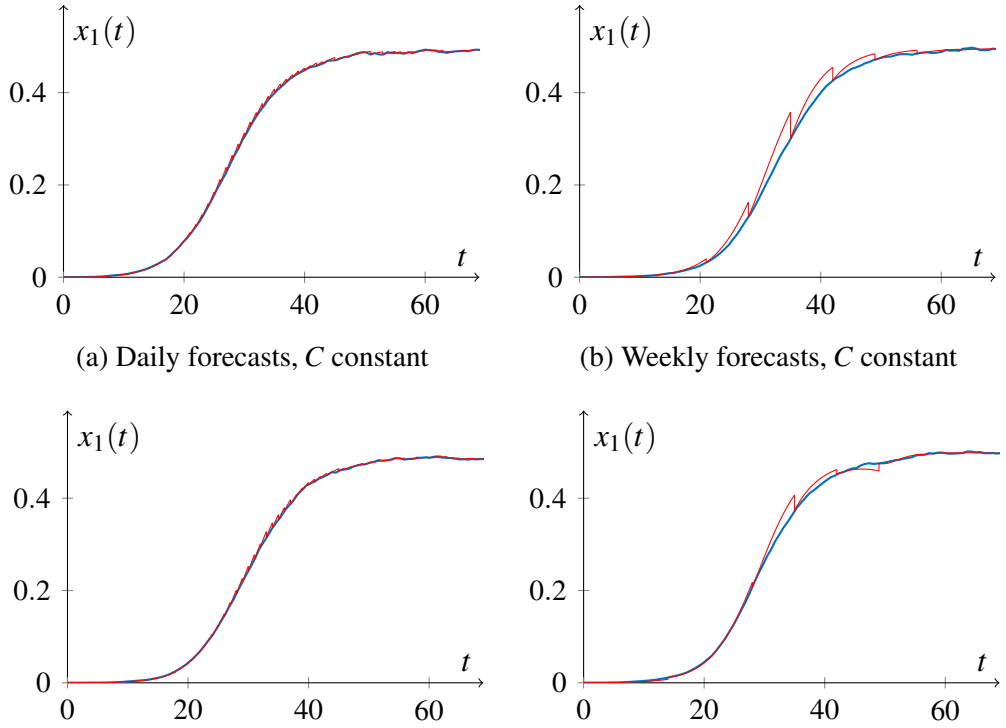

(a) Daily forecasts, C constant

(b) Weekly forecasts, C constant

(c) Daily forecasts, C adaptive

(d) Weekly forecasts, C adaptive

Fig. 3.5 Simulation of a discrete-time continuous-distribution ADN (blue), for the flu case study, and our predictions over a finite time horizon of one day and one week (red). Predictions in (a) and (b) are obtained with a constant estimate for C, while those in (c) and (d) are based on the on-line adaptive update in (3.56) with $\beta = 1$. A similar result for the Twitter case study is presented in the Supplemental Material of [40].

the algorithm by setting $C_0 = \alpha_2$. Then, fixing a real constant $\beta > 0$, at the end of each iteration, C_h is updated as

$$C_{h+1} = C_h \left(1 + \beta \frac{X_{(h+1)T} - x_1^{(h)}((h+1)T)}{1 - 2X_{(h+1)T}} \right). \tag{3.56}$$

Here, C is incremented by a term that is proportional to the prediction error at the inception of a new prediction window. The effect of the denominator is to change the sign of the increment when $X_{(h+1)T} > 1/2$, following a line of reasoning similar to the one used to define $\phi_{\varepsilon,x_2}(x_1)$ in (3.54). In Fig. 3.5, we demonstrate the improvement of the approach, which is successful in closely predicting population level dynamics even with only data available on a weekly basis.

3.4 Conclusion

In this chapter, we have adapted our general theory to study the SIS epidemic model. The formalism developed in Chapter 2 and the technical results presented in Appendix A have been leveraged to gain new insights into the epidemic process.

In Section 3.2, we have dealt with the computation of the time to extinction of an epidemic process. Specifically, we have focused our analysis on the tail probabilities of its distribution, improving the results available in the literature, which are mostly concerned with its expected value. The new insights into the epidemic process have enabled us to deepen the characterization of the slow-extinction regime of the process. Specifically, we have proved that, under some conditions, the disease becomes endemic and diffuses in the population for a time that grows at least exponentially with the number of individuals, with probability converging to 1 for large populations. The technique proposed here also allows for an explicit estimation of the rate of such an exponential time, depending on i) the model parameters, ii) topological properties of the graph related with the structure of its bottlenecks, and iii) the initial condition of the system.

Our analysis has also a methodological purpose for the analysis of more complex dynamics on networked systems. In fact, the central observation of our proving argument is that, under some conditions, the system has a drift, yielding the disease to diffuse faster than the spontaneous regression due to recover. A similar strategy can be applied to any other model exhibiting this feature. Therefore, one future research line consists in extending our results to more general epidemic models and other diffusion dynamics on networks.

In Section 3.3, we have applied the deterministic approximation of the system (detailed in Section 2.5) to study disease spreading on heterogeneous, time-varying large-scale networks of interactions, putting forward a mathematically tractable approach to study these complex phenomena from their onset to the endemic equilibrium. Techniques from the field of differential inclusions have been leveraged to gather insight on the transient response and endemic equilibrium. Toward connecting the theoretical framework with real data, we have introduced an adaptive estimation technique that affords the accurate prediction of the epidemics from coarse information only seldom acquired.

Although we specialized the treatment to SIS processes, the framework could be extended to other processes, by tailoring the individual dynamics. Details on this extension to a general epidemic model can be found in [41]. Several improvements to our model are envisaged and will be subject of further research. First, future work should seek to clarify the relationship between our predictions based on analytical bounds and model parameters. Second, a further effort should be devoted to cast the finite-time-horizon prediction techniques in an optimization context, to ease the selection of sampling periods and assess accuracy a priori. Finally, we aim at further empowering our framework with realistic phenomena, relevant from an epidemic modeling point of view, such as memory processes in link formation, spatial locality, and formation of communities. Some preliminary results in this direction can be found in [52], in which a model that includes self-excitement mechanisms has been proposed and analyzed, and in [53], in which the authors present a model for activity driven networks with communities.

Chapter 4

Model for Diffusion of Innovation

In this chapter, we study the spread of a new technological item (e.g., a smartphone application) in a population. We model its diffusion using a two-step adoption dynamics: the word-of-mouth yields a learning channel, through which potential users get aware of the existence of the item, whereas the probability of adoption increases the more the product is already diffused in the population, thanks to an effect known in economics as positive externalities [54].

In Section 4.1, we present the mathematical model within the general framework introduced in this dissertation. Then, we analyze its asymptotic behavior, in order to understand how the topology of the network of interactions and the model parameters influence the outcome of the diffusion of the asset. First, we study the model in two mean field topologies. Specifically, in Section 4.2, we consider a community connected through a complete graph, whereas in Section 4.3 the case of two isolated (mean field) communities is considered. This second analysis allows us to discuss the effect of the positive externalities, even in absence of direct connections between the two communities. Then, in Section 4.4 we extend our analysis to a general network of interaction, studying the effect of the topology of the graph in the asymptotic behavior of the system. The chapter is concluded by Section 4.5, where our theoretical results are applied to some specific topologies (such as Erdős-Rényi random graphs, configuration models, and other network structures) corroborated by Monte Carlo simulations. Part of the work described in this chapter has been previously published in [55, 56].

4.1 Model

In the literature, the spread of innovations and of new behaviors is often modeled and studied under a network game scenario [19, 20, 23, 24]. In this setting each agent tends to maximize its own payoff by coordinating its choice with that of its neighbors. This hypothesis seems to be realistic when dealing with what we might call "big choices", such as the terms of economic contracts [20] or the choice of an operating system [19]. In such cases, a wrong decision can be very costly for the one who took it, therefore it is reasonable that an individual contacts many of his or her friends/colleagues (i.e. the neighbors) before taking the "big choice". In this work we instead focus on those we might call "light choices", (e.g. downloading an application for smartphone or joining an online community/social network). In such cases, negative consequences of the choice are usually mild, hence we can assume that individuals take their own choices after a pairwise interaction with one of their neighbors (a recent survey [57] supports our hypothesis highlighting the centrality of the world-of-mouth in the spread of assets), instead of involving their whole neighborhood in the choice.

The original feature of this model, with respect to classical epidemic models as the SIS model analyzed in Chapter 3, lays in the fact that the strength of the gossip persuasion depends on the global diffusion already reached by the new technological item in the population. Instead of a diffusion channel, the gossip mechanism plays here the role of a learning channel. It is the media through which agents gets aware of the existence of this new item, while its attraction for a potential new adopter in the end depends on the size of the diffusion of such an item not just among the neighbors, but in the whole population. This is a phenomenon known in economics as a "positive externalities" effect [58]. It should also be remarked that the model for diffusion of innovation (DoI) differs, substantially, from network dynamical model with neighborhood effects (typically cascade dynamics) where the driving force depends on the number of neighbors possessing the new feature. Notice that this does not mean that in our model the probability that an agent adopts the asset is not influenced by the numbers of neighbors having it, since the more the innovation is diffused in the neighborhood of an agent, the more it is likely that the agent gets aware of the existence of the asset. However, once the agent is informed of the existence of the new asset and considers whether to adopt it or not, then this decision is not influenced by the neighborhood, but by the global diffusion of the innovation.

The presence of the spontaneous dropping mechanism has various motivations. It may model a tendency to abandon technologies that have a maintenance cost or, also, a limitation of the time during which an agent can influence their neighbors. Mathematically, the case when only the persuasion mechanism is present is not particularly interesting as in this case the item, if originally present, will eventually diffuse to the whole population, independently of the strength of the mechanism and on the topology of the network. Our analysis, however, covers also, as a limit case, the situation when the dropping mechanism is not present.

We develop the DoI model within the general framework presented in Chapter 2. Similarly to an SIS model, the probabilities m_{01} and p_{10} are set equal to 0. Then, without any loss in generality, we set $\lambda = m_{10} = 1$. Edges activate at rate $W_{ij} = \beta \bar{d}^{-1}$, where $\bar{d}$ is the average degree of the graph, $\forall (i,j) \in E$. When edge (i,j) activates, agent i has the possibility to revise its state from 0 to 1 if $X_j(t) = 1$. This happens with probability $p_{01} = \phi(Z(t))$, where $\phi : [0,1] \to [0,1]$ is a C^2 function, called *persuasion strength*, satisfying the following properties:

(A1) ϕ is nondecreasing: $\phi'(z) \geq 0, \forall z$;

(A2) ϕ is concave: $\phi''(z) \leq 0, \forall z$;

(A3) $\phi'(0) > \phi(0)$.

From this moment on, we refer to a ϕ satisfying properties (A1) to (A3) as to an *admissible persuasion strength*. Fig. 4.1 depicts the admissible state transitions.

Remark 4.1. *We briefly motivate these properties. Property (A1) is a natural consequence of the "positive externalities effect" [58] cited before: the more the new item is diffused, the higher is its persuasion strength. Regarding property (A2), a sub-linear growth of the persuasion strength with respect to the diffusion of the new item can be inferred from real world observations: trivially, an increase of a single new agent adopting the item has a bigger impact when adopters are still few than when they are more numerous. Finally, (A3) is assumed for the sake of simplicity: the case $\phi'(0) < \phi(0)$, studied in [55], leads to a theory with essentially no novelties with respect to the SIS model, whose long-run behavior is analyzed in Section 3.2.*

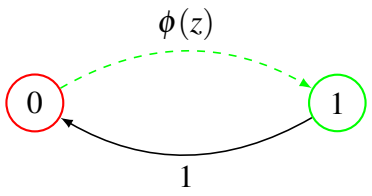

Fig. 4.1 State transitions characterizing the DoI model. Black solid lines are spontaneous mutation, colored dashed lines are transitions taking place after a pairwise interaction with a node with the other state.

The jump Markov process $X(t)$ has transition rates

$$\begin{cases} \lambda_i^+(\mathbf{x}) = \beta \bar{d}^{-1}(1-x_i) \sum\limits_{j \in \mathcal{N}_i} x_j \phi(z(\mathbf{x})) \\ \lambda_i^-(\mathbf{x}) = x_i. \end{cases} \tag{4.1}$$

Remark 4.2. *When ϕ is constant, this model reduces to the standard SIS model analyzed in Chapter 3 with $p_{01} = \phi$.*

The main feature and novelty of this model is the fact that, when the function ϕ is instead not constant, the gossip dynamics is affected by the global distribution of the state in the population of agents. In this model agents influence each other through two "information channels": the one determined by the graph edges and the another one due to the pressure of the global population state. These two channels are coupled through the persuasion mechanism described above.

Similar to the SIS dynamics, the pure configuration $0\mathbb{1}$ is the only absorbing state of $X(t)$ and from every configuration there is a non zero probability of reaching it in finite time. Consequently, $X(t)$ enters the absorbing state $0\mathbb{1}$ in a finite time with probability 1. Our aim is to study the behavior of the system in the transient phase, i.e. before the occurrence of the absorbing event.

In the SIS model, we witness the presence of two different regimes determined by a threshold value that is function of connectivity features of the graph. If the strength of the contagion mechanism with respect to the rate of regression is below this threshold, the epidemic quickly decades to the absorbing state. Whereas if it is above this threshold, the epidemic expands and remains persistent in the population for a time exponentially large in the size of the population. Further details can be found in Chapter 3 that is devoted to the analysis of the SIS model.

Here, we show that for many network topologies (comprising complete graphs, two complete isolated communities, expander graphs,...) a double bifurcation phenomenon occurs, with probability converging to 1 as $N \to \infty$. The first bifurcation takes place with respect to the parameter β. If β is smaller than a given threshold, the process $Z(t)$ enters forever into an ε-neighborhood of 0 in a time independent of the size of the graph. If β is larger than another threshold, $Z(t)$ reaches a level $z_s(\beta)$ in a time that does not depend on N and remains above that level for an exponentially (in N) long time. Furthermore, for intermediate values of the parameter β, we witness a further bifurcation with respect to the initial condition $Z(0)$, governed by a threshold $z_u(\beta)$ such that, if $Z(0) < z_u(\beta)$, we have the analogous fast extinction phenomenon that takes place for β small, whereas if $Z(0) > z_u(\beta)$, we have the analogous slow extinction phenomenon as for large values of β.

In plain words, in the DoI model, besides these two regimes, we witness in many cases the presence of a third intermediate regime where the behavior strictly depends on the initial condition, namely the original fraction of agents in state 1 in the population. In this third regime, if the initial fraction of 1's in the population is below a certain level, the item will not be able to spread. Whereas if it is sufficiently large, the persuasion mechanism will be able to push towards a wide and persistent diffusion. This is the main novelty of our model with respect to standard SIS, where the initial condition instead (as long as the fraction of infected agents is initially non zero) never influences qualitatively the behavior of the system.

Coherently with to our interpretation of the model, from now on the two behaviors described above, namely the fraction of 1's that quickly becomes smaller than ε, or instead that remains large for a long time are respectively called, a *failure* and a *success*. As already pointed out, the main novelty of the DoI model is the presence of the intermediate regime where failure and success depend on the initial condition.

Due to the specificities of the model, the transition rates of process $Z(t)$ depend only on the boundary $B_{01}(t)$ and not on $B_{10}(t)$. Hence, we can drop the indices and denote $\xi(t) := \xi_{01}(t)$. Hence, the fransition rates (2.21) read

$$\begin{cases} \lambda^+(z,\xi) = \beta \bar{d}^{-1} \xi \phi(z) \\ \lambda^-(z) = Nz. \end{cases} \tag{4.2}$$

Of course, the difficulty arises from the fact that the process $\xi(t)$ is not explicitly known. The next section is devoted to the analysis of the process when G is a

complete graph, which is essentially the only case in which $\xi(t)$ can be expressed as a deterministic function of $Z(t)$, so that $Z(t)$ is Markovian itself. The general case will be taken up in Section 4.4.

4.2 Mean Field I: Complete Graph

In this section we assume the graph to be complete, so $\xi(t) = N^2 Z(t)(1-Z(t))$, implying that $Z(t)$ is a Markov birth and death process and (4.2) reduces to

$$\begin{cases} \lambda^+(z) = N\beta z(1-z)\phi(z) \\ \lambda^-(z) = Nz. \end{cases} \tag{4.3}$$

Of course, in this case, the local gossip interaction and the global influence are somehow mixed together but some key interesting phenomena can already be observed here. For such processes a quite complete analysis is available and its results are gathered in the following Theorem.

Theorem 4.1. *Consider the birth and death jump Markov process $Z(t)$ whose transition rates are given in (4.3) where $\beta > 0$ and ϕ is an admissible persuasion strength (i.e. properties (A1), (A2), and (A3) are satisfied). Put*

$$\beta^* = \left[\max_{z\in[0,1]} (1-z)\phi(z) \right]^{-1}. \tag{4.4}$$

Then, for every $\varepsilon > 0$ we can find $C_\varepsilon(\beta) > 0$ and $T_\varepsilon > 0$ for which the following holds true, if N is sufficiently large,

1. *$\beta < \beta^*$, then $\forall z$,*
$$\mathbb{P}_z \left(\sup_{t \geq T_\varepsilon} Z(t) > \varepsilon \right) < e^{-C_\varepsilon N}; \tag{4.5}$$
2. *$\beta^* < \beta < \phi(0)^{-1}$, then $\forall z < z_u(\beta) - \varepsilon$,*
$$\mathbb{P}_z \left(\sup_{t \geq T_\varepsilon} Z(t) > \varepsilon \right) < e^{-C_\varepsilon N}, \tag{4.6}$$

and $\forall z > z_u(\beta) + \varepsilon$,

$$\mathbb{P}_z\left(\inf_{t\in[T_\varepsilon, T_\varepsilon + e^{C\varepsilon N}]} Z(t) < z_s(\beta) - \varepsilon\right) < e^{-C_\varepsilon N}; \tag{4.7}$$

3. $\beta > \phi(0)^{-1}$, *then* $\forall z > \varepsilon$,

$$\mathbb{P}_z\left(\inf_{t\in[T_\varepsilon, T_\varepsilon + e^{C\varepsilon N}]} Z(t) < z_s(\beta) - \varepsilon\right) < e^{-C_\varepsilon N}. \tag{4.8}$$

With the understanding that if $\phi(0) = 0$ *case 3. does not show up. Points* $z_s(\beta)$ *and* $z_u(\beta)$*, when they exist, can be characterized as follows*

$$\begin{aligned} z_u(\beta) &= \min\{z > 0 \,:\, \beta(1-z)\phi(z) - 1 = 0\}, \\ z_s(\beta) &= \min\{z > z_u(\beta) \,:\, \beta(1-z)\phi(z) - 1 = 0\}. \end{aligned} \tag{4.9}$$

The proof of this theorem is based on three steps: at first we consider the hydrodynamic limit, analyzing a deterministic approximation of the stochastic process [59]. Then, a couple of technical lemmas combined with the results of the analysis of the hydrodynamic limit allow to bound the probabilities that appear in Theorem 4.1. Finally, algebraic manipulations allow for guaranteeing the exponential decay of the probabilities, when N is sufficiently large.

4.2.1 Hydrodynamic Limit

At first, according to Theorem 2.1, we approximate $Z(t)$ with $\zeta(t)$, solution of the following Cauchy problem:

$$\begin{cases} \zeta'(t) = F(\zeta) = \beta\zeta(1-\zeta)\phi(\zeta) - \zeta \\ \zeta(0) = Z(0). \end{cases} \tag{4.10}$$

The analysis of (4.10) follows from the analysis of the zeros of $F(\zeta)$.

Lemma 4.1. *Let* β^* *from* (4.4)*,* $z_u(\beta)$ *and* $z_u(\beta)$ *from* (4.9)*. Then,*

1. $\beta < \beta^*$*, then* F *has one zero in* 0 *and* $F'(0) < 0$*;*

2. $\beta^* < \beta < \phi(0)^{-1}$, *then* F *has three zeros* $0 < z_u(\beta) < z_s(\beta)$ *and* $F'(0) < 0$, $F'(z_u(\beta)) > 0$, *and* $F'(z_s(\beta)) < 0$.

3. $\beta > \phi(0)^{-1}$, *then* F *has two zeros* $0 < z_s(\beta)$ *and* $F'(0) > 0$ *and* $F'(z_s(\beta)) < 0$.

With the understanding that if $\phi(0) = 0$ *case 3. does not show up.*

Proof. Let $F(\zeta) = f(\zeta)\zeta$, where $f(\zeta) = \beta(1-\zeta)\phi(\zeta) - 1$. It is straightforward to check that $f(\zeta)$ is a concave function, that $f(1) < 0$ and that $f'(1) < 0$. Moreover, since $f'(\zeta) = \beta(1-\zeta)\phi'(\zeta) - \beta\phi(\zeta)$, $\phi'(0) > \phi(0)$ implies $f'(0) > 0$. The function $f(\zeta)$ is thus concave, increasing in a neighborhood of 0 and decreasing in a neighborhood of 1, so it possesses a global maximum point $z_{\max} \in (0,1)$ and $f(z_{\max}) = \beta(\beta^*)^{-1} - 1$. In case 1., $f(z_{\max}) < 0$. In case 2., $f(0) < 0$ and $f(\zeta_{\max}) > 0$, hence $f(\zeta) = 0$ has two distinct solutions $z_u(\beta) < z_s(\beta)$. Finally, in case 3. $f(0) > 0$, implying a single solution of $f(0) = 0$, that is $z_s(\beta)$. Sign of derivatives in 0 can be checked directly, while other signs follow from the monotonicity properties of f. □

Then, the asymptotic behavior of (4.10) is an immediate consequence of previous result:

Lemma 4.2. *The following hold:*

1. *if* $\beta < \beta^*$, *then* $\zeta(t) \to 0\ \forall z_0$;

2. *if* $\beta^* < \beta < \phi(0)^{-1}$, *then* $\zeta(t) \to 0\ \forall \zeta_0 < z_u(\beta)$ *and* $z(t) \to z_s(\beta)\ \forall \zeta_0 > z_u(\beta)$;

3. *if* $\beta > \phi(0)^{-1}$, *then* $\zeta(t) \to z_s(\beta)\ \forall \zeta_0 \neq 0$.

With the understanding that if $\phi(0) = 0$ *case 3. does not show up.*

Corollary 4.1. *The following holds true:*

1. *if* $\beta < \beta^*$, *then* $\forall \varepsilon > 0\ \exists T(\varepsilon,\beta) > 0$ *and* $\exists C(\varepsilon,\beta) > 0$ *such that*

$$\mathbb{P}_z(Z(T) \geq \varepsilon/2) \leq 4\exp(-CN) \quad \forall z, \tag{4.11}$$

where $T(\varepsilon,\beta)$ *is bounded and* $C(\varepsilon,\beta)$ *does not annihilates for any* ε *bounded away from* 0 *and* β *bounded away from the upper limit of the case* ($\phi(0)^{-1}$ *or* β^*).

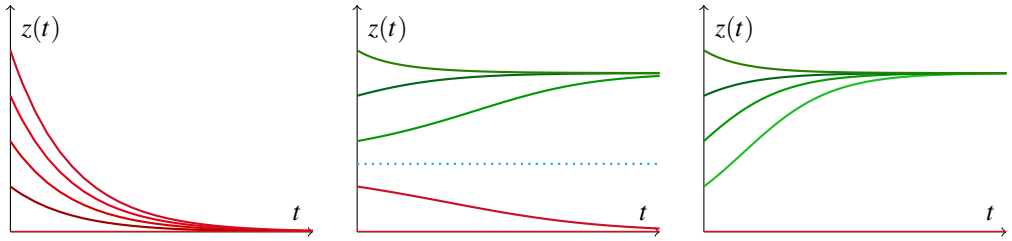

(a) Case 1. (b) Case 2. (c) Case 3.

Fig. 4.2 Simulations of (4.10) with different values of β and functions ϕ show the existence of the three regimes.

2. *if* $\beta^* < \beta < \phi(0)^{-1}$, *then* $\forall \varepsilon > 0\ \exists T(\varepsilon,\beta) > 0$ *and* $\exists C(\varepsilon,\beta) > 0$ *such that*

$$\mathbb{P}_z(Z(T) \geq \varepsilon/2) \leq 4\exp(-CN) \quad \forall z < z_u(\beta) - \varepsilon; \tag{4.12}$$

and

$$\mathbb{P}_z(Z(T) \leq z_s(\beta) - \varepsilon/2) \leq 4\exp(-CN) \quad \forall z > z_u(\beta) + \varepsilon, \tag{4.13}$$

where $T(\varepsilon,\beta)$ *is bounded and* $C(\varepsilon,\beta)$ *does not annihilates for any* ε *bounded away from* 0 *and* β *bounded away from* β^* *and* $\phi(0)^{-1}$.

3. *if* $\beta^* > \phi(0)^{-1}$, *then* $\forall \varepsilon > 0\ \exists T(\varepsilon,\beta) > 0$ *and* $\exists C(\varepsilon,\beta) > 0$ *such that*

$$\mathbb{P}_z(Z(T) \leq z_s(\beta) - \varepsilon/2) \leq 4\exp(-CN) \quad \forall z > \varepsilon, \tag{4.14}$$

where $T(\varepsilon,\beta)$ *is bounded and* $C(\varepsilon,\beta)$ *does not annihilates for any* ε *bounded away from* 0 *and* β *bounded away from* $\phi(0)^{-1}$. *With the understanding that if* $\phi(0) = 0$ *case 3. does not show up.*

Proof. In item 1. the equation $\zeta(t)$ converge to the equilibrium 0, from Lemma 4.2. It follows that $\forall \varepsilon > 0\ \exists T(\varepsilon,\beta) > 0$ for which $\zeta(T) < \varepsilon/4$ for any initial condition. We notice that $T(\varepsilon,\beta)$ is bounded when ε is bounded away from 0 and when β is bounded away from β^*. The proof is completed combining this result with the bound on $\mathbb{P}(|Z(T) - \zeta(T)| > \varepsilon/4)$ from Theorem 2.1. Properties of $C(\varepsilon,\beta)$ comes from those of $T(\varepsilon,\beta)$. The other two items are obtained using a similar argument. □

4.2.2 Markov Process

In this second step, we prove a slightly different formulation of Theorem 4.1, which can be state for any value of N (instead of N sufficiently large) at the cost of losing the exponential decay. Finally, at the end of this section, we will derive our original formulation using some algebraic manipulations.

Theorem 4.2. *Consider the birth and death jump Markov process $Z(t)$ whose transition rates are given in (4.3) where $\beta > 0$ and ϕ is an admissible persuasion strength (i.e. properties (A1), (A2), and (A3) are satisfied). For every $\varepsilon > 0$ we can find $C_\varepsilon > 0$ and $T_\varepsilon > 0$, both depending on β, for which the following holds true*

1. *if $\beta < \beta^*$, then $\forall z$,*

$$\mathbb{P}_z\left(\sup_{t\geq T_\varepsilon} Z(t) > \varepsilon\right) < 5Ne^{-C_\varepsilon N}; \tag{4.15}$$

2. *if $\beta^* < \beta < \phi(0)^{-1}$, then $\forall z < z_u(\beta) - \varepsilon$,*

$$\mathbb{P}_z\left(\sup_{t\geq T_\varepsilon} Z(t) > \varepsilon\right) < 5Ne^{-C_\varepsilon N}, \tag{4.16}$$

   and $\forall z > z_u(\beta) + \varepsilon$,

$$\mathbb{P}_z\left(\inf_{t\in[T_\varepsilon, T_\varepsilon + e^{C_\varepsilon N}]} Z(t) < z_s(\beta) - \varepsilon\right) < 14(1+\beta)^2 N^2 e^{-C_\varepsilon N}; \tag{4.17}$$

3. *if $\beta > \phi(0)^{-1}$, then $\forall z > \varepsilon$,*

$$\mathbb{P}_z\left(\inf_{t\in[T_\varepsilon, T_\varepsilon + e^{C_\varepsilon N}]} Z(t) < z_s(\beta) - \varepsilon\right) < 14(1+\beta)^2 N^2 e^{-C_\varepsilon N}. \tag{4.18}$$

The constant $T(\varepsilon,\beta)$ is bounded for any ε bounded away from 0 and β bounded and bounded away from β^* and $\phi(0)^{-1}$, whereas $C(\varepsilon,\beta)$ is bounded away from 0 in the same cases. If $\phi(0) = 0$ case 3. does not show up.

Proof. As a general remark notice that the sign of the right-hand side of (4.10) is positive (negative) if and only if $\lambda^+(z)/\lambda^-(z)$ is, respectively, above (below) 1.

In case 1. we estimate as follows:

$$\mathbb{P}_z\left(\sup_{t\geq T_\varepsilon} Z(t) > \varepsilon\right) \leq \mathbb{P}_z\left(\sup_{t\geq T_\varepsilon} Z(t) > \varepsilon \mid Z(T_\varepsilon) < \frac{\varepsilon}{2}\right) + \mathbb{P}_z\left(Z(T_\varepsilon) \geq \frac{\varepsilon}{2}\right), \quad (4.19)$$

where T_ε is defined, according to Corollary 4.1, as $z(T_\varepsilon) = \varepsilon/4$, where $z(t)$ is the solution of (4.10) with $z(0) = 1$. Conclusion now follows by estimating the first term using Lemma A.2, where the parameter δ in the inequality $\lambda^-(z) \geq (1+\delta)\lambda^-(z)$ is exactly

$$\delta = \left[\beta \max_{z\leq\varepsilon}(1-z)\phi(z)\right]^{-1} - 1, \quad (4.20)$$

and clearly depends on both β and ε, therefore the constant $C = \ln(1+\delta)$ that comes from Lemma A.2 depends itself on β and ε, so we denote it as $C_{\varepsilon,\beta}$, and it is bounded away from 0 when β is bounded away from the upper limit of the case ($\phi(0)^{-1}$ or β^*). The second term is bounded using item 1 from Corollary 4.1, where the constant is denoted as $C'_{\varepsilon,\beta}$. Therefore we conclude

$$\begin{aligned} \mathbb{P}_z\left(\sup_{t\geq T_\varepsilon} Z(t) > \varepsilon\right) &\leq \frac{\varepsilon}{4} N \exp\{-C_{\varepsilon,\beta}\varepsilon N\} + 4\exp\{-C'_{\varepsilon,\beta} N\} \\ &\leq 5N\exp\{-\min\{C_{\beta,\varepsilon}\varepsilon, C'_{\varepsilon,\beta}\}N\} \\ &\leq 5N\exp\{-C(\varepsilon,\beta)N\}, \end{aligned} \quad (4.21)$$

where $C(\varepsilon,\beta)$ is bounded away from zero for ε bounded away from zero and β bounded away from the upper limit of the case.

In case 3. we estimate as follows:

$$\begin{aligned} \mathbb{P}_z\left(\inf_{t\geq T_\varepsilon} Z(t) < z_s - \varepsilon\right) \leq \mathbb{P}_z\left(Z(T_\varepsilon) \leq z_s - \frac{\varepsilon'}{2}\right) + \\ + \mathbb{P}_z\left(\inf_{t\geq T_\varepsilon} Z(t) < z_s - \varepsilon' \mid Z(T_\varepsilon) > z_s - \frac{\varepsilon'}{2}\right). \end{aligned} \quad (4.22)$$

where $\varepsilon' = \min\{\varepsilon, z_u(\beta)\}$. T_ε is defined, according to Corollary 4.1, as $|z(T_\varepsilon) - z_s(\beta)| = \varepsilon/4$, where $z(t)$ is the solution of (4.10) with $z(0) = \varepsilon$. Conclusion now follows by estimating the first term using using item 2 from Corollary 4.1, naming the constant $C'_{\varepsilon,\beta}$, and the second term using Lemma A.1, where the parameter δ in

the inequality $\lambda^-(z) \geq (1+\delta)\lambda^-(z)$ depends again on β and ε, being

$$\delta = \beta \cdot \min_{z \leq z_s(\beta)-\varepsilon'/8} (1-z)\phi(z) - 1, \tag{4.23}$$

Therefore the constant C depends itself on the two parameters and the exponent is now linear in ε' (that may depend on β itself). We collect all these terms in the constant denoted by $C_{\varepsilon,\beta}$ and we notice that this constant is bounded away from 0 if ε is bounded away from 0 and β from $\phi(0)^{-1}$. Finally, the energy of the Poisson process $\mu \leq (1+\beta)N$, therefore we conclude

$$\begin{aligned} \mathbb{P}_z\left(\inf_{t \geq T_\varepsilon} Z(t) < z_s - \varepsilon\right) &\leq 10(1+\beta)^2 N^2 \exp\{-C_{\varepsilon,\beta}N\} + 4\exp\{-C'_{\varepsilon,\beta}N\} \\ &\leq 14(1+\beta)^2 N^2 \exp\{-\min\{C_{\varepsilon,\beta}, C'_{\varepsilon,\beta}\}N\} \\ &\leq 14(1+\beta)^2 N^2 \exp\{-C(\varepsilon,\beta)N\}, \end{aligned} \tag{4.24}$$

where $C(\varepsilon,\beta)$ is bounded away from 0 for ε bounded away from zero and β bounded away from $\phi(0)^{-1}$.

Finally, case 2. follows by similar arguments in dependence of the initial condition of the process using item 3 from Corollary 4.1 and, in one case Lemma A.2, in the other one Lemma A.1. □

Theorem 4.2 is not sufficient to prove the existence of the three different regimes. In fact, depending on the parameters and on N, the bounds on the probability in the right-hand-sides of the inequalities may be not informative. For this reason, and in order to give a nicer presentation of our results, we can manipulate these (quasi) exponential terms, obtaining an exponential decay when N is sufficiently large. Here we consider, as an example, the case 1., where the right-hand-side can be bounded by a purely exponential function as follows:

$$5N\exp\{-C(\varepsilon,\beta)N\} = \exp\{-C(\varepsilon,\beta)N + \ln(5N)\} \leq \exp\left\{-\frac{C(\varepsilon,\beta)}{2}N\right\}, \tag{4.25}$$

when $N \geq \tilde{N}_\varepsilon(\beta)$, where $N_\varepsilon(\beta)$ is the only solution of $C(\varepsilon,\beta)N = 2\ln(5N)$.

Using a similar argument on 2. and 3., the exponential decay is obtained on all the right-hand-sides when N is greater that all the different values of $\tilde{N}_\varepsilon(\beta)$, proving Theorem 4.1.

4.3 Mean Field II: Two Disconnected Graphs

Here, we present the analysis of the DoI model on a graph made of two complete sub-graphs (with self-loops) with respectively N_1 and $N_2 = N - N_1$ agents, without any edge between them. This is one of the simplest example (and it is indeed analytically tractable) where the local gossip interaction and the global influence depend on different parameters. In fact, for an agent of the i-th sub-graph, the first effect depends on the fraction of 1's in the i-th community $Z_i(t)$, while the second one is a function of the global fraction of 1's in the whole graph, denoted by $\bar{Z}(t)$. The goal of this analysis is to show the effect of positive externalities, in interconnecting the dynamics into the two different communities, comparing with the case of the SIS model, where two isolated communities evolve totally independently one of the other.

In this work, we will limit our study to the hydrodynamic limit of the model. The increased dimensionality of the system of ODEs poses some more issues in the analysis. Without loss of generality we can consider the first sub-graph to be the biggest one, i.e. $N_1 \geq N_2$. In order to observe the spread of the asset in the two sub-graphs we introduce the bi-dimensional process $Z(t) = (Z_1(t), Z_2(t))$, where $Z_i(t) = Z_i(X(t))$ is a process taking values in S_{N_i} denoting the fraction of 1's in the i-th sub-graph. Clearly, we have that the total fraction of 1's can be obtained as

$$\bar{Z}(t) = \frac{N_1 Z_1(t) + N_2 Z_2(t)}{N}. \tag{4.26}$$

At first we notice that the process $Z(t)$ is a bi-dimensional Markov jump process and its transition rates, from (z_1, z_2) to, respectively, $(z_1 \pm N_1^{-1}, z_2)$ and $(z_1, z_2 \pm N_2^{-1})$ are the following:

$$\begin{cases} \lambda_1^+(z_1, z_2) &= N_1 \beta z_1 (1 - z_1) \phi(\bar{z}) \\ \lambda_1^-(z_1, z_2) &= N_1 z_1 \\ \lambda_2^+(z_1, z_2) &= N_2 \beta z_2 (1 - z_2) \phi(\bar{z}) \\ \lambda_2^-(z_1, z_2) &= N_2 z_2, \end{cases} \tag{4.27}$$

where $\bar{z}$ denotes the global fraction of 1's.

In order to take the hydrodynamic limit, we suppose that N_1 is such that $N_1/N \to \eta$, as $N \to \infty$, for some $\eta \in [1/2, 1)$. Consequently, also $N_2/N \to 1 - \eta$.

Theorem 2.2 guarantee that, for finite time ranges, the stochastic process is exponentially close to the solution $\zeta(t) = (\zeta_1(t), \zeta_2(t))$ of the following system of ODEs:

$$\begin{cases} \dot{\zeta}_1 = \beta\zeta_1(1-\zeta_1)\phi(\bar{\zeta}) - \zeta_1 \\ \dot{\zeta}_2 = \beta\zeta_2(1-\zeta_2)\phi(\bar{\zeta}) - \zeta_2, \end{cases} \tag{4.28}$$

where $\bar{\zeta} = \eta\zeta_1 + (1-\eta)\zeta_2$.

Notice first that the diagonal $\zeta_1 = \zeta_2$ as well the two axis $\zeta_1 = 0$ and $\zeta_2 = 0$ are invariant lines for the dynamics.

To complete the theoretical analysis of the system, put

$$F(\zeta_1, \zeta_2) = (F_1(\zeta_1, \zeta_2), F_2(\zeta_1, \zeta_2)), \tag{4.29}$$

to be the right-hand side of (4.28) and notice that

$$\begin{aligned} \frac{\partial F_1}{\partial \zeta_2} &= (1-\eta)\beta\zeta_1(1-\zeta_1)\phi'(\bar{\zeta}) \geq 0; \\ \frac{\partial F_2}{\partial \zeta_1} &= \eta\beta\zeta_2(1-\zeta_2)\phi'(\bar{\zeta}) \geq 0. \end{aligned} \tag{4.30}$$

This implies that the system is monotone [50], which means that for any couple of initial conditions $x_0 \geq y_0$ (component-wise), then the same ordering holds for the solutions, namely $x(t) \geq y(t)$, $\forall t > 0$. Monotonicity provides many important properties to the system. In particular limits cycles are excluded. Hence, compactness of the domain insures all solutions to converge to critical points of the system, namely to solutions of the equation $F(\zeta_1, \zeta_2) = 0$. The following result gives a complete characterization of critical points. A further consequence of (4.30) is that Jacobian eigenvalues are always real so that critical points are either nodes (stable or unstable) or saddle points.

Proposition 4.1. *Assume $\phi(\bar{\zeta})$ is an admissible persuasion strength. Let β^* from* (4.4) *and put*

$$\begin{aligned} \beta_1^* &= \left[\max_\zeta (1-\zeta)\phi(\eta\zeta)\right]^{-1}; \\ \beta_2^* &= \left[\max_\zeta (1-\zeta)\phi((1-\eta)\zeta)\right]^{-1}. \end{aligned} \tag{4.31}$$

Then, the following critical points show off in (4.28):

1. *if $\beta < \beta^*$, the origin is the only critical point and it is a stable node;*

2a. *if* $\beta^* < \beta < \beta_1^*$*, two more critical points are added,* $(z_u(\beta), z_u(\beta))$*, which is a saddle and* $(z_s(\beta), z_s(\beta))$*, which is a stable node;*

2b. *if* $\beta_1^* < \beta < \beta_2^*$*, two more critical points are added,* $(z_{u1}(\beta), 0)$*, which is an unstable node and* $(z_{s1}(\beta), 0)$*, which is a saddle;*

2c. *if* $\beta_2^* < \beta < \phi^{-1}(0)$*, two more critical points are added,* $(0, z_{u2}(\beta))$*, which is an unstable node and* $(0, z_{s2}(\beta))$*, which is a saddle;*

3. *if* $\beta > \phi^{-1}(0)$*, the origin becomes unstable and critical points* $(z_{u1}(\beta), 0)$*,* $(0, z_{u2}(\beta))$ *and* $(z_u(\beta), z_u(\beta))$ *disappear.*

Proof. Critical points on the diagonal (ζ, ζ) are simply the critical points in the one-dimensional case (see Section 4.2), which are $(0,0)$, and, depending on β, two more $(z_u(\beta), z_u(\beta))$ and $(z_s(\beta), z_s(\beta))$.

Notice now that any critical points (ζ_1, ζ_2) for which $\zeta_1 \neq \zeta_2$ must be such that $\zeta_1 = 0$ or $\zeta_2 = 0$. Indeed, if $\zeta_1 \neq 0$ and $\zeta_2 \neq 0$, by dividing the two equations $F_i(\zeta_1, \zeta_2)$ by ζ_i and taking the difference, we immediately obtain that $\zeta_1 = \zeta_2$. Clearly, $(\zeta_1, 0)$ is a critical point if and only if

$$\beta \zeta_1 (1 - \zeta_1) \phi(\eta \zeta_1) - \zeta_1 = 0, \tag{4.32}$$

leading to one or two more critical points $(z_{s1}(\beta), 0)$ and $(z_{u1}(\beta), 0)$ depending if $\beta > \beta_1^*$ or if $\beta_1^* < \beta < \phi(0)^{-1}$ with $z_{u1}(\beta) < z_{s1}(\beta)$. Similarly, for $\zeta_2 = 0$, we finally obtain one or two more critical points $(0, z_{s2}(\beta))$ and $(0, z_{u2}(\beta))$ if $\beta > \beta_2^*$ or if $\beta_2^* < \beta < \phi(0)^{-1}$ with $z_{u2}(\beta) < z_{s2}(\beta)$. Considering that $\beta_2^* \geq \beta_1^*$ and assembling all these information we obtain the existence results of the various critical points. It remains to be analyzed their stability.

Notice first of all that

$$F'(0,0) = \begin{pmatrix} \beta\phi(0) - 1 & 0 \\ 0 & \beta\phi(0) - 1 \end{pmatrix}, \tag{4.33}$$

so that $(0,0)$ is a stable node if $\beta < \phi^{-1}(0)$ and unstable otherwise.

In order to analyze the stability of the other two points on the diagonal notice first of all that along the diagonal $(z_s(\beta), z_s(\beta))$ is always stable and $(z_u(\beta), z_u(\beta))$ always unstable. It remains to be studied the stability of the other eigendirection of

the Jacobian. To this aim put $\delta = \zeta_1 - \zeta_2$ and consider

$$\dot{\delta} = F_1(\zeta_1, \zeta_2) - F_2(\zeta_1, \zeta_2) = \delta[\beta\phi(\bar{\zeta})(1 - \zeta_1 - \zeta_2) - 1]. \tag{4.34}$$

Notice that at any critical point (ζ_1, ζ_2) with $\zeta_1 = \zeta_2 = \zeta > 0$, it holds

$$\beta\phi(\bar{\zeta})(1 - \zeta_1 - \zeta_2) - 1 = \beta\phi(\zeta)(1 - 2\zeta) - 1 < \beta(1 - \zeta)\phi(\zeta) - 1 = 0. \tag{4.35}$$

This says that in a neighborhood of such a point $\delta = \zeta_1 - \zeta_2$ is always monotonically decreasing, and clearly implies that the eigenvalue corresponding to the non diagonal eigendirection must necessarily be negative (indeed, if positive, moving along that direction there would be a local increase in δ). Therefore, when present, $(z_s(\beta), z_s(\beta))$ is a stable node while $(z_u(\beta), z_u(\beta))$ a saddle point.

Finally, regarding the critical point on the boundaries, notice that, for symmetry arguments, we can restrict our analysis to $(z_{u1}(\beta), 0)$ and $(z_{s1}(\beta), 0)$. Along the invariant axis $\zeta_2 = 0$, usual one-dimensional considerations imply that, when present, $(z_{s1}(\beta), 0)$ is always stable while $(z_{u1}(\beta), 0)$ is always unstable. To study the stability of the other Jacobian eigendirection, remember that the points considered show up only when $\beta > \beta_1^*$ and notice that

$$\begin{aligned} F_2(\zeta_1, \zeta_2) &= \zeta_2[\beta(1 - \zeta_2)\phi(\bar{\zeta}) - 1] \\ &\geq \zeta_2[(1 - \zeta_2)\beta(1 - \zeta_1)\phi(\eta\zeta_1) - 1] \\ &\geq \zeta_2[(1 - \zeta_2)\beta(\beta_1^*)^{-1} - 1]. \end{aligned} \tag{4.36}$$

Therefore, for ζ_2 sufficiently small, $F_2(\zeta_1, \zeta_2) > 0$. This implies that the other eigendirection is always unstable. Therefore, $(z_{s1}(\beta), 0)$ is always a saddle point while $(z_{u1}(\beta), 0)$ is always an unstable node. This completes the proof. □

Critical points of (4.28), their characterization and their stability can therefore be summarized in Table 4.1.

The asymptotic behavior of this model is thus quite similar to the one-dimensional case. In fact, for almost all initial conditions (i.e those which are not critical points or on stable manifolds of saddle points), it holds

1. if $\beta < \beta^*$, then $\zeta(t) \to 0$;

2. if $\beta^* < \beta < \phi^{-1}(0)$, then $\zeta(t) \to 0$ or $\zeta(t) \to (z_s(\beta), z_s(\beta))$, depending on the initial condition;

3. if $\beta > \phi^{-1}(0)$, then $\zeta(t) \to (z_s(\beta), z_s(\beta))$.

Table 4.1 Critical points of (4.28)

Coordinates	Characterization	Existence	Stability
$(0,0)$	Node	$\forall \beta$	$\beta < \phi^{-1}(0)$
$(z_u(\beta), z_u(\beta))$	Saddle	$\beta \in (\beta^*, \phi^{-1}(0))$	Unstable
$(z_s(\beta), z_s(\beta))$	Node	$\beta > \beta^*$	$\forall \beta > \beta^*$
$(z_{u1}(\beta), 0)$	Node	$\beta \in (\beta_1^*, \phi^{-1}(0))$	Unstable
$(z_{s1}(\beta), 0)$	Saddle	$\beta > \beta_1^*$	Unstable
$(0, z_{u2}(\beta))$	Node	$\beta \in (\beta_2^*, \phi^{-1}(0))$	Unstable
$(0, z_{s2}(\beta))$	Saddle	$\beta > \beta_2^*$	Unstable

In the intermediate regime $\beta^* < \beta < \phi^{-1}(0)$, where two stable nodes show up, the study of the dependence on the initial condition is more involved than in the one-dimensional case. Denote by D_0 and D_{z_s} the two basin of attractions of, respectively, $(0,0)$ and $(z_s(\beta), z_s(\beta))$. The stable manifold corresponding to the saddle point $(z_u(\beta), z_u(\beta))$ separates the two basins. Because of the monotonicity properties of the system, such manifold admits a parameterization of the form $(\zeta_1, \sigma(\zeta_1))$ with $\zeta_1 \in [a,b]$ and where

$$\begin{aligned} a &= \inf\{\zeta_1 : (\zeta_1, \zeta_2) \in D_{z_s}\}; \\ b &= \sup\{\zeta_1 : (\zeta_1, \zeta_2) \in D_0\}; \\ \sigma(\zeta_1) &= \inf\{\zeta_2 : (\zeta_1, \zeta_2) \in D_{z_s}\} = \sup\{\zeta_2 : (\zeta_1, \zeta_2) \in D_0\}. \end{aligned} \tag{4.37}$$

Another immediate consequence of the monotonicity of the system is that $\sigma = \sigma(\zeta_1)$ is a monotone decreasing function. Standard considerations which use continuous dependence on the initial conditions, the fact that trajectories can not intersect and the absence of limit cycles, lead to claim that the stable manifold parametrized by σ is a curve defined between two points on the boundary of the domain, namely $(a, \sigma(a))$ and $(b, \sigma(b))$. Moreover, for the same reasons, these two points, if on the invariant axis $\zeta_1 = 0$ or $\zeta_2 = 0$, must coincide with the corresponding unstable nodes $(z_{u1}(\beta), 0)$ and/or $(0, z_{u2}(\beta))$. In this case $a = 0$ and $b = z_{u1}(\beta)$. Otherwise the extremes are point of the form $(a, 1)$ and/or $(1, \sigma(1))$.

The various possible cases are summarized in the following Corollary.

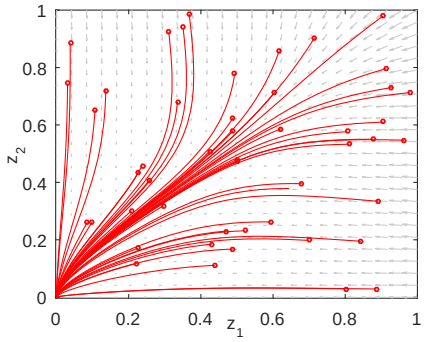

(a) Regime 1. ($\beta = 3$).

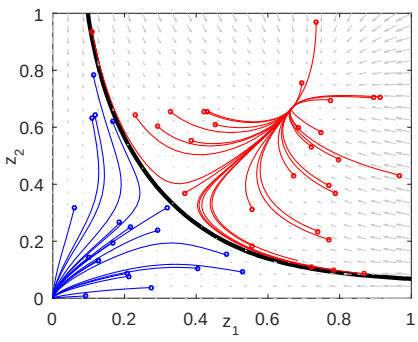

(b) Regime 2a. ($\beta = 4.5$).

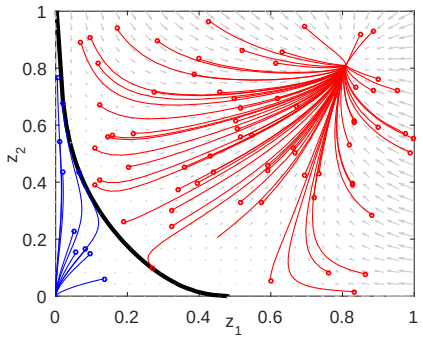

(c) Regime 2b. ($\beta = 6.5$).

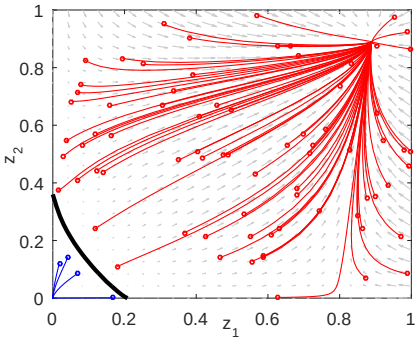

(d) Regime 2c. ($\beta = 11$).

Fig. 4.3 Simulations of (4.28) with $\eta = 0.6$ and $\phi(z) = z$ show the different regimes of Proposition 4.1 and Corollary 4.2. The black line is a numerical approximation of σ.

Corollary 4.2. *Under the assumptions of Proposition 4.1,*

a. if $\beta^* < \beta < \beta_1$, *then* $a > 0$, $b = 1$, $\sigma(a) = 1$, $\sigma(1) > 0$;

b. if $\beta_1^* < \beta < \beta_2^*$, $a > 0$, $b = z_{u1}(\beta)$, $\sigma(a) = 1$, $\sigma(b) = 0$;

c. if $\beta_2^* < \beta < \phi^{-1}(0)$, *then* $a = 0$, $b = z_{u1}(\beta)$, $\sigma(a) = z_{u2}(\beta)$, $\sigma(b) = 0$.

The key qualitative difference among the three regimes is the following: in case (a) even if we start from an initial condition where the asset is present in all members of one of the two communities, the dynamics will converge to 0 unless the asset has a sufficient spread also in the other community. In case (b) instead, for any non zero initial spread of the asset in the smaller community, a sufficiently high spread of the asset in the largest community is sufficient to guarantee convergence to the non zero equilibrium. In case (c), finally, also the smaller community acquires this

leading capability. Figure 4.3 shows the various possible behaviors when $\phi(0) = 0$, highlighting the separatrix σ.

4.4 Analysis on General Graphs

Finally, we partially extend Theorem 4.1, proving the existence of the three regimes (in particular of the intermediate one), for a large family of expander graphs.

For the epidemic SIS model, an estimation of the mean absorbing time has been carried on general graphs [11, 10, 60]. Notably, fast extinction results have been obtained [10] by upper bounding the original process with another one whose transition rates depend linearly on the state variable $\mathbf{x}$ and for which, consequently, the moment analysis turns out to be particularly simple. The key graph parameter in this estimation is the spectral radius of the corresponding adjacency matrix. On the other hand, slow extinction has been analyzed by essentially estimating the active boundary in terms of bottleneck ratios of the graph and then lower bounding the process with a simple birth and death process.

However, the techniques developed in [10] can not be straightforwardly applied to the DoI model. Indeed, the presence of the persuasion strength ϕ poses a number of technical issues that are absent in the SIS model. This will be particularly evident in the analysis of the intermediate regime where success or failure depends on the initial condition.

In the next three subsections we determine a series of lower and upper bounds of process $Z(t)$ using standard coupling techniques, inspired by the results in [11, 10, 60]. Specifically, in 4.4.1 we propose a lower bound based on bottleneck estimation that allows to prove the existence of the success regimes - thereby extending the second part of item 2. and item 3. of Theorem 4.1. In 4.4.2 instead, we propose a quite simple upper bound sufficient to prove the existence of the failure regime - extending item 1. of Theorem 4.1. Finally, in 4.4.3 we develop a stronger upper bound using a linearization technique and a second moment analysis in order to prove the existence of the failure regime depending on the initial condition - extending the first part of item 2. of Theorem 4.1. This last case is the most original technical part of this chapter. Though inspired by [11, 10, 60], our technique is based on a detailed second order analysis of the bounding process, which is not needed in the analysis of

the SIS model. All these partial results are assembled in 4.4.4 where the main result is finally stated and proved. Specifically, our main result is formulated for general graphs as Theorem 4.2, then the standard formulation can be derived, similarly to the mean field cases, for many families of expander graphs.

Fixed a strongly connected graph $G = (V, E)$, its Cheeger constant [61] is defined as

$$\gamma = \gamma_G = \inf_{S \subset V} \frac{|\{(i, j) : i \in S,\, j \notin S\}|}{\min\{|S|, |V \setminus S|\}}. \tag{4.38}$$

We notice that there is a straight relation between Cheeger constant and isoperimetric constants (3.8), in fact, if G is undirected, then

$$\gamma = \min_{m \leq n/2} \eta(m). \tag{4.39}$$

We recall that $X(t)$ is a jump Markov process on the state-space $\{0,1\}^V$ having transition rates given by (4.1). $Z(t) = z(X(t))$ denotes the total fraction of 1's in the population and $\xi(t) = \xi(X(t))$ is the active boundary.

4.4.1 Bottleneck-Based Lower Bound

The following result, inspired by an argument used in [62], yields a lower bound of the process $Z(t)$ in terms of a birth and death jump Markov process.

Proposition 4.2. *There exists a coupling of the process $X(t)$ with a birth and death jump Markov process $\tilde{Z}(t)$ over $\mathcal{S}_N$ having transition rates*

$$\begin{cases} \tilde{\lambda}^+(z) = N\beta\bar{d}^{-1}\gamma z(1-z)\phi(z) \\ \tilde{\lambda}^-(z) = Nz, \end{cases} \tag{4.40}$$

in such a way that $Z(t) \geq \tilde{Z}(t)$ for all t.

Proof. From (4.38), choosing as S the set of all agents with state equal to 0, we obtain

$$\gamma \leq \frac{|\{(i, j) : X_i = 0, X_j = 1\}|}{\min\{z|V|, (1-z)|V|\}} \leq \frac{\xi}{z(1-z)|V|} = \frac{\xi}{z(1-z)|V|} = \frac{\xi}{z(1-z)N}. \tag{4.41}$$

This implies that the active boundary satisfies the inequality $\xi \geq \gamma N z(1-z)$. This yields, using (4.2),

$$\lambda^+(z,\xi) \geq \tilde{\lambda}^+(z) \qquad \text{and} \qquad \lambda^-(z,\xi) = \tilde{\lambda}^-(z). \tag{4.42}$$

The proof is now concluded by applying a simple coupling argument, similarly to the one used to prove Theorem 8.8 in [11]. □

The following Corollary proves the existence of the two success regimes, extending the second part of item 2. and item 3. of Theorem 4.1 to general graphs.

Corollary 4.3. *Let $Z(t)$ follow* (4.2) *and let ϕ be an admissible persuasion strength. Put $z_u = z_u(\beta \bar{d}^{-1}\gamma)$ and $z_s = z_s(\beta \bar{d}^{-1}\gamma)$ as defined in (4.9). For every $\varepsilon > 0$ we can find $C_\varepsilon > 0$ and $T_\varepsilon > 0$ for which the following hold true*

1. *if $\bar{d}\gamma^{-1}\beta^* < \beta$, then, $\forall z > z_u + \varepsilon$,*

$$\mathbb{P}_z\left(\inf_{t\in[T_\varepsilon, T_\varepsilon + e^{C\varepsilon N}]} Z(t) < z_s - \varepsilon\right) \leq AN^2 e^{-C\varepsilon N}; \tag{4.43}$$

2. *if, moreover, $\bar{d}\gamma^{-1}\phi(0)^{-1} < \beta$, then, $\forall z > \varepsilon$,*

$$\mathbb{P}_z\left(\inf_{t\in[T_\varepsilon, T_\varepsilon + e^{C\varepsilon N}]} Z(t) < z_s - \varepsilon\right) \leq AN^2 e^{-C\varepsilon N}, \tag{4.44}$$

where $A = 14(1+\beta)^2$. The constants C_ε and T_ε only depend on the quantity $\bar{d}^{-1}\gamma\beta$ and are, respectively, bounded away from 0 and bounded, when this quantity is bounded away from β^* and $\phi(0)^{-1}$.

Proof. Using Proposition 4.2, process $Z(t)$ can be lower bounded by a birth and death jump Markov process $\tilde{Z}(t)$ having transition rates (4.40). Hence $\mathbb{P}_z[Z(t) < \bar{z}] \leq \mathbb{P}_z[\tilde{Z}(t) < \bar{z}]$, $\forall z, \bar{z}$. A comparison with (4.3) shows that the transition rates of $\tilde{Z}(t)$ coincide with the ones of the mean field model (4.3) with β replaced by $\beta \bar{d}^{-1}\gamma$. Results then follow from items 2. and 3. of Theorem 4.1. □

4.4.2 Degree-Based Upper Bound

In this subsection we provide a simple upper bound that depends only on the degrees of the nodes in the graph. Let Δ_{in} be the maximum in-degree in G, then the following proposition holds.

Proposition 4.3. *There exists a coupling of the process $X(t)$ with a birth and death jump Markov process $\tilde{Z}(t)$ over $\mathcal{S}_N$ having transition rates*

$$\begin{cases} \tilde{\lambda}^+(z) = N\Delta_{in}\bar{d}^{-1}\beta z\phi(z) \\ \tilde{\lambda}^-(z) = Nz, \end{cases} \tag{4.45}$$

in such a way that $Z(t) \leq \tilde{Z}(t)$ for all t.

Proof. This follows from $\xi = |\{(i,j) : X_i = 0, X_j = 1\}| \leq \Delta_{in} N z$. □

The following Corollary proves the existence of the failure regime, extending item 1. of Theorem 4.1 to general graphs.

Corollary 4.4. *Let $Z(t)$ follow* (4.2) *and let ϕ be an admissible persuasion strength. If $\beta < \bar{d}\Delta_{in}^{-1}\phi(1)^{-1}$, then, for every $\varepsilon > 0$ we can find $C_\varepsilon > 0$ and $T_\varepsilon > 0$ for which*

$$\mathbb{P}_z\left(\sup_{t \geq T_\varepsilon} Z(t) > \varepsilon\right) \leq 5Ne^{-C_\varepsilon N}, \quad \forall z. \tag{4.46}$$

For every $\varepsilon > 0$, the constants C_ε and T_ε only depend on the quantity $\beta\bar{d}^{-1}\Delta_{in}$ and are, respectively, bounded away from 0 and bounded, when this quantity is bounded away from $\phi(1)^{-1}$.

Proof. From Proposition 4.3, process $Z(t)$ can be upper bounded by a birth and death jump Markov process $\tilde{Z}(t)$ having transition rates (4.45). Hence $\mathbb{P}_z[Z(t) > \bar{z}] \leq \mathbb{P}_z[\tilde{Z}(t) > \bar{z}]$, $\forall z, \bar{z}$. We now apply (2.30) to the process $\tilde{Z}(t)$. The assumption $\beta < \bar{d}\Delta_{in}^{-1}\phi(1)^{-1}$ implies that 0 is asymptotically stable in (4.10). More precisely, the solution $\zeta(t)$ of (4.10) with $\zeta(0) = 1$ converges to 0 when $t \to +\infty$ and this clearly implies that, for every fixed $\varepsilon > 0$, there exists $T_\varepsilon > 0$ such that $\zeta(t) < \varepsilon/2$ for every $t \geq T_\varepsilon$ and for every initial condition $z(0) = \zeta$. Moreover, T_ε only depends monotonically on the quantity $\bar{d}^{-1}\beta$ and blows up when this quantity approaches

$\phi(1)^{-1}$. Using (2.30) with $T = T_\varepsilon$ we thus obtain that there exists $C'_\varepsilon > 0$ such that

$$\mathbb{P}_z\left(\tilde{Z}(T_\varepsilon) > \varepsilon/2\right) \leq 4e^{-C'_\varepsilon N} \quad \forall z. \tag{4.47}$$

It follows from (2.30) and from the considerations above on T_ε that C'_ε only depends on $\bar{d}^{-1}\beta$ and it is bounded away from 0, when this quantity is bounded away from $\phi(1)^{-1}$. If we apply Lemma A.2 to $\tilde{Z}(t)$ with $1+\delta = \bar{d}\Delta_{in}^{-1}\beta^{-1}\phi(1)^{-1} > 1$, we obtain that, for every $z < \varepsilon/2$,

$$\mathbb{P}_z\left(\exists t \geq 0 : \tilde{Z}(t) > \varepsilon\right) \leq \frac{\varepsilon}{2} N e^{-[\ln(1+\delta)]\varepsilon/2N}. \tag{4.48}$$

From (4.47) and (4.48) we finally obtain that, $\forall z$

$$\mathbb{P}_z\left(\sup_{t\geq T_\varepsilon} Z(t) > \varepsilon\right) \leq \mathbb{P}_z\left(\sup_{t\geq T_\varepsilon} \tilde{Z}(t) > \varepsilon\right) \leq 5Ne^{-C_\varepsilon N},$$

where $C_\varepsilon = \min\{C'_\varepsilon, [\ln(\bar{d}\Delta_{in}^{-1}\beta^{-1}\phi(1)^{-1})]\varepsilon/2\}$. In consideration of the properties already discussed for the quantity C'_ε, the result is now proven. □

4.4.3 Linearization-Based Upper Bound

What remains to be shown is the existence, for general graphs, of the failure regime as described in the first part of item 2. of Theorem 4.1. This is fundamental in order to prove the existence of the bifurcation with respect to the initial condition. In this subsection we tackle this issue by upper bounding the process $Z(t)$ with another jump Markov process whose transition rates depend linearly on the configuration vector. In [10] a similar idea was used to analyze the SIS model. However, while in [10] it was sufficient to carry on a first moment analysis of the linearized process to prove the existence of the fast extinction regime, here a much more complex analysis is needed. In fact, differently from the SIS model, in our model the fraction of 1s influences the persuasion strength and, ultimately, the behavior of the system. In the study of the bifurcation in dependence on the initial condition, to make our bounding technique effective, we must make sure that the fraction of 1s always remains below a certain threshold. For this, a first moment analysis of the linearized process is no longer sufficient. It must be coupled with a concentration result based on a second moment analysis.

Consider the jump Markov process $Y(t)$ over $\Theta = \mathbb{N}^V$, with transition rates

$$\begin{cases} \bar{\lambda}_i^+ &= \mu \sum_{j \in \mathcal{N}_i} y_j \\ \bar{\lambda}_i^- &= y_i, \end{cases} \tag{4.49}$$

where $\mu = \beta \bar{d}^{-1} \phi(1)$.

Notice that the original process $Z(t)$, taking values in $\{0,1\}^V$, can be naturally extended to Θ by simply putting $\lambda_i^+ = 0$ if $y_i > 0$ and using the same expression for $\lambda_i^- = y_i$. In the case when $\beta < \bar{d}\rho_A^{-1}\phi(1)^{-1}$, it follows that $\bar{\lambda}_i^+ \geq \lambda_i^+$ for all $\mathbf{y}$ and for all $i \in V$. We now consider any coupling between $X(t)$ and $Y(t)$ such that $X(0) = Y(0)$ and $X(t) \leq Y(t)$ (entry-wise) for all t. Clearly, it holds $Z(t) \leq Z_Y(t) := z(Y(t))$ for all t.

For the sake of readability, we present this detailed analysis in Appendix B, and we report here our final result, that is Lemma 4.3 (whose proof is in Appendix B, along with the rest of the analysis of the linearized jump Markov process), where the asymptotic behavior of $Z_Y(t)$ is analyzed.

Lemma 4.3. *Let $Z_Y(t) = z(Y(t))$ with $Y(t)$ following* (4.49)*. Assume that $\mu\rho_A < 1$. For every $\varepsilon > 0$ there exists a time $T_\varepsilon > 0$ and a constant $K_\varepsilon > 0$ such that*

1. *if $Z_Y(0) \leq a^2$, it holds*

$$\mathbb{P}(\exists t \geq 0 : Z_Y(t) > a + \varepsilon) \leq K_\varepsilon N^{-1/2}; \tag{4.50}$$

2. *for every $Z_Y(0)$, it holds*

$$\mathbb{P}(\exists t \geq T_\varepsilon : Z_Y(t) > \varepsilon) \leq K_\varepsilon N^{-1/2}. \tag{4.51}$$

Moreover, for every $\varepsilon > 0$, the constants K_ε and T_ε only depend on the quantity $\mu\rho_A$ and are bounded when this quantity is bounded away from 1.

We are now ready to go back to our original process $Z(t)$. The following Corollary proves the existence of two failure regimes, one that does not depend on the initial condition and the second one that does depend on it, extending items 1. and the first part of item 2. of Theorem 4.1 to general graphs, respectively. Notice that a

different extension of item 1. was already obtained in Corollary 4.4. Later on we will comment on the relation between these two estimations.

Corollary 4.5. *Let $Z(t)$ follow* (4.2) *and let ϕ be an admissible persuasion strength. For every $\varepsilon > 0$, there exist $K_\varepsilon > 0$, $K'_\varepsilon > 0$, $T_\varepsilon > 0$, and $T'_\varepsilon > 0$ such that*

1. *if $\beta < \bar{d}\rho_A^{-1}\phi(1)^{-1}$, then for every z,*

$$\mathbb{P}_z(\exists t \geq T_\varepsilon : Z(t) > \varepsilon) \leq K_\varepsilon N^{-1/2}; \tag{4.52}$$

2. *if $\bar{d}\rho_A^{-1}\phi(1)^{-1} < \beta < \bar{d}\rho_A^{-1}\phi(0)^{-1}$, let z^* be the unique solution of the equation $\phi(z^*) = \beta^{-1}\bar{d}\rho_A^{-1}$ and assume that $\varepsilon < z^*/2$. Then, for every $z \leq (z^* - 2\varepsilon)^2$, it holds*

$$\mathbb{P}_z(\exists t \geq T'_\varepsilon : Z(t) > \varepsilon) \leq K'_\varepsilon N^{-1/2}. \tag{4.53}$$

Moreover, the constants K_ε and T_ε only depend on the quantity $\beta\bar{d}^{-1}\rho_A$ and are bounded when this quantity is bounded away from $\phi(1)^{-1}$. The constants K'_ε and T'_ε only depend on ε.

Proof. Item 1. is a straightforward consequence of the stochastic domination between $Z(t)$ and $Z_Y(t)$ and of item 2. is a consequence of Lemma 4.3 with $\mu = \beta\bar{d}^{-1}\phi(1)$.

Regarding item 2., notice first of all that because of the assumptions on ϕ, we have that $|\{z : \phi(z) = w\}| = 1$ for every $w \in [\phi(0), \phi(1))$. This implies the uniqueness of z^*. At this stage, we consider the jump Markov process $Y(t)$ with transition rates given by (4.49) and $\mu = \beta\bar{d}^{-1}\phi(z^* - \varepsilon)$. We notice that

$$\mu\rho_A = \beta\bar{d}^{-1}\phi(z^* - \varepsilon)\rho_A = \frac{\phi(z^* - \varepsilon)}{\phi(z^*)} < 1, \tag{4.54}$$

and that $\bar{\lambda}_{\mathbf{y},\mathbf{y}+\delta_\mathbf{v}} \geq \lambda_{\mathbf{y},\mathbf{y}+\delta_\mathbf{v}}$ as long as $\mathbf{y}$ is such that $z(\mathbf{y}) \leq \mathbf{z}^* - \varepsilon$. Put

$$\bar{T} = \inf\{t : Y(t) > z^* - \varepsilon\}. \tag{4.55}$$

We can establish a coupling between $X(t)$ and $Y(t)$ such that $X(0) = Y(0)$ and $X(t) \leq Y(t)$ for all $t < \bar{T}$. Choose now T_ε that satisfies item 2) of Proposition 4.3. It

holds

$$\begin{aligned}
&\mathbb{P}(\exists t \geq T_\varepsilon : Z(t) > \varepsilon) = \\
&\quad = \mathbb{P}(\exists t \geq T_\varepsilon : Z(t) > \varepsilon\,, \bar{T} = +\infty) + \mathbb{P}(\exists t \geq T_\varepsilon : Z(t) > \varepsilon\,, \bar{T} < +\infty) \quad (4.56)\\
&\quad \leq \mathbb{P}(\exists t \geq T_\varepsilon : Z_Y(t) > \varepsilon) + \mathbb{P}(\exists t \geq 0 : Z_Y(t) > z^* - \varepsilon).
\end{aligned}$$

Result now follows from Proposition 4.3 with $a = z^* - 2\varepsilon$ and $\delta = \varepsilon$. The fact that we get constants K'_ε and T'_ε that only depend on ε is due to the fact that for every $\varepsilon > 0$ the quantity $\mu\rho_A$ in (4.54) is uniformly bounded away from 1 when β varies in the specified interval. □

4.4.4 The Core Result

The main result of this chapter can be finally obtained by combining Corollaries 4.3, 4.4 and 4.5. For the sake of readability, we recall here the standing assumptions.

Let $G = (V,E)$ be a fixed graph having average degree $\bar{d}$, maximum degree Δ, Cheeger constant γ and spectral radius of the adjacency matrix ρ_A. We recall that $X(t)$ is a jump Markov process on $\{0,1\}^V$ governed by the transition rates (4.1) and $Z(t) = z(X(t))$ is a process counting the fraction of nodes having state 1. The persuasion strength ϕ is assumed to be admissible, namely it satisfies properties (A1), (A2), and (A3). The following result holds true.

Theorem 4.3. *Let $z'_u \leq z''_u < z_s$ be points in $[0,1]$ defined by*

$$\phi(\sqrt{z'_u}) = \beta^{-1}\bar{d}\rho_A^{-1}, \qquad z''_u = z_u(\Delta_{in}\bar{d}^{-1}\beta), \qquad z_s = z_s(\Delta_{in}\bar{d}^{-1}\beta), \qquad (4.57)$$

where $z_u(\cdot)$ and $z_s(\cdot)$ have been defined in (4.9). Depending on the conditions of the various parameters each of this point may exist or not. Below, whenever we write them, we are implicitly affirming their existence. Let $A = 14(1+\beta)^2$.

For every $\varepsilon > 0$ we can find $C^i_\varepsilon > 0$, $T^i_\varepsilon > 0$ for $i = 1,2,3$, $K_\varepsilon > 0$, and $S_\varepsilon > 0$ such that

1. *if* $\beta < \bar{d}\Delta_{in}^{-1}\phi(1)^{-1}$, *then* $\forall z$,

$$\mathbb{P}_z\left(\sup_{t\geq T_\varepsilon^1} Z(t) > \varepsilon\right) \leq 5Ne^{-C_\varepsilon^1 N}; \tag{4.58}$$

2. *if* $\bar{d}\gamma^{-1}\beta^* < \beta < \bar{d}\rho_A^{-1}\phi(0)^{-1}$, *then*

   - $\forall z < z'_u - 4\varepsilon$,

$$\mathbb{P}_z\left(\sup_{t\geq S_\varepsilon} Z(t) > \varepsilon\right) \leq K_\varepsilon N^{-1/2}, \tag{4.59}$$

   - $\forall z > z''_u + \varepsilon$,

$$\mathbb{P}_z\left(\inf_{t\in[T_\varepsilon^2, T_\varepsilon^2 + e^{C_\varepsilon^2 N}]} Z(t) < z_s - \varepsilon\right) \leq AN^2 e^{-C_\varepsilon^2 N}; \tag{4.60}$$

3. *if* $\bar{d}\gamma^{-1}\phi(0)^{-1} < \beta$, *then* $\forall z > \varepsilon$,

$$\mathbb{P}_z\left(\inf_{t\in[T_\varepsilon^2, T_\varepsilon^2 + e^{C_\varepsilon^2 N}]} Z(t) < z_s - \varepsilon\right) \leq AN^2 e^{-C_\varepsilon^2 N}. \tag{4.61}$$

With the understanding that if $\phi(0) = 0$, *then case 3. does not show up. Moreover, for every* $\varepsilon > 0$, *the various constants exhibit the following dependence on the parameters.* C_ε^1 *and* T_ε^1 *only depend on the quantity* $\beta\bar{d}^{-1}\Delta$ *and are, respectively, bounded away from* 0 *and bounded, when this quantity is bounded away from* $\phi(1)^{-1}$. C_ε^2 *and* T_ε^2 *only depend on the quantity* $\beta\bar{d}^{-1}\gamma$ *and are, respectively, bounded away from* 0 *and bounded, when this quantity is bounded away from* β^* *and* $\phi(0)^{-1}$. *Finally,* K_ε *and* S_ε *only depend on* ε.

Proof. Item 1. is a consequence of Corollary 4.4. Regarding item 2), notice first that the following inequalities hold

$$\gamma \leq \rho_A \leq \bar{d} \leq \Delta_{in} \quad \text{and} \quad \phi(1)^{-1} \leq \beta^* \leq \phi(0)^{-1}. \tag{4.62}$$

The first and third inequalities of the first expression are trivial, while the second one comes form [63]. The second expression is a direct consequence of the monotonicity of $\phi(z)$. This yields, in particular, $\gamma^{-1}\beta^* \geq \rho_A^{-1}\phi(1)^{-1}$. Item 2. now follows from

item 2. of Corollary 4.5 and from item 1) of Corollary 4.3. Finally, item 3. comes from item 2. of Corollary 4.3. □

Remark 4.3. *Using item 1. of Corollary 4.5, we can obtain the following variant of item .) of Theorem 4.3: 1 bis. if* $\beta < \bar{d}\rho_A^{-1}\phi(1)^{-1}$*, then* $\forall z$*,*

$$\mathbb{P}_z\left(\sup_{t\geq T'_\varepsilon} Z(t) > \varepsilon\right) \leq C'_\varepsilon N^{-1/2}, \tag{4.63}$$

where the constants C'_ε *and* T'_ε *only depend on the quantity* $\beta\bar{d}^{-1}\rho_A$ *and are bounded when this quantity is bounded away from* $\phi(1)^{-1}$*. On the one hand, 1 bis. improves the result by widening the interval for* β*, as* $\rho_A \leq \Delta$ *and the gap between the two quantities may actually be large. On the other hand, it weakens the result in terms of probability decay. Bound 1 bis. can be useful when dealing with large-scale random graphs, where results on the concentration of* ρ_A *and* Δ *have already a slow decay in probability, so that the exponential decay would be lost in any case.*

Theorem 4.3 is a result that holds true for any possible graph. Of course, its most interesting use is for sequences of graphs having size $N \to +\infty$. Since the various thresholds and constants involved in the statement depend on graph properties (and thus ultimately on N), suitable assumptions on the sequence of graphs are needed in order for the three regimes to be observed in the large scale limit, similarly to the mean field case. Notably, in order to ensure the existence of the intermediate regime with the bifurcation with respect to the initial condition, we need to consider graphs where the Cheeger constant (4.38) and the average degree have the same asymptotic behavior, as the population size N grows. In the next section we will show some very interesting topologies with this property. To sum up, in Theorem 4.3 we notice two important differences with respect to the results established in Theorem 4.1. First, the cases considered in Theorem 4.3 are not exhaustive as the various intervals considered for the parameter β do not cover the whole positive line. Second, exponential decay of probabilities is not always insured.

4.5 Application on Specific Topologies

In this section, we discuss the application of Theorem 4.3 to specific sequences of graphs with increasing size N. For the sake of simplicity we stick to the case

$\phi(z) = z$. This choice of the persuasion strength yields $\beta^* = 4$ and to the occurrence of only the cases depicted in items 1. and 2. of Theorem 4.3.

First we introduce the notion of a regularly expansive sequence of graphs that includes popular random graphs examples like Erdős-Rényi graphs and random configuration models. For such graphs, we show that Theorem 4.3 guarantees the existence of the two regimes: the first one where failure always occurs and the second one where both failure and success may occur, depending on the initial condition. Finally we present some numerical simulations on Erdős-Rényi graphs and random configuration models corroborating our analytical results. We conclude with some simulations on graphs for which Theorem 4.3 does not give any information. Such simulations suggest that these bifurcation phenomena should hold under less stringent assumptions than those assumed in results.

We recall below the graph parameters that need to be computed (or at least estimated) in order to use Theorem 4.3:

- $\bar{d}$ and Δ_{in} are, respectively, the average and the largest in-degree of the graph;
- γ is the Cheeger constant of the graph, defined in (4.38);
- ρ_A is the spectral radius of the adjacency matrix.

A sequence of graphs G_N with increasing number of nodes N is called (a, e_1, e_2)-*regularly expansive* if, for every N,

$$\bar{d}\Delta_{in}^{-1} \geq a \qquad \text{and} \qquad e_1 \leq \bar{d}\rho_A^{-1} \leq \bar{d}\gamma^{-1} \leq e_2. \tag{4.64}$$

Notice that, because of (4.62), we can always choose $e_1 \geq a$.

For such graph sequences, Theorem 4.3 can be reformulated as follows.

Corollary 4.6. *Assume that $\phi(z) = z$ and that G_N is a (a, e_1, e_2)-regularly expansive sequence of graphs. Let $z'_u \leq z''_u < z_s$ be points defined by*

$$\begin{aligned} z'_u &= \beta^{-2} e_1^2, \\ z''_u &= \frac{1}{2} - \frac{1}{2}\sqrt{1 - \frac{4e_2}{\beta}}, \\ z_s &= \frac{1}{2} + \frac{1}{2}\sqrt{1 - \frac{4e_1}{\beta}}. \end{aligned} \tag{4.65}$$

Let $A = 14(1+\beta)^2$. For every $\beta > 0$ and for every $\varepsilon > 0$ we can find $C_\varepsilon > 0$, $K_\varepsilon > 0$, and $T_\varepsilon > 0$ for which the following holds true for every N:

1. *if $\beta < a$, then $\forall z$,*

$$\mathbb{P}_z\left(\sup_{t \geq T_\varepsilon} Z(t) > \varepsilon\right) \leq 5Ne^{-C_\varepsilon N}; \tag{4.66}$$

2. *if $\beta > 4e_2$, then $\forall z < z'_u - 4\varepsilon$,*

$$\mathbb{P}_z(\exists t \geq T_\varepsilon : Z(t) > \varepsilon) \leq K_\varepsilon N^{-1/2}; \tag{4.67}$$

and $\forall z > z''_u + \varepsilon$,

$$\mathbb{P}_z\left(\inf_{t \in [T_\varepsilon, T_\varepsilon + e^{C_\varepsilon N}]} Z(t) < z_s - \varepsilon\right) \leq AN^2 e^{-C_\varepsilon N}. \tag{4.68}$$

Proof. It is an immediate consequence of Theorem 4.3, of the explicit computation of (4.9), and the inequalities (4.62). □

Remark 4.4. *We stress the fact that the quantities C_ε, K_ε and T_ε appearing in the statement of Corollary 4.6, only depend on the graph parameters $a, e, 1, e_2$ and on the choice of β, but not on the size N.*

We notice that, the condition $a > 0$ ensures that there exists a transition with respect to the parameter β from the failure regime to the intermediate regime. Instead, the condition $e_1 > 0$ ensures the presence of the transition with respect to the initial condition in the second regime.

Below we present two fundamental examples of random graph ensembles which yield, under specific assumptions, regularly expansive graphs sequences.

Example 4.1. (Erdős-Rényi graphs) *We consider the ER model $G(N,p)$, presented in Example 2.6. We restrict our analysis to the case above connectivity threshold, i.e. when $\frac{\ln N}{Np} \to 0$. In this regime, w.h.p. $G(N,p)$ is connected [11, 32] and*

$$\bar{d}\gamma^{-1} = 2 + o(1) \qquad \text{and} \qquad \bar{d}\rho_A^{-1} = 1 + o(1). \tag{4.69}$$

This implies that in the connectivity regime, $G(N,p)$ is w.h.p. $(1-\delta, 1-\delta, 2+\delta)$-regularly expansive for any $\delta > 0$.

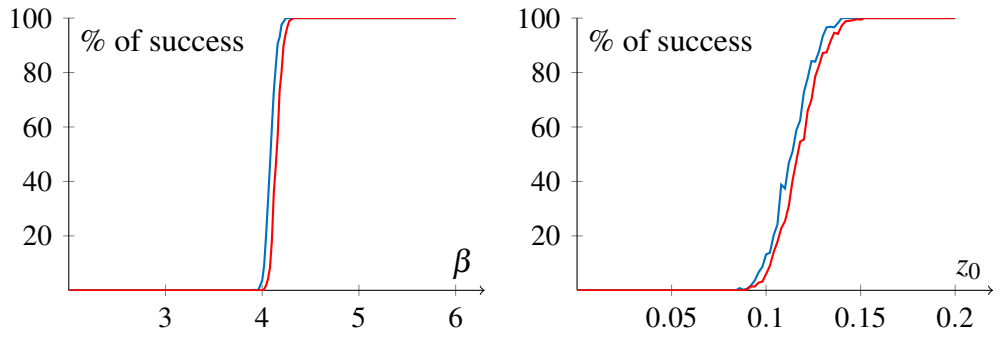

(a) Success varying β, $z_0 = 1$. (b) Success varying z_0, $\beta = 10$.

Fig. 4.4 Simulations of the DoI model on random expander graphs with $N = 1000$. In blue ER with $p = 0.05$, in red regular configuration model with $\bar{d} = 20$.

Example 4.2. (Configuration model) *Consider a probability distribution q_d over $\{3,\dots,d_{max}\}$. The configuration model $G(N,q_d)$ is a random undirected simple graphs with N nodes whose degrees are independent random variables distributed according to q_d and where edges are created through a random permutation [45]. Notice that, by construction, $3 \leq \bar{d} \leq \Delta_{in} \leq d_{max}$. Moreover, $\exists \alpha > 0$ such that $\gamma \geq \alpha$ for all finite N and w.h.p. as $N \to \infty$ [45]. Consequently, $G(N,q_d)$ is w.h.p. $(3/d_{max}, 3/d_{max}, d_{max}/\alpha)$-regularly expansive.*

Numerical simulations with Erdős-Rényi graphs and with regular configuration models are shown in Figs. 4.4 and 4.5. In particular, Fig. 4.4 shows the bifurcation with respect to β and the bifurcation with respect to the initial condition in the intermediate regime for $\beta = 10$. Simulations seem to show that such bifurcations are sharp as it was happening in the mean field case (notice also that the bifurcation with respect to β is placed in the same position $\beta^* = 4$). Fig. 4.5 deepens the analysis of the bifurcation with respect to the initial condition that seems to become sharper for larger and larger values of N.

In this final paragraph we consider some examples of graph sequences that are not regularly expansive and for which, consequently, Theorem 4.3 can not infer the presence of the phase transitions. Nevertheless, we show through numerical simulations that such phenomena (or at least some of them) do take place.

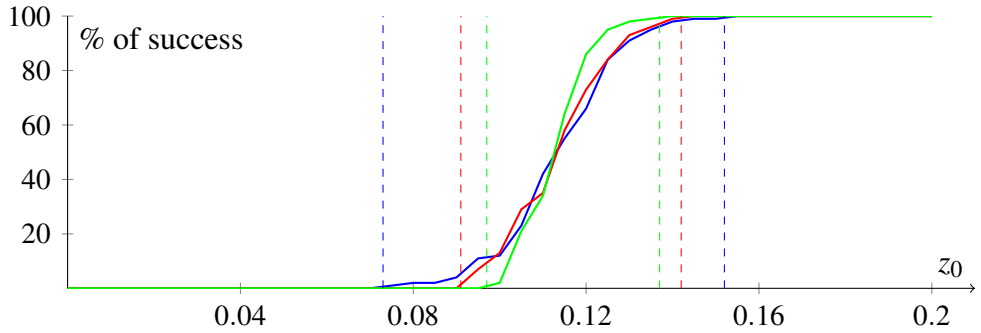

Fig. 4.5 Simulations of the DoI model on ER random graphs with $\beta = 10$ and $N = 800$ (blue), $N = 1200$ (red) and $N = 1600$ (green). The vertical dotted lines are the estimated thresholds z'_u and z''_u. As N increases the transition seems to be sharper. Notice that the analytical thresholds from Corollary 4.6 are $z'_u = 0.01$ and $z''_u \simeq 0.2764$.

Example 4.3. (Barábasi-Albert model) *Consider a Barábasi-Albert graph, presented in Ex. 2.7. As $N \to \infty$ we know that [32], $\exists\, \alpha > 0$ such that w.h.p.*

$$\bar{d} = m + o(1), \quad \Delta_{in} = \sqrt{N}(1 + o(1)), \quad \rho_A = \sqrt[4]{N}(1 + o(1)), \text{ and } \quad \gamma \geq \alpha. \tag{4.70}$$

Therefore, Barábasi-Albert graphs are only $(0, 0, m/\alpha + \delta)$-regularly expansive, for any $\delta > 0$.

Example 4.4. (Toroidal graphs) *A 1-torus is a simple ring graph C_n (Ex. 2.3. A k-torus can be defined as a k-dimensional generalization of this topology: the 2-torus is a toroidal grid, and so on. In general, a k-torus can be formally defined as the cartesian product between k 1-tori with $\sqrt[k]{N}$ nodes each, details can be found in [64]. For a k-torus we have that $\gamma \asymp N^{-k/2}$ and $\bar{d} = 2k$ is constant. Therefore, $\bar{d}/\gamma$ always diverges.*

Therefore, in these two examples Corollary 4.6 can not be applied to prove any phase transitions neither on β, nor on the initial condition. Nevertheless, in the case of Barábasi-Albert graphs, simulations presented in Fig. 4.6 show the existence of the two different regimes: the failure regime, and a regime where success and failure are both possible depending on the initial condition. However, from our simulations, the phase transition in this intermediate regime seems to be smooth, even increasing N (see Fig. 4.6b).

Similarly, even in the case of k-tori, simulations (see Fig. 4.6) seem to show the existence of the intermediate regime. In this case the transition with respect

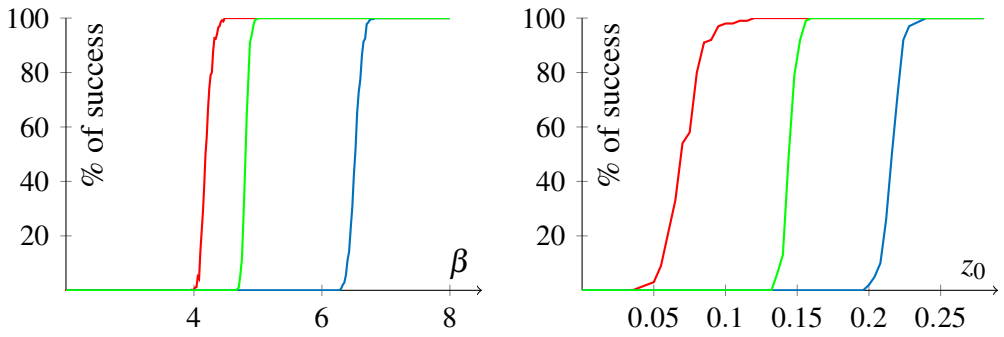

(a) Success varying β, $z_0 = 1$.

(b) Success varying z_0, $\beta = 10$.

Fig. 4.6 Simulations of the DoI model on nonexpander topologies: Barábasi-Albert graphs with $N = 1000$ and $m = 6$ (red), k-tori (blue $k = 1$, green $k = 2$) with $N = 1024$.

to the initial condition seems to be sharp, as one can see in Fig. 4.6b. Finally, the simulations in Fig. 4.6 also suggest that the various thresholds for a k-torus are monotonically decreasing in the dimension k. This is intuitive for the role played by the connectivity features of the graph in the diffusion dynamics.

4.6 Conclusion

In this Chapter, we have used our theory to develop a novel network dynamics modeling the adoption of a new technological item, such as a smart-phone application or a software, in a networked system. To model this phenomenon, we have proposed a gossip spreading mechanism whose strength depends on the global diffusion of the item in the community through a positive externalities effect, coupled with a spontaneous regression drift. This model, named diffusion of innovation (DoI) model, can also be interpreted as a generalization of an SIS epidemic model (studied in Chapter 3) with a nonfixed state-dependent infection probability.

We have performed our analysis in three steps. First, in Section 4.2, we have studied the system under the assumption of a fully connected network of interactions. In particular, we have been able to prove that, depending on the strength of the gossip mechanism, three possible regimes may show up: i) a failure regime; ii) a success one; and iii) an intermediate regime where failure and success are both are possible, depending on the initial fraction of users. This intermediate regime presenting the bistability phenomenon is the main novelty of the DoI model with respect to

a standard SIS epidemic model, where, instead, the outcome of the dynamics is always independent of the initial condition. Then, Sections 4.3 and 4.4 are devoted to extend our results to non fully connected topologies, showing the existence of the intermediate regime in more realistic scenarios. First, we have studied the case of two isolated communities, proving that, under some conditions, the presence of a sufficiently high initial condition in one of the two is sufficient to diffuse the product in both the communities, due to the effect of positive externalities. Finally, a general network of interactions has been considered, enabling us to define a family of network topologies in which the intermediate regime is present. We have concluded this chapter by presenting a number of numerical results to corroborate our theoretical results and to suggest that the transitions phenomena which characterize the intermediate regime could be present even in more general graphs, non encompassed by our theoretical result, paving the way for future research to extend our theoretical findings.

Besides the extension of our results to other families of network topologies, a relevant line of future research consists in testing the DoI model in real world case studies. Our aim is to acquire temporal data describing the spread of a technological asset in a social community (e.g., the use of a service or the downloads of an application for smartphone) and, against them, to test our model also in comparison with classical epidemic models and with standard model used for “big choices”.

Chapter 5

Controlled Diffusive Systems for Evolutionary Dynamics

Evolutionary dynamics [27] study the spread of a new species (usually called mutants) in a geographic area. An important application is thus to analyze the effects of the introduction of a genetically modified organism (GMO) in a certain area, with the goal of replacing a native species. This problem is a hot topic in epidemics control, since several diseases are transmitted by intermediate hosts (e.g., dengue, malaria, and, more recently, Zika). In the last few years, many efforts have been done by researchers to create GMOs similar to the intermediate hosts, but in such a way that they can not transmit the pathogen. Furthermore, some trials in which these mutants are introduced in nature have been done, with different outcomes [28, 29].

The main goals of the analysis of such a processes is to compute the probability that the mutants diffuse widely in the area (called fixation probability) and to estimate the duration of the spreading process, depending on the topology of the network. However, very few analytical results are available, since the results in the literature are mainly based on extensive Monte Carlo simulations [27, 65, 66], but for the computation of the fixation probability in some very specific network topologies [67, 68], and the computation of loose bounds on the absorbing time for regular directed graph [69]. As a consequence of this lack of results, at now, very few control policies for evolutionary dynamics have been proposed and studied.

In this chapter, inspired by evolutionary dynamics, we propose a new model for mutant diffusion that presents two different features with respect to the one previously

mentioned: i) the diffusion process is modeled through link-based (instead of node-based as in the cited work) activation mechanisms; and ii) an explicit control action is incorporated. This change of perspective enables us to obtain, on the one hand, new analytical insights, notably concerning the expected duration of the spreading mechanism. On the other hand, it also allows for the development of control policies to speed up the spread of the mutant. With this in mind, we propose and analyze an effective feedback control strategy based on few knowledge on the network topology and on the evolution of the spreading process.

The chapter is organized as follows. In Section 5.1, we introduce the stochastic evolutionary model. In Section 5.2, we present our main results on the time needed for the mutants to occupy the whole network, along with practical examples of their use on specific network topologies. Then, in Section 5.3, we propose and analyze a feedback control policy which allows for a remarkable speed up of the diffusion of the mutant using few observables and topological data. Finally, two examples show the increased performance of our feedback control policy with respect to the constant one, both for synthetic artificial networks and for a case study. Part of the work described in this chapter has been previously published [70], accepted for pubblication [71] and is part of current working papers [72] .

5.1 Model

In our model the geographical setting is described as a graph whose nodes are locations that we assume to be fully occupied by just one species, either the native one or the mutant one. A spreading mechanism and an external control are the mechanisms through which species occupation varies with time. Below we detail the various definitions. Here, we present these two mechanisms using a slight different formulation with respect to the standard one proposed for pairwise-based diffusion processes in Chapter 2. This is because it allows for an easier and clearer presentation of the external control strategy. Then, we show how this model fits the formalism we developed in this dissertation.

- *The geographical graph.* We consider an undirected connected weighted graph $G = (V, E, W)$ whose node set $V = \{1, \dots, N\}$ represents locations of a geographical network, whose links $\{i, j\} \in E$ represent proximity of nodes i and

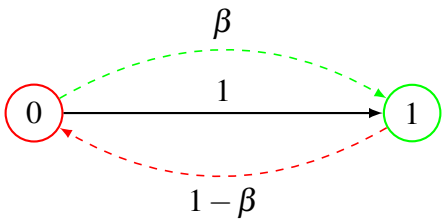

Fig. 5.1 State transitions characterizing the Controlled Diffusive System. Black solid lines are spontaneous mutation, colored dashed lines are transitions taking place after a pairwise interaction with a node with the other state.

j, and whose nonnegative weights W_{ij} measure the frequency of interactions between neighbor nodes. We suppose W to be symmetrical and that $W_{ij} > 0$ if and only if $\{i, j\} \in E$.

- *The spreading mechanism.* We assume each link $\{i, j\}$ to be equipped with an independent Poisson clock with rate W_{ij}, modeling the times the two species in nodes i and j come in contact. When the clock associated with the link $\{i, j\}$ clicks, if both locations i and j are occupied by the same species, nothing happens, whereas, if the two species in i and j differ, then a conflict takes place and the winning species occupies both locations. Conflicts are solved according to a stochastic law: the probability for mutants to win a conflict is assumed to be a constant $\beta \in [0, 1]$.

- *The external control.* We fix an integrable function $U(t) = (u_1(t), \ldots, u_N(t)) \in \mathbb{R}_+^N$ where $t \in \mathbb{R}_+$. $u_i(t)$ represents the rate at which mutants are introduced in node i at time t.

Remark 5.1. *The formulation as pairwise-based diffusion processes is straightforward. The probabilities are set as follow:* $p_{01} = \beta$, $p_{10} = 1 - \beta$, $m_{01} = 0$, *and* $m_{10} = 1$, *wheres, a heterogeneous time-varying activation rate is given to each node, where* $\lambda_i(t) = u_i(t)$. *Possible state transitions are represented in Fig. 5.1.*

The triple $(G, \beta, U(t))$ is called a *Controlled Diffusive System* (CDS). To it, we now associate a Markov process describing the spreading of the mutants. Nodes are characterized by a binary state $X_i(t) \in \{0, 1\}$. We assume that each geographical node i at a certain time t is either fully occupied by the native species $X_i(t) = 0$ or by the mutant $X_i(t) = 1$. States of the various nodes is assembled in a vector $X(t)$ that is called the *configuration* at time t. $X(t)$ is a time inhomogeneous jump Markov

process on the configuration space $\{0,1\}^N$, whose initial condition is assumed to be a deterministic vector $X(0)$. Typically, we will choose the initial condition to be the mutant-free pure configuration, i.e., $X(0) = 0\mathbb{1}$. Its transition rates from (2.16) reads:

$$\begin{cases} \lambda_i^+(\mathbf{x}) &= (1-x_i)\left(\beta \sum_{j\in V} W_{ij}x_j + u_i(t)\right) \\ \lambda_i^-(\mathbf{x}) &= x_i(1-\beta)\sum_{j\in V} W_{ij}(1-x_j). \end{cases} \tag{5.1}$$

Remark 5.2. *We observe that, in the special case without external control (i.e., $U(t) = 0$, $\forall t \geq 0$), when all links have the same weight, and when $\beta = 1/2$, this model reduces to an isothermal voter model [1] (recalling that, in its original formulation, voter model was actually developed for biological applications), whereas when $\beta \neq 1/2$ it leads to a biased isothermal voter model [73]. Therefore our model generalizes isothermal voter models (both fair and biased) through the inclusion of external control and heterogeneity of link activation rates. Moreover, an (homogeneous) agent-based version of our model without control, where clocks are associated with nodes instead of links, has been proposed as an evolutionary model [27]. Notice that isothermal models and homogeneous agent-based ones coincide only on regular networks. However, as already mentioned, the very few analytical results on evolutionary models are limited to the computation or the estimation of the probability that the whole network is eventually occupied by mutants, before the native species does (the so told, fixation probability) and to a deeper analysis only on some very specific network topologies [67, 68], while convergence times are tackled only through extensive Monte Carlo simulations.*

Remark 5.3. *Also, observe that a different interpretation of our model consists in thinking the external control as the addition of a fictitious stubborn node s with constant state $X_s(t) = 1$, $\forall t \geq 0$, linked to each one of the nodes of the target set $i \in M_0(t)$ with $W_{si} = W_{is} = u_i(t)/\beta$. In the case of a time-varying control policy, this interpretation yields a time-varying network, where the nodes connected to the stubborn node and the weight of the relative links change in time. Models with stubborn nodes have been analyzed, e.g., within opinion dynamics [4]. However, despite this interesting different point of view, the presence of a single stubborn node in our model poses different issues with respect to those usually analyzed in the literature.*

In order to model the evolutionary advantage given to the GMO with respect to the native species and the presence of an external control, we focus on the case where

$$\beta \in (1/2, 1] \quad \text{and} \quad X(t) = 0\mathbb{1} \implies \exists i : u_i(t) > 0\,. \tag{5.2}$$

From (5.1) and (5.2), it follows that the pure configuration $\mathbb{1}$, the one with the whole network occupied by mutants, is the only absorbing state and that it is reachable from any other state. Therefore, in the long run, mutants will almost surely occupy the whole network. What is of interest, from the applicative viewpoint, is the transient behavior of our system that we capture in two indices: the *expected absorbing time* and the *expected control cost*.

$$\tau = \mathbb{E}\left[\inf\{t \geq 0 : X(t) = \mathbb{1}\}\right], \quad J = \mathbb{E}\left[\int_0^\infty \mathbb{1}^T U(t)\mathrm{dt}\right]. \tag{5.3}$$

with the understanding that, once the process is absorbed in $\mathbb{1}$, then $U(t)$ is set to 0. We notice that, under constant control policies, $J = \tau U$. It is evident that τ and J will exhibit a trade-off behavior and fundamental limitations will show up from our analysis. The effectiveness of various control policies will be compared through the analysis of these two quantities. Another natural bound on the expected control cost, holding true under any control policy, ties J with the number of nodes in which mutants are introduced through the external control, as formalized in the following statement.

Proposition 5.1. *Let $(G, \beta, U(t))$ be a controlled diffusive system and let $X(t)$ be its associated diffusive dynamics. If, during the evolution of the system, mutants are introduced via the external control in K nodes, then $J \geq K$.*

Proof. The duration of each introduction is an exponentially distributed random variable with expected value equal to the inverse of the rate. Hence, the expected contribution of each introduction to the total expected control cost is equal to 1, which yields the inequality. □

We observe that, in general, the expected control cost J could be greater than the bound in Proposition 5.1 because further effort could be wasted by controlling nodes already occupied by the mutants, or by controlling nodes that will be occupied by mutants due to the spreading mechanism.

There are typically some constraints that we want to enforce on the control policies we want to use. In general, the external control $U(t)$ is constrained to be active only at certain specified nodes. We define the support of $U(t)$ as

$$M_U(t) = \{i \in V : u_i(t) > 0\}. \tag{5.4}$$

Given $M \subseteq V$, we say that $U(t)$ is M-supported if $M_U(t) \subseteq M$ for every t. In this case the triple $(G, \beta, U(t))$ is called an M-controlled diffusive system.

Below we will consider, in particular, *constant control* policies $U(t) = U, \forall t \geq 0$ and, more generally, *feedback control* policies where $U(t)$ is chosen to be a function of the process $X(t)$ itself. Precisely, we consider a function $\mathcal{U} : \{0,1\}^N \to \mathbb{R}_+^N$ and we take $U(t) = \mathcal{U}(X(t))$. The triple $(G, \beta, \mathcal{U})$ is called a *feedback controlled diffusive system*. If $M_{\mathcal{U}(\mathbf{x})} \subseteq M$, $\forall \mathbf{x} \in \{0,1\}^N$, we say that $\mathcal{U}$ is M-supported and that $(G, \beta, \mathcal{U})$ is a *feedback M-controlled diffusive system*. Considering that each configuration $\mathbf{x} \in \{0,1\}^N$ can be equivalently characterized by its support $M_{\mathbf{x}} = \{i : x_i = 1\}$, we will also use the notation $\mathcal{U}(M_{\mathbf{x}})$ for $\mathcal{U}(\mathbf{x})$. In particular, defining the process

$$M_X(t) = \{i : X_i(t) = 1\}, \tag{5.5}$$

we will also write $U(t) = \mathcal{U}(M_X(t))$.

5.2 Main Results on Controlled Diffusive Systems

In this section, we study the performance that can be achieved by a controlled evolutionary dynamics depending on the control policy adopted and on the network topology. Specifically, in Section 5.2.1 we define two fundamental limitations on the performance, while an upper bound on τ is presented in Section 5.2.2. From these technical results, we establish some easy-to-use Corollaries for some specific choices of the control policy.

Finally, we propose some examples of the application of our findings on relevant network topologies presenting different large-scale behaviors.

In order to present our results, let us recall some notion related to the isoperimetric constants of a symmetric weighted graph, we have already used in Chapters 3 and 4.

We briefly recall that the cut of a subset of nodes $S \subseteq V$ of a weighted graph G is

$$c[S] = \sum_{i \in S} \sum_{j \notin S} W_{ij}. \tag{5.6}$$

Definition 5.1. *Given an undirected weighted graph $G = (V, E, W)$ with $|V| = N$, its* (minumum) conductance profile *is a function $\phi : \{1, \dots, N-1\} \to \mathbb{R}$, defined as*

$$\phi(z) = \min_{S \subset V, |S| = z} c[S], \tag{5.7}$$

while its (maximum) expansiveness profile *is a function $\psi : \{1, \dots, N-1\} \to \mathbb{R}$, defined as*

$$\psi(z) = \max_{S \subset V, |S| = z} c[S], \tag{5.8}$$

We remark that, conductance profile can be seen as a re-scaling of the isoperimetric constants in Definition 3.2, since $\phi(z) = z\eta(z)$. Finally, in order to tackle the analysis of this evolutionary dynamics and present our results, we define three stochastic processes, obtained as one-dimensional observables of the process $X(t)$. Two of them are well known objects, i.e., $\tilde{Z}(t)$ and $\xi(t)$, measuring the number of locations occupied by mutants and the overall weights of the links connecting nodes with different state, i.e., $\xi(t) = c[M_X(t)]$, respectively. Then, we introduce

$$C(t) := (\mathbb{1} - X(t))^T U(t), \tag{5.9}$$

which measures the total effective control rate in nodes occupied by the native species.Given this set of one-dimensional observables of the process, one can express the intensity of the non-homogeneous Poisson process $X(t)$ through the following Proposition.

Proposition 5.2. *The intensity of the non-homogeneous Poisson process $X(t)$ can be written as a function of the one-dimensional observables $B(t)$ and $C(t)$ as*

$$\mu(t) = \xi(t) + C(t). \tag{5.10}$$

Proof. From (5.1), we write

$$\begin{aligned}\mu(t) &= \sum_{i\in\mathcal{V}}\left[\lambda_i^+(X(t))+\lambda_i^-(X(t))\right]\\ &= (\mathbb{1}-X(t))^T\beta WX(t)+(\mathbb{1}-X(t))^TU(t)\\ &\quad +X(t)^T(1-\beta)W(\mathbb{1}-X(t))\\ &= \beta\xi(t)+(1-\beta)\xi(t)+C(t),\end{aligned} \tag{5.11}$$

where the last equality is verified since $W=W^T$. □

5.2.1 Fundamental Limitations on the Performance

Here, we present a number of results showing fundamental limitations for the performance of feedback controlled diffusive systems. They are expressed in the form of lower bounds on the average absorbing time τ, depending on topological properties of the network and on the specific form of the external control adopted.

Before presenting our results, we state a pair of lemmas, presenting some relevant monotonicity properties for the controlled diffusive systems. In order to improve the readability of this section, some technical proofs of the results presented here will be detailed in Appendix C.

Lemma 5.1. *Let $(G,\beta,U(t))$ and $(G,\gamma,U(t))$ be two controlled diffusive systems with diffusive dynamics $X(t)$ and $Y(t)$, respectively. If*

$$\beta\leq\gamma,\quad X(0)\leq Y(0),$$

then there exists a coupling $Z(t)=(X(t),Y(t))$ of the two processes such that

$$X(t)\leq Y(t),\qquad \forall t\geq 0.$$

In particular, $\tau_Y\leq\tau_X$ and $J_Y\leq J_X$, where the subscript denotes the two processes.

Remark 5.4. *Here, we remark that Lemma 5.1 holds true for any control policy $U(t)$. We emphasize that, if $U(t)=\mathcal{U}(Y(t))$ is a feedback control policy, where $U(t)$ is a function of the process $Y(t)$, then, when considering the process $X(t)$, $U(t)$ is not a feedback control policy for $X(t)$.*

Lemma 5.2. *Let $(\mathcal{G},1,U(t))$ and $(\mathcal{G},1,0)$ be two controlled diffusive systems with state $X(t)$ and $Y(t)$, respectively. If*

$$(\mathbb{1}-Y(0))^T U(t)=0\,,\qquad \forall t\geq 0\,,$$

i.e., if the control of the first process is supported on a subset of the support of the initial state of the second process, then, there exists a coupling $Z(t)=(X(t),Y(t))$, such that

$$X(t)\leq Y(t)\,,\qquad \forall t\geq 0\,.$$

In particular, $\tau_Y\leq\tau_X$, where the subscript denotes the two processes.

Lemma 5.2 implies that, for a controlled diffusive system where mutants always win (i.e., when $\beta=1$) it is always optimal for the control to insert the mutants as soon as possible in the system. We wish to emphasize that controlled diffusive systems with $\beta<1$ do not enjoy this monotonicity property and, as a consequence, their optimal control design problem is much more difficult.

The main result is obtained considering the limitations on the admissible trajectories of the diffusive dynamics posed by the spreading mechanism and by the control policy, and then solving a minimization problem. Given an M-controlled diffusive system $(G,1,U(t))$, the following definition captures the limitations that the process $M_X(t)$ inherently receives from the way jumps can occur.

Definition 5.2. *Given a graph $G=(V,E)$, a* neighborhood monotone crusade *(NMC) from $S\subseteq V$, denoted by $\boldsymbol{\omega}=(\omega_1,\dots,\omega_{k+1})$ where $k=N-|S|$, is a sequence of subsets of V such that:*

- $\omega_1=S$;
- $\omega_j=\omega_{j-1}\cup\{v_j\}$, *with* $v_j\in\mathcal{N}_{\omega_{j-1}}\setminus\omega_{j-1}$;
- $\omega_{k+1}=V$.

The set Ω_S collects all the NMCs from S. Finally, let

$$\underline{\tau}(S)=\min_{\boldsymbol{\omega}\in\Omega_S}\sum_{j=0}^{n-|S|-1}\frac{1}{c[\omega_j]}\,,\tag{5.12}$$

act a lower bound on the expected duration of a NMC from S.

Given a set $S \subseteq V$, we define the quantity

$$\mathcal{C}[S] := \left(\mathbb{1} - \delta^{(S)}\right)^T \mathcal{U}(S), \tag{5.13}$$

which measures the sum of the control rates in the nodes occupied by the native species under the feedback control policy $\mathcal{U}$. Similarly to the relation between the cut of a subset c and the process $B(t)$, we remark that $C(t) = \mathcal{C}[M_X(t)]$.

Before presenting the main result of this section, we prove a technical lemma, in which we estimate the expected contribution to the control cost given by the insertion of mutants in a single location.

Lemma 5.3. *Let $(\mathcal{G}, 1, U(t))$ and be a controlled diffusive system and let*

$$J_i := \int_0^\infty u_i(t)dt \tag{5.14}$$

be the contribution to the control cost given by the insertion of mutants in node $i \in \mathcal{V}$. Namely, $J = \sum_{i\in\mathcal{V}} J_i$. Let E_i be the following event:

$$E_I :=" X_i \text{ turns to } 1 \text{ as an effect of the external control}". \tag{5.15}$$

Then it holds $\mathbb{E}[J_i|E_i] \geq 1$.

Proof. Let T be a random variable modeling the time node i turns to 1. Since the transition is triggered by the external control, then it holds

$$\mathbb{P}[T \leq t] = 1 - \exp\left\{-\int_0^t u_i(s)ds\right\} =: F(t).$$

Then, we estimate

$$\begin{aligned}
\mathbb{E}[J_i|E_i] &\geq \mathbb{E}\left[\int_0^T u_i(t)dt \,|\, E_i\right] \\
&= \mathbb{E}\left[\int_0^\infty \left(\int_0^t u_i(s)ds\right) F'(t)dt \,|\, E_i\right] \\
&= \lim_{t\to\infty} \mathbb{E}[F(t)|E_i] - \mathbb{E}[F(0)|E_i] = 1.
\end{aligned}$$

□

We remark that the actual expected control cost can be larger than its bound in Lemma 5.3 due to wastes of external control in nodes already occupied by mutants, or in nodes that will be occupied by mutants because of the spreading mechanism, without the need of external control. Moreover, if $\beta < 1$, further contributions to the control cost can be consequences of multiple introductions of mutants in the same node.

Theorem 5.1. *Let $G = (V,E,W)$ be a graph, $M \subseteq V$ a subset of nodes, and $\beta \in [0,1]$. Then, for any M-controlled diffusive system $(\mathcal{G},\beta,U(t))$ with initial condition $X(0) = 0\mathbb{1}$, the expected absorbing time τ and the expected cost J satisfy*

$$\tau \geq \min_{\mu \in \mathcal{M}_J} \sum_{S \subseteq M} \mu_S \underline{\tau}(S), \tag{5.16}$$

where $\underline{\tau}$ is defined as in (5.12)*, μ is a probability measure over the power set of $\mathcal{U}$ that belongs to $\mathcal{M}_J$, defined as*

$$\mathcal{M}_J := \left\{ \mu : \sum_{S \subseteq M} \mu_S |S| \leq J \right\}. \tag{5.17}$$

Proof. Let $X(t)$ be the state of the M-controlled diffusive system $(\mathcal{G},\beta,U(t))$. Let $K \subseteq M$ be the set of nodes controlled during the evolution of the system. The set K is a random variable and depends on the whole evolution of the controlled diffusive system from $t = 0$ till the occurrence of the absorbing event. The argument we use in this proof is based on the conditioning of the the evolutionary dynamics on the realization of K. Under this conditioning, we are able to compute the (conditioned) expected value of τ. Finally, we obtain the result by using the law of total probability and minimizing over all the admissible probability distributions for K.

Let us condition on $K = S$, then it holds $J \geq |S|$ as a straightforward consequence of the application of Lemma 5.3 for the $|S|$ nodes controlled during the dynamics. The process $Y(t)$ associated with the diffusive system $(\mathcal{G},1,\mathrm{U(t)})$, with $Y(0) = 0\mathbb{1}$ has, because of Lemma 5.1 an expected absorbing time $\tau_Y \leq \tau$. The process $Y_S(t)$ associated with the diffusive system $(\mathcal{G},1,0)$, with $Y_S(0) = \delta^{(S)}$ has, because of Lemma 5.2 an expected absorbing time $\tau_{Y,S} \leq \tau_Y \leq \tau$.

We estimate $\tau_{Y,\mathcal{W}}$ by using the following observation. The set of all admissible trajectories of $Y_S(t)$ coincides with the set Ω_S of all NMCs from S. Let $\boldsymbol{\omega} = (\omega_0,\ldots,\omega_{n-|S|})$ be the trajectory followed by the process, and let T_j be time

spent in state $M_Y(t) = \omega_j$, for $j = 0, \dots, n - |S| - 1$. Due to linearity of the average operator, it holds

$$\tau_Y = \mathbb{E}\left[\sum_{j=0}^{n-|S|-1} T_j\right] = \sum_{j=0}^{n-|S|-1} \mathbb{E}[T_j]. \tag{5.18}$$

We also observe that, when we condition the process to follow a given trajectory, the random variable T_j depends on $\boldsymbol{\omega}$ only through ω_j. In fact, T_j is an exponentially distributed random variable with parameter equal to the intensity of the Poisson process $Y_S(t)$, computed according to Proposition 5.2, that is $c[\omega_j]$. Then, by conditioning on the NMC $\boldsymbol{\omega}$ followed by the process $Y_S(t)$, we estimate

$$\begin{aligned} \tau_{Y,S} &= \sum_{\boldsymbol{\sigma} \in \Omega_S} \mathbb{E}[T_k \,|\, \boldsymbol{\omega} = \boldsymbol{\sigma}] \mathbb{P}(\boldsymbol{\omega} = \boldsymbol{\sigma}) \\ &= \sum_{\boldsymbol{\sigma} \in \Omega_{\mathcal{W}}} \mathbb{P}(\boldsymbol{\omega} = \boldsymbol{\sigma}) \sum_{j=0}^{n-|S|-1} \mathbb{E}[T_j | \, \omega_j = \sigma_j] \\ &= \sum_{\boldsymbol{\sigma} \in \Omega_{\mathcal{W}}} \mathbb{P}(\boldsymbol{\omega} = \boldsymbol{\sigma}) \sum_{j=0}^{n-|S|-1} \frac{1}{c[\sigma_j]} \geq \underline{\tau}(S). \end{aligned} \tag{5.19}$$

Then, we obtain the result which relates the two indices τ and J by means of the law of total probability for the conditioning on the set $K = S$ and, finally, by minimizing over all the probability distributions for the set K for which the expected control is at most J, that is the set $\mathcal{M}_J$ in (5.17). □

This result, can be applied to detect hard controllable topologies, where no feedback control policy is able to achieve fast diffusion. Rings are a relevant example of hard controllable network structures. In the following, we prove the impossibility of designing a fast diffusive control policy for large-scale ring graphs. For the sake of simplicity, in all our examples we consider isothermal models, i.e., we set $W_{ij} = w$, for any $\{i, j\} \in \mathcal{E}$. Moreover, to avoid the weights from blowing up, in all our examples we parametrize $w = \alpha/\Delta$, where Δ is the maximum degree of the graph.

Example 5.1 (Impossibility of fast diffusion on rings)**.** *Let $\mathcal{G} = C_n$ be a ring graph with n nodes, all the weights of the links equal to $\alpha/2$, and let us consider a M-controlled diffusive system $(\mathcal{G}, \beta, U(t))$ with $X(0) = 0\mathbb{1}$, where M can possibly coincide with the whole V. In order to prove impossibility of fast diffusion of the mutants on the ring for any control policy, we derive a bound on $\underline{\tau}(S)$ that depends only on the cardinality of S. If fact, we observe that the spreading mechanism cannot*

increase the boundary of the process: after an occurrence of the spreading process, the boundary decreases by α (if the node that changes state is surrounded by two nodes occupied by the other species) or it remains the same (otherwise). Moreover, given a subset $S \subseteq \mathcal{V}$, it holds $c[S] \leq \alpha|S|$. Hence, we bound

$$\underline{\tau}(S) \geq \frac{1}{\alpha|S|}N - \frac{1}{\alpha}, \tag{5.20}$$

which enables us to write (5.16) *and its constraints* (5.17) *as a minimization problem involving only the variable $|\mathcal{W}|$. Since* (5.20) *is a convex function of $|\mathcal{W}|$, Jensen's inequality yields*

$$\begin{aligned}\tau &\geq \min_{\mu\in\mathcal{M}_J} \sum_{S\subseteq M} \mu_S \frac{1}{\alpha|S|}N - \frac{1}{\alpha} \\ &\geq \min_{\mu\in\mathcal{M}_J} \frac{1}{\alpha\sum_{S\subseteq M}\mu_S|S|}N - \frac{1}{\alpha} \\ &\geq \frac{1}{\alpha J}N - \frac{1}{\alpha},\end{aligned}$$

which proves that the diffusion is slow on large-scale graphs, unless letting the expected control cost to blow up as n grows large.

Even though the result in Theorem 5.1 is very general, some limitations on its direct use hamper its applicability. First, the computation of the exact solution of (5.16) is not always a simple problem as it is for the ring graphs in Example 2.3, whose topological properties pose strong constraints on the boundary of the sets along a NMC. Second, the result in Theorem 5.1 is conditioned to the knowledge (or the estimation) of the number of nodes controlled during the process, which is in general a random variable for non-constant control policies $U(t)$. To address these issuse, we present two simple but immediate corollaries, which provide weaker but easier-to-use bounds on τ.

In the first corollary, we give an immediate bound on τ for M-controlled diffusive systems, not depending on the specific form of the control policy adopted (which could be even a non-feedback one, as remarked below), nor on the control rates. Our estimation depends only on structural limitations posed by the topology of G and on the support of the control M, depending on the presence of bottlenecks in the sub-graph that cannot be controlled.

Corollary 5.1. *For any feedback M-controlled diffusive system $(G,\beta,U(t))$, it holds*

$$\tau \geq \left(\min_{M \subseteq R \subset V} c[R] \right)^{-1}. \tag{5.21}$$

Proof. Consider a set $R \supseteq M$ and let $Y(t)$ be the M-controlled diffusive system $(G,\beta,U(t)=U(t)))$ with initial condition $Y(0)=\delta^{(R)}$. Lemma 5.1 yields $\tau \geq \tau_Y$. Finally, Theorem 5.1 can be used and the sum in (5.12) can be lower bounded by its first term, that is $c[R]^{-1}$, since $C'[R]=0$. The inequality holds for any $R \supseteq M$, so the maximum of these quantities (that is achieved by the subset R that minimizes $c[R]$) yields the tighter bound. □

Remark 5.5. *We remark that this result depends only on the network topology and on the controllable set of nodes. Hence, it holds for any M-controlled diffusive systems, not depending on the specific control policy adopted.*

We propose now an intuitive but explanatory application of Corollary 5.1 to prove slow diffusion of the spreading process on barbel graphs.

Example 5.2 (Slow diffusion for barbell graph)**.** *Let $G=B_n$ be a barbell graph with N (even) nodes equally divided into two complete sub-communities V_1 and V_2, linked by a single link and let us consider any M-controlled diffusive dynamics, where $M \subseteq V_1$ and with initial condition $X(0)=\delta^{(S)}$ with $S \subseteq V_1$. Since $\Delta = n/2$ we parametrize $w = 2\alpha/n$. Corollary 5.1 yields*

$$\tau \geq \left(\min_{M \subseteq R \subset V} c[R] \right)^{-1} = c[V_1]^{-1} = \frac{N}{2\alpha}, \tag{5.22}$$

which grows linearly in the size of the system.

In the second Corollary, we relax the lower bound on the expected absorbing time by dropping its dependence on the feasibility of a trajectory. This relaxation yields the simplified expression for (5.16) in the following.

Corollary 5.2. *Let $G=(V,E,W)$ be a graph, $M \subseteq V$ a subset of nodes, and $\beta \in [0,1]$. Then, for any M-controlled diffusive system $(G,\beta,U(t))$ with initial condition $X(0)=0\mathbb{1}$, then the expected absorbing time τ and the expected cost J satisfy*

$$\tau \geq \min_{\mu \in \tilde{M}_J} \sum_{m \leq |S|} \mu_m \sum_{z=m}^{n-1} \frac{1}{\psi(z)} \tag{5.23}$$

where ψ is defined as in (5.8) *and μ is a probability measure over $\{0,\dots,|S|\}$ that belongs to $\tilde{M}_J$, defined as*

$$\tilde{M}_J := \left\{ \mu : \sum_{m\leq|S|} \mu_m m \leq J \right\}. \tag{5.24}$$

Proof. The proof comes from the definition of maximum expansiveness profile in (5.8) which implies $c[S] \leq \psi(|S|)$, for any set $S \subseteq V$. □

We remark that the estimation of the expected absorbing time from Corollary 3.1 is a simpler and more treatable problem than the minimization problem in Theorem 5.1. The drawback of using this result, is that the fundamental limit computed therein could be in some cases unreachable and far from the achievable values of τ and J. This gap is due to the fact that we do not take into account the admissibility of high expansiveness trajectories due to local topological constraints. For example, Corollary 3.1 cannot be used to prove slow diffusion for ring graphs. In fact, the maximum expansiveness profile of a ring graph is $\psi(z) = \alpha \min\{z, N-z\}$, so (5.23) yields a lower bound that grows as $\ln N$, which is far from the linear growth in N, proved using Theorem 5.1).

We present now a second Theorem, providing a lower bound on the expected absorbing time τ, under some conditions verified by the controlled diffusive system, during the evolution of the process. We remark that this result is not directly applied to the process, but a relevant corollary in which a fundamental limit that ties τ and J is provided, will be established using it.

Theorem 5.2. *For any controlled diffusive system (G,β,U) with $X(0) = \delta^{(S)}$, if the following inequality is verified:*

$$\xi(t) + C(t) \leq g(\tilde{Z}(t)), \quad \forall t \geq 0, \tag{5.25}$$

where $g : \{0,\dots,N-1\}] \to \mathbb{R}_+$ is a positive function. Then

$$\tau \geq \sum_{z=|S|}^{N-1} \frac{1}{g(z)}. \tag{5.26}$$

The detailed proof of this Theorem, as well as the one of Theorem 5.3, that is its upper bound counter-part, goes through some technical results for the analysis of the

stochastic process $X(t)$ and it will be extensively presented in Appendix C. However, an intuitive heuristic can be found in the analysis of a mean field deterministic relaxation of the evolutionary process, which is presented in the next section, in Remark 5.6.

5.2.2 Upper Bound on the Expected Absorbing Time

In this section we present our upper bound on τ and we provide a simple interpretation of this result in terms of a mean-field approximation of the stochastic process. Then, we show how this result can be directly applied in the case of constant control, presenting an explanatory example on expander graphs.

We state now the main contribution of this Section, that gives an upper bound on the expected absorbing time τ, under some conditions verified by the controlled diffusive system, during the evolution of the process. Similarly to the lower bound in Theorem 5.2, we remark that also this result is not directly applied to the process, but two relevant corollaries will be established using it, for constant control policy (in this section) and for a specific feedback control policy (in the following section), respectively.

Theorem 5.3. *For any controlled diffusive system (G,β,U) if the following inequality is verified:*

$$\xi(t)+C(t)\geq f(\tilde{Z}(t)),\quad \forall t\geq 0, \tag{5.27}$$

where $f:\{0,\dots,N-1\}]\to\mathbb{R}_+$ is a positive function. Then

$$\tau\leq \frac{\beta}{(2\beta-1)f(0)}+\frac{1}{2\beta-1}\sum_{z=1}^{N-1}\frac{1}{f(z)}. \tag{5.28}$$

As already mentioned, the detailed proof of this result is presented in Appendix C. Here, we propose an intuitive heuristic for the results in Theorems 5.2 and 5.3 can be found in the following analysis of a mean field deterministic relaxation of the evolutionary process in the following.

Remark 5.6. *Let the state of each node to assume a continuous value $\rho_i\in[0,1]$, representing the probability that mutants occupy that location. According to a N-Intertwined Mean Field Approximation [74], the variables ρ evolve according to the*

following ODE:

$$\dot{\rho} = \beta diag(\mathbb{1}-\rho)(W\rho+U) - (1-\beta)diag(\rho)W(\mathbb{1}-\rho). \tag{5.29}$$

Similar to the stochastic process, let $\zeta(t) = \mathbb{1}^T\rho(t)$, $\chi(t) = \rho(t)^T W(\mathbb{1}-\rho(t))$, *and* $\kappa(t) = (\mathbb{1}-\rho(t))^T U(t)$, *then* $\zeta(t)$ *is the solution of the Cauchy problem*

$$\begin{cases} \dot{\zeta} = (2\beta-1)\chi + \kappa. \\ \zeta(0) = 0 \end{cases} \tag{5.30}$$

Let $\bar{\tau} = \inf\{t \geq 0 : \zeta(t) = N\}$. *If* $f(\zeta) \leq \chi + \kappa \leq g(\zeta)$, *with* f *and* g *strictly positive functions in* $[0,N)$. *Then it holds*

$$\int_0^N \frac{ds}{g(s)} \leq \bar{\tau} \leq \frac{1}{2\beta-1}\int_0^N \frac{ds}{f(s)}. \tag{5.31}$$

In fact, positivity of f *and* g *implies strict monotonicity of* $\zeta(t)$. *On the one hand,* $\chi+\kappa \leq g(\zeta) \implies \dot{\zeta} \leq g(\zeta)$. *Thus, both sides can be divided by* $g(\zeta)$ *and integrated with respect to* t, *from* 0 *to* $\bar{\tau}$, *obtaining*

$$\int_0^{\bar{\tau}} \frac{\dot{\zeta}(t)dt}{f(\zeta)} \leq \int_0^{\bar{\tau}} dt \implies \bar{\tau} \geq \int_0^N \frac{ds}{g(s)}, \tag{5.32}$$

by substituting $s = \zeta(t)$ *in the first integral and recalling the boundary condition* $\zeta(0) = 0$. *Similarly, we obtain the second inequality.*

As already mentioned, Theorem 5.3 is used in the following of the paper to establish upper bounds on τ under specific control policies. First, the case of constant control is considered. In this case, Theorem 5.3 yields an upper bound in which the expected absorbing time is related to the evolutionary advantage of the mutants given by the parameter β and to topology of the network through its minimum conductance profile.

Corollary 5.3. *For any controlled diffusive system* (G,β,U) *under fixed control policy* $U(t) = U$, *let* ϕ *be the minimum conductance profile of* G. *Then it holds*

$$\tau \leq \frac{\beta}{(2\beta-1)\mathbb{1}^T U} + \frac{1}{2\beta-1}\sum_{z=1}^{N-1}\frac{1}{\phi(z)} \tag{5.33}$$

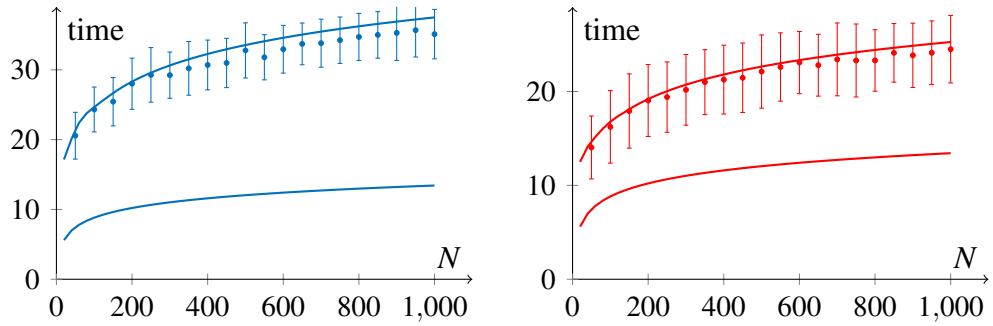

(a) $\beta = 0.7$. (b) $\beta = 0.8$.

Fig. 5.2 Monte Carlo estimation (200 simulations) of the expected absorbing time τ of a CDS on complete graphs for different values of N ($\alpha = 1$), with 90% confidence intervals. The two solid lines are the theoretical bounds from (5.34).

Proof. We observe that, for any $z \in \{1,\dots,N\}$, for all subsets $S \subset V$ with $|S| = z$, it holds $\phi(a) \leq c[S]$. Therefore, if $\tilde{Z}(t) = z \implies \xi(t) + C(t) \geq \phi(x)$. If $X(t) = 0$, then $C(t) = \mathbb{1}^T U$. Hence, (5.28) from Theorem 5.3 is applied with $f(z) = \phi(z)$, for $z \neq 0$, and $f(0) = \mathbb{1}^T U$. □

Here, we present an application of Corollary 5.3, which characterizes the family of expander graphs as easy controllable network structures. In fact, we ensures fast diffusion to be achieved under any constant control policies.

Example 5.3 (Fast diffusion on expander graphs)**.** *Let G be an expander graph with N nodes. Expander graphs, such as complete graphs, Erdős-Rényi random graphs, small-world networks [75] and Ramanujan graphs [76], have high conductance profile in the sense that $\exists \gamma > 0$ such that $\phi(i) \geq \gamma \min\{i, N-i\}$. We parametrize $w = \alpha/\Delta$ and we notice that any set S has at least $c[S] \geq \alpha\phi(|S|)$. Therefore, Theorem 5.2 and Corollary 5.3 yield*

$$\frac{2}{\alpha} \ln \frac{N}{2} \leq \tau \leq \frac{2}{\gamma(2\beta - 1)} \ln \frac{N}{2} + \frac{\beta}{(2\beta - 1)\mathbb{1}^T U}. \tag{5.34}$$

Expander graphs can be considered as a benchmark for fast-diffusive topologies. In fact, in large-scale expander graphs (i.e., $N \to \infty$), the bounds (5.34) *are (order-)tight, guaranteeing τ to grow logarithmically with N. Figure 5.2 presents Monte Carlo estimations of the expected absorbing time, together with the two analytical bounds from* (5.34) *for complete graphs.*

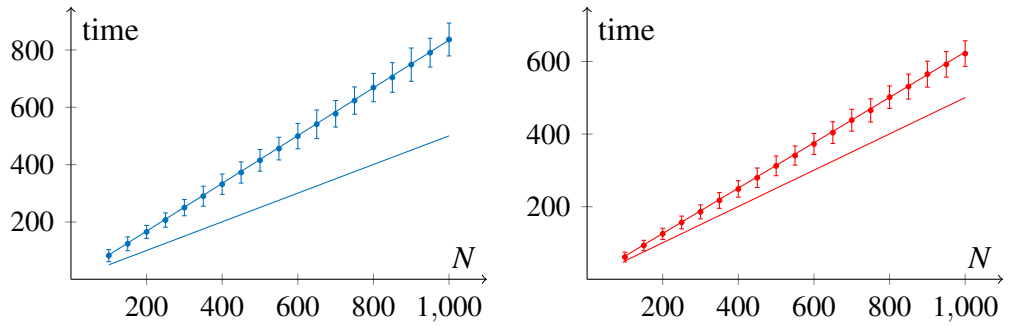

(a) $\beta = 0.8$. (b) $\beta = 0.9$.

Fig. 5.3 Monte Carlo estimation (200 simulations) of the expected absorbing time τ of a CDS on ring graphs for different values of N ($\alpha = 1$), with 90% confidence intervals. The two solid lines are the theoretical bounds computed.

In a similar fashion, Corollary 5.3 can be used to compute an upper bound on τ under a constant control for the two Examples presented in Section 5.2.1, i.e., ring graphs and barbell graphs. In both cases, order-thigh upper bounds are computed, ensuring τ to grow linearly with N.

Example 5.4 (Ring Graphs cont'd)**.** *In Example 5.1 we proved that fast diffusion is not achievable on ring graphs, since τ is bounded to grow at least linearly with N. Here, we show that this lower bound is actually order-tight. Computation of the conductance profile is straightforward. In fact, it holds $\phi(z) = \alpha$. Therefore, Theorem* (5.3) *yields*

$$\tau \leq \frac{\beta}{(2\beta-1)\mathbb{1}^T U} + \frac{1}{(2\beta-1)\alpha}(N-1). \tag{5.35}$$

Numerical simulations in Fig. 5.3 are consistent with our analytical results.

Example 5.5 (Barbell Graphs cont'd)**.** *Let us consider the barbell graph studied in Example 5.2. Since the two sub-communities V_1 and V_2 form complete graphs, the conductance profile is*

$$\phi(z) = \begin{cases} \alpha z\left(\frac{1}{2} - \frac{z}{N}\right) & \text{if } z < N/2 \\ \alpha/N & \text{if } z = N/2 \\ \alpha(N-z)\left(\frac{z}{N} - \frac{1}{2}\right) & \text{if } z > N/2, \end{cases} \tag{5.36}$$

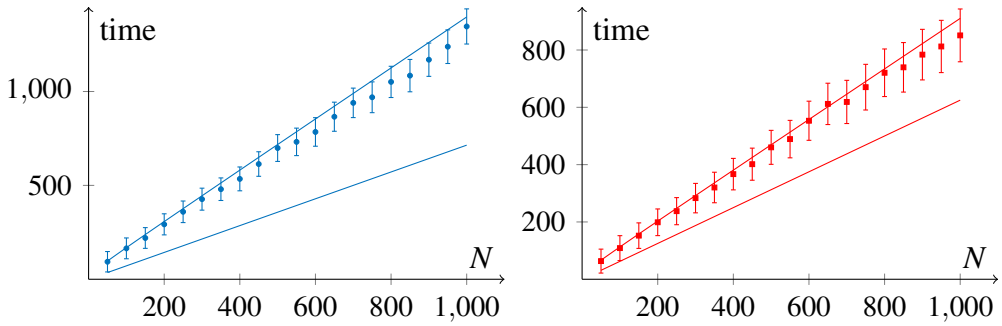

(a) $\beta = 0.7$. (b) $\beta = 0.8$.

Fig. 5.4 Monte Carlo estimation (200 simulations) of the expected absorbing time τ on barbell graphs for different values of N ($\alpha = 2$), with 90% confidence intervals. The two solid lines are the theoretical bounds computed.

Hence we obtain

$$\tau \leq \frac{1}{\alpha(2\beta-1)}\left(N+4\ln\frac{N}{2}\right)+\frac{\beta}{(2\beta-1)\mathbb{1}^T U}, \tag{5.37}$$

leading to τ to grow linearly with N. Numerical simulations can be found in Fig. 5.4.

We conclude the section by presenting an example where the upper- and the lower bound we developed are not sufficient to understand an order-thigh bound. In this example, we consider a square lattice, where a single node can be controlled, and the initial condition is the mutant-free configuration. From the Monte Carlo simulations we performed, it seems that the lower bound is the weak result, paving the way for further efforts to improve it.

Example 5.6 (Square Lattices)**.** *Let G be a square lattice with N (square number) nodes. We parametrize $w = \alpha/4$. The conductance profile can be estimated, for large-scale networks, as*

$$\phi(z) = \begin{cases} [\alpha/2+o(1)]\sqrt{z} & \text{if } z \leq N/2 \\ [\alpha/2+o(1)]\sqrt{N-z} & \text{if } z > N/2, \end{cases} \tag{5.38}$$

see [10]. On the other hand, Corollary 5.1 is ineffective, yielding $\tau \geq 1/\alpha$, and the minimization problem in Theorem 5.1 cannot be trivially solved. However, its minimum can be estimated through the following two (order-)tight bounds. At first, since after each node addition in a NMC the weighted boundary cannot increase by

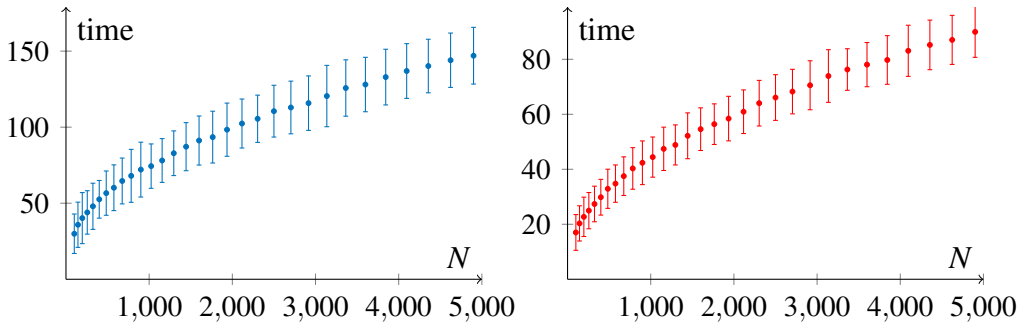

(a) $\beta = 0.6$. (b) $\beta = 0.7$.

Fig. 5.5 Monte Carlo estimation (200 simulations) of the expected absorbing time τ of a CDS on square lattices for different values of N ($w = 1$), with 90% confidence intervals.

more than $\alpha/2$, a natural upper bound is $c[\omega_i] \leq \alpha i/2$. On the other hand, a NMC in which $\boldsymbol{\omega}$ the mutants at first spread in the first line and in the first column, then they invade all the other odd lines (columns) in increasing order, finally they occupy the remaining nodes, has $\sum c[\omega_i]^{-1} = \left[\frac{2}{\alpha} + o(1)\right] \ln N$, giving a tight lower bound. Therefore $\exists K_1, K_2 > 0$ such that

$$\frac{K_1}{\alpha} \ln N \leq \tau \leq \frac{K_2}{(2\beta - 1)\alpha} \sqrt{N}. \tag{5.39}$$

In large-scale networks, this yields nontight asymptotic bounds: τ grows at least logaritmically in N, at most with its square root. Numerical simulations in Fig. 5.5 suggest τ to be close to its upper bound and to grow, thus, with the square root of N.

5.3 Feedback Control Policy

In the examples proposed in the previous section, we have been able to see different behaviors of the evolutionary dynamics on different network topologies. Some cases, such as expander graphs, are easy to be controlled. In fact, for these topologies, a very simple constant control policy provides fast diffusion of the mutants. On the other hand, we presented examples of hard controllable topologies such as ring graphs and barbell graphs (at least under constant control policies). Moreover, we show that some of these topologies exhibit structural limitations to achieve fast diffusion (e.g., ring graphs), while for other topologies no fundamental limitations are present (e.g., barbell graphs).

In this section, we focus on the design of a feedback control policy capable of speeding up the process, for these cases where no structural limitations prevent us from achieving fast diffusion, but constant control policies fail. Theorem 5.3 will be used to evaluate the effectiveness of our control strategy. The case of barbell graphs will be presented as an effective example where our feedback control policy is able to ensure fast diffusion of the spreading process.

The first stage to develop our feedback control policy consists in noticing that it is useless to insert mutants in locations already occupied by them, therefore we move the support of the control $M_U(t)$ during the spreading mechanism in such a way that the nodes in it have always state 0. As we shall discuss later, the optimal choice for $M_U(t)$ to maximize its influence, which in general is a computationally hard problem [21], is not required in our policy, therefore, we simply set $M_U(t)$ to be a singleton $m(t)$ in such a way that $U(t) > 0 \implies X_{m(t)}(t) = 0$. From Theorem 5.3, we argue that the diffusion process mainly depends on the number of locations occupied by mutants $\tilde{Z}(t)$ and on the boundary of the process $\xi(t)$. Therefore, we set $U(t)$ to be a feedback function of these two observables, i.e., $U(t) = \mathcal{U}(X(t)) = \mathcal{U}(\tilde{Z}(t), \xi(t))$.

In [70], we have proposed a preliminary effort in this direction. Therein, we set $\mathcal{U}(X(t)) = \xi(t) f(\tilde{Z}(t))$. This control policy allowed for a simple analysis and its effectiveness in speeding up the diffusion process had been shown, e.g., for barbell graphs. However, less regular network topologies (typical in real-world applications) may arise issues, restricting the usability of the proposed control policy. In fact, that control policy i) is very sensible to small errors in the data (e.g. if a node is added to one of the two components of the barbell graph, the control policy fails in activating in correspondence to the real bottleneck); and ii) could waste energy uselessly, inserting mutants when the process is already evolving fast.

Then, we have addressed these two issues by proposing a feedback control policy in which the knowledge of $\xi(t)$ is exploited in a more thoughtful way, improving the robustness of our control technique for its real-world use, as the two applications we will propose at the end of this section suggest.

In view of all our observations on the importance of $\xi(t)$, the goal of our control policy should intuitively be that of speeding up the process when $\xi(t)$ is small. To

this aim, fixed a positive parameter $C > 0$ and $i \in V$ with $X_i(t) = 0$, we define

$$\mathcal{U}_i(X(t)) = \begin{cases} C - \xi(t) & \text{if } \tilde{Z}(t) < N, \xi(t) < C \\ 0 & \text{else,} \end{cases} \tag{5.40}$$

and $\mathcal{U}_j(t) = 0, \forall\, j \neq i$. We remark that $C > 0$ guarantees convergence to the absorbing state.

In this new setting, we want to estimate the absorbing time τ to the state $X(t) = \mathbb{1}$ as well the expected cost of the control policy J_U. First, we define the following modification of the conductance profile.

Definition 5.3. *Given an undirected weighted graph $G = (V, E, W)$ with $|V| = n$ and a constant $C \geq 0$, its* C-floor conductance profile *is a function $\phi_C : \{1, \ldots, N-1\} \to \mathbb{R}$, defined as*

$$\phi_C(z) := \max\{\phi(z), C\} = \max\left\{ \min_{S \subset V, |S| = z} c[S], C \right\}. \tag{5.41}$$

We observe that, for $C \leq \min_{S \subseteq V} \phi(S)$, and in particular in the case $C = 0$, the C-floor conductance profile coincides with the minimum conductance profile ϕ. Moreover, due to its definition, the monotonicity $\phi_C \geq \phi_{C'}$ holds true for any $C \geq C'$. Using this notion of C-floor conductance profile, we deduce the following corollary of Theorem 5.3, which establish an upper bound on the expected absorbing time and on the expected cost of the feedback control policy.

Corollary 5.4. *For the feedback controlled diffusive system $(G, \beta, \mathcal{U})$, where $\mathcal{U}$ follows the control policy* (5.40)*, let ϕ_C be the C-floor conductance profile of G. Then it holds*

$$\tau \leq \frac{\beta}{(2\beta - 1)C} + \frac{1}{2\beta - 1} \sum_{z=1}^{N-1} \frac{1}{\phi_C(z)}; \tag{5.42}$$

and

$$J \leq \frac{\beta}{2\beta - 1} + \frac{1}{2\beta - 1} \sum_{z : \phi(z) < C} \frac{C - \phi(z)}{C} \leq \frac{\beta}{2\beta - 1} + \frac{1}{2\beta - 1} \left| \{ z : \phi(z) < C \} \right|. \tag{5.43}$$

Proof. The upper bound (5.42) comes straightforward from Theorem 5.3, being $\mu(t) = \xi(t) + C(t) = \xi(t) + \mathbb{1}^T U(t) \geq \phi_C(z)$.

To prove (5.43), if $\tilde{Z}(t)$ jumps in z at time t, from Proposition (5.2) we estimate

$$\begin{aligned} \mu(t) &= \xi(t^+) + \mathbb{1}^T U(t^+) \\ &= \max\{\xi(t^+), C\} \\ &\geq \max\{\phi(z), C\} = \phi_C(z), \end{aligned} \tag{5.44}$$

while the control rate is $\mathbb{1}^T U(t^+) = C - \xi(t^+)$ if $\xi(t^+) < C$, and 0 otherwise. Hence, the expected contribution to control cost of a sojourn in z, denoted by J_z, depends on the boundary of the process: if $\xi(t^+) < C$, then the intensity in (5.44) is equal to C, and we have

$$J_z = \frac{C - \xi(t^+)}{C} \leq \frac{C - \phi(z)}{C} \leq 1. \tag{5.45}$$

Otherwise, if $\xi(t^+) \geq C$, $J_z = 0$. We remark that, being $\xi(t^+) \geq \phi(z)$, if $\phi(z) \geq C$, it holds $J_z = 0$.

Finally, the upper bound in (5.43) is obtained by summing up the bounds in (5.45) over all the sojourns in all the states of process $\tilde{Z}(t)$ that give a nonnull contribution. In the worst-case scenario, these states are $z : \phi(z) < C$, which completes the proof. □

The upper bounds of the expected absorbing time and on the control cost are functions of the control policy $\mathcal{U}$ (through the choice of the parameter C) and of the minimum conductance profile ϕ so, ultimately, of the network topology. Due to the monotonicity property of ϕ_C pointed out above, the upper bound in (5.42) is a nonincreasing function in C, while (5.43) is nondecreasing in C, yielding typically a trade-off between faster diffusion and higher cost. Therefore, an optimization problem for our control policy consists in finding an optimal value for the parameter C, representing the best compromise between fast diffusion (obtained for large values of C) and affordable cost (achieved by small values of C).

To sum up, despite i) the very myopic choice of our control policy in which no optimization is done on the choice of the support of the control policy $M_U(t)$, ii) the few a-priori knowledge on the topology (only ϕ), and iii) the use of only two observables in the design of the feedback function (from a N-dimensional state variable), we have been able to obtain an effective control policy that can be used in optimization over networks, far beyond the usually analyzed mean field case.

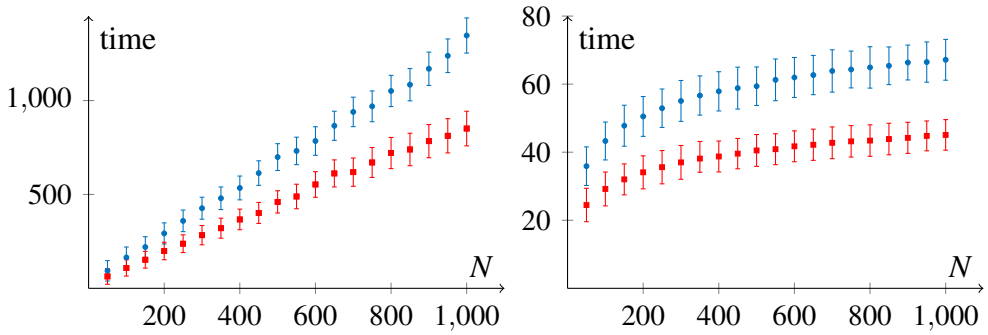

(a) Constant control policy (b) Feedback control policy

Fig. 5.6 Monte Carlo estimation (200 simulations) and 90% confidence intervals of the expected absorbing time τ of a CDS on barbell graphs for different N ($w = u_0 = 1$), with $\beta = 0.7$ (blue circles) and $\beta = 0.8$ (red squares), under the constant control policy (a) and the feedback one (b).

An immediate application of our control technique allows to achieve fast diffusion in barbell graphs, as we show in the following example.

Example 5.7 (Feedback control policy for a barbell graph)**.** *Let us consider the barbell graph analyzed in Examples 5.2 and 5.5. Let us fix any* $C < \alpha(\frac{1}{2} - \frac{1}{N})$*. Then,* $\phi_C(z) = \phi(z)$*,* $\forall z \neq N/2$*, and* $\phi(N/2) = C$*, yielding*

$$\tau \leq \frac{4}{\alpha(2\beta-1)} \ln \frac{N}{2} + \frac{1+\beta}{C(2\beta-1)}, \tag{5.46}$$

which is a great improvement from (5.37)*, obtained with constant control policy. In fact, if constant control policy yields* τ *to grow linearly with N, our feedback control policy ensures* τ *to grow logaritmically with N, with a bounded expected cost. Fig. 5.6 shows the magnitude of the improvement from constant control policy to the feedback one.*

We conclude this chapter by presenting two relevant applications of the feedback control policy we proposed. First, we apply it on a synthetic realistic network created according to a stochastic block model [77]. In this framework we are able to prove analytically the high performance obtained by our control strategy. Then, we apply it on a case study, where the network structure as well as the model parameters have been estimated from real-world data. Even though an analytical treatment cannot be performed due to the complexity of the network structure, Monte Carlo simulations

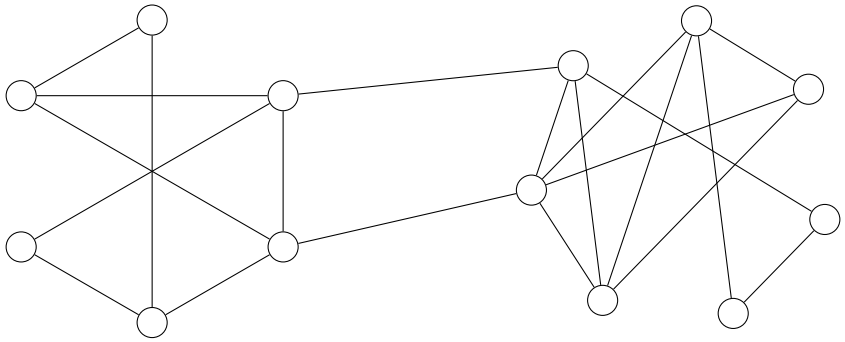

Fig. 5.7 Realization of a SBM with $p = 0.3$, $L = 2$ $N = 13$ and $c = 6/13$.

allows us to prove a statistically significant improvement with respect to the constant control policy adopted in the trials [28, 29].

5.3.1 Synthetic Network: Stochastic Block Model

Here, we propose a relevant application of our feedback control policy, far beyond the toy example of barbell graphs. We consider a realistic situation consisting in a geographical network made by densely connected communities, linked by few connections. The presence of communities is a typical features of spatial and geographical networks [78, 79], being a consequence of to the physiography of the area: e.g., the presence of mountain ranges and isthmuses separates a geographic area into communities. For the sake of simplicity, we only consider the case of two communities, modeled by a stochastic block models (SBM) [77] as described below. Then, our results can be intuitively generalized to SBMs with more communities. Due to the stochastic nature of SBMs, then all the following results hold true with high probability. Fig. 5.7 depicts an realization of a SBM.

First, we a constant control policy. In order to simplify the computations we set $U(t) = \delta^{(1)}$, $\forall t$. The result can be easily generalized for any control with support in V_1 and for any U. Then, we show how our feedback control policy can dramatically improve the speed of convergence.

Let G be a SBM made by two nonoverlapping communities V_1 and V_2 of cardinality $|V_1| = cN$ and $|V_2| = (1-c)N$, with $c \in (0, 1/2]$. Here, we consider an implementation of a SMB useful to model network presenting highly interconnected communities with few connections between them: the two communities are Erdős-Rényi random graphs, i.e. each link is present with constant probability

$p > 0$, independently on the others [44]. Then, a set of L links positioned uniformly at random connects nodes belonging to different communities. We parametrize $w = \alpha[Np(1-c)]^{-1}$.

Remark 5.7. *Barbell graphs can be seen as a limit case of SBMs with* $p = L = 1$.

Corollary 5.1 yields

$$\tau \geq \frac{Np(1-c)}{L\alpha} \tag{5.47}$$

In order to compute an upperbound o τ, we can consider that, if the graph is not an expander graph, the communities considered on their own are so. In particular they have $\gamma = \frac{c}{2}Npw = \frac{c\alpha}{2(1-c)}$ [10], which means that, if z_i is the number of locations occupied by mutants in the i-th community at time t, then $\xi(t) \geq \gamma z_i$. Therefore, we can bound $\phi(z)$ by considering the worst case scenario as follows:

$$\phi(z) \geq \frac{c\alpha}{2(1-c)} \min_{z_1,z_2:z_1+z_2=z} \{\min\{z_1, cN - z_1\} + \min\{z_2, (1-c)N - z_2\}\}. \tag{5.48}$$

For $z = z_1$ or $z = z_2$, (5.48) yields the trivial bound $\phi(z) \geq 0$. However, the presence of L links between the two communities ensures

$$\phi(z) \geq \frac{L\alpha}{Np(1-c)}, \quad \text{if } z \in \{z_1, z_2\}. \tag{5.49}$$

combining (5.48) and (5.49), we deduce

$$\sum_{i=1}^{N} \frac{1}{\phi(z)} \leq \left(\frac{2Np}{L\alpha} + \frac{4(1-c)}{c\alpha} \ln N \right). \tag{5.50}$$

Hence,

$$\tau \leq \frac{2}{\alpha(2\beta-1)} \left(\frac{Np}{L} + \frac{2(1-c)\ln N}{c} \right) + \frac{\beta}{2\beta-1}. \tag{5.51}$$

This implies slow diffusion of the mutants, since τ grows at least linearly with N.

We consider now the control policy in (5.40) for any $C \leq \frac{c\alpha}{2(1-c)}$. Expansiveness in (5.48) guarantees the mutants to diffuse fast when not in correspondence of a bottleneck, that is where one community is occupied by the mutants and the other one by the native species. The choice of the parameter C ensures the control function to be equal to zero when the process is not in a bottleneck [80]. Therefore, $\phi_C(z)$ verifies inequality (5.48) and $\phi_C(z) \geq C$ for $z \in \{cN, (1-c)N\}$. Proposition 5.4

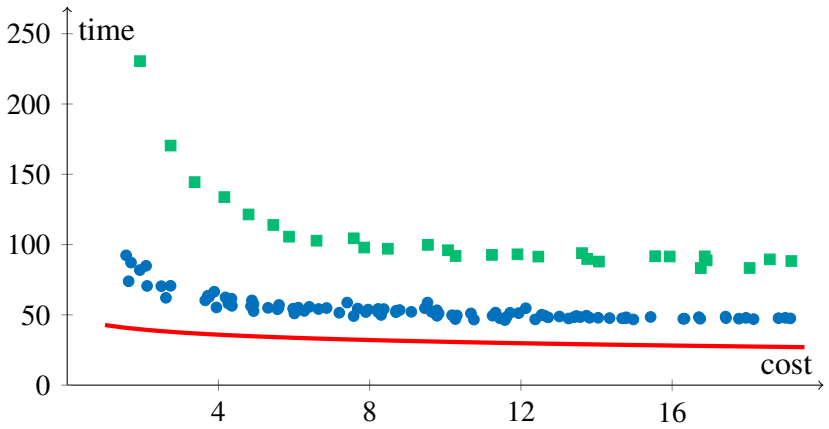

Fig. 5.8 Monte Carlo estimation (200 simulations) of the expected absorbing time τ and expected cost J_U of CDSs on SBMs with $N = 800$, $u_0 = 1$, $\alpha = 1$, $\beta = 0.8$, $c = 0.4$, $p = 0.1$ and $L = 5$ for different values of the parameter C. The red line is a numerical solution of the fundamental limit in Corollary 5.2. Green squares are Monte Carlo estimation of the expected absorbing time τ and expected cost under a control policy where the control is always moved to a node occupied by the native species, but the observable $\xi(t)$ is not used.

concludes that

$$\tau \leq \frac{\beta}{(2\beta-1)} + \frac{2(1-c)}{c\alpha(2\beta-1)} \ln N + \frac{2}{C(2\beta-1)}. \tag{5.52}$$

On the other hand, activation of the control function only in correspondence of bottlenecks ensures (5.43) to read

$$J_U \leq \frac{2+\beta}{2\beta-1}. \tag{5.53}$$

To sum up, our feedback control policy ensures τ to grow logarithmically with N, bounding the cost not to grow with the dimensionality of the problem.

In Fig. 5.8 we analyze the trade-off between absorbing time and cost of the control policy by increasing C: after a first phase presenting a fast improvement, the time decreases slowly as the cost increases. In the same figure, our feedback control policy is also compared with the fundamental limit computed numerically according to Corollary 5.2 and with an even simpler control policy, under which the observable $\xi(t)$ is not used and mutants are introduced with a constant rate in a singleton, moved in such a way that it has always state 0. From this comparison, we claim that the use of the observable $\xi(t)$ in our feedback control policy provides a great improvement in the results. Then, Fig. 5.9 shows the great improve provided

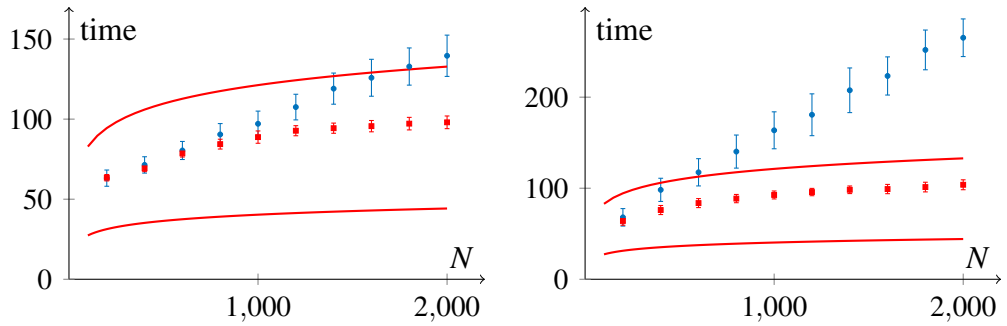

(a) $p = 0.1$ (b) $p = 0.3$

Fig. 5.9 Monte Carlo estimation (200 simulations) and 90% confidence intervals of the expected absorbing time τ of a CDS on SBMs for different N with $u_0 = 1$, $\alpha = 1$, $\beta = 0.8$, $c = 0.4$ and $L = 5$, under the feedback control policy (red squares), compared with those obtained with the constant one (blue circles), for different values of p. The red solid lines are the theoretical upper bound from Proposition 5.4 and a numerical solution of the fundamental limit in Proposition 5.2 with the expected cost estimated from the simulations.

by the feedback control policy, in particular as N increases. We also notice that, for highly connected communities (i.e., for large values of p) the improvement with respect to the constant control policy increases in magnitude.

As already pointed out above, the main strength of this control policy consists in the fact that only few data and information about the network topology are required: notably, the two observables $\tilde{Z}(t)$ and $\xi(t)$ are used in the feedback control function, and the conductance profile allows for thoughtfully set the trade-off between the speed of the process and the cost of the control. For example, in this application on SBMs, the control strategy is designed without the knowledge of the exact partition of the nodes into the two communities, and even the cardinality of each community is not used. This property of our control policy is very important since it provides robustness in real-world situations, where few data might be available and some uncertainty on the exact network structure can be present.

5.3.2 Case-study: Zika Virus in Rwanda

In this section, we present a case study to show the potentiality our feedback control policy to speed up evolutionary dynamics in networked systems. Inspired by a current hot topic in epidemic control, we consider a possible strategy to control the Zika outbreak in Rwanda [81] by substituting *Aedes aegypti* mosquitoes with genetically

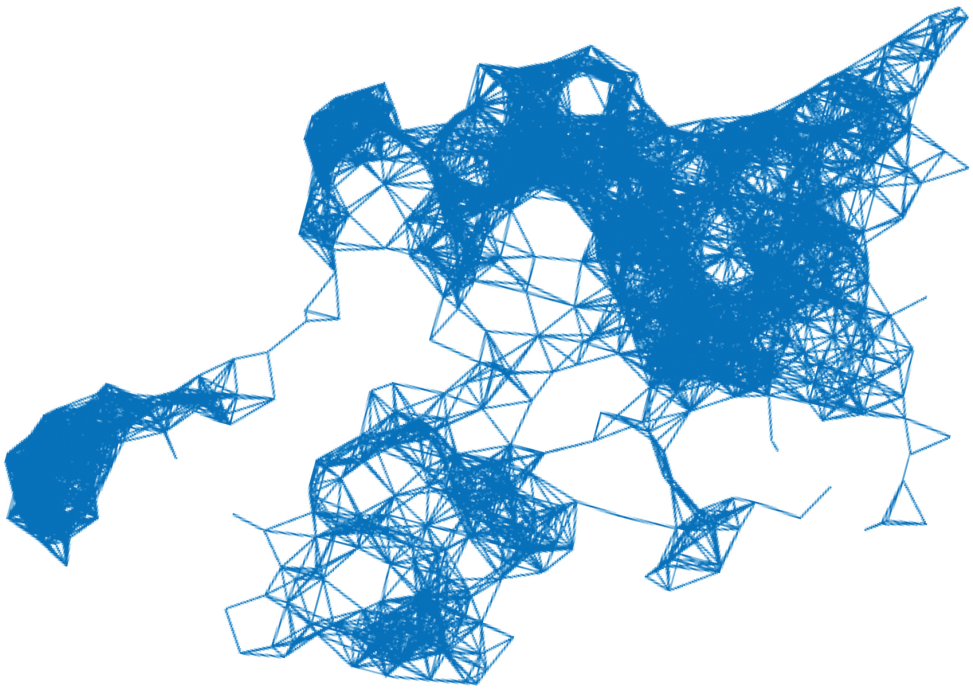

Fig. 5.10 Topological network of the considered geographic area. Links connect locations within 11.7 km.

modified organisms (GMOs) that are similar to the original mosquitoes but do not transmit the Zika virus. Similar control strategies that use GMOs have been proposed and adopted in trials and experiments for fighting other mosquitoes-borne diseases such as dengue fever [28, 29].

The geographical network is constructed as follows. We consider a data set of 1621 locations in Rwanda with their GPS coordinates [82]. Two nodes should be connected, if and only if the mosquitoes in the two locations can contact. Hence, we establish a threshold corresponding to 11.7 km, that is the maximum distance

Table 5.1 Parameters of the Rwanda case study

Parameter	Meaning	Value
N	Number of locations	1621
W_{ij}	Activation rate	0.1
β	Evolutionary advantage	0.53
$\mathbb{1}^T U$	Control rate (constant)	2
C	Control parameter (feedback)	1.5
t	Time unit	day

traveled by mosquitoes to lay their eggs [83]: locations reachable within this distance are connected. The so obtained network is represented in Fig. 5.10. Since the duration of the life cycle of an *Aedes aegypti* lasts in average 10 days [84], we set the activation rate of each link $(i, j) \in E$ equal to $W_{ij} = 0.1$. Finally, we give the GMOs a little evolutionary advantage. In our simulations this advantage is modeled by setting $\beta = 0.53$.

We performed 200 Monte Carlo simulations of the evolutionary dynamics on the networked system for each control policy (constant control policy and the new feedback one). Simulations are generated according to a Gillespie algorithm [35].

In order to compare the two policies, we set the specific parameters of the two control policies in such a way that the two estimated costs coincide. As we remarked above, the cost of a constant control policy grows linearly with the absorbing time. However, in order to have a more challenging benchmark to improve on, we consider only the cost for the constant policy when controlling a node occupied by the native species. Following the trials [28, 29], we set the support of the constant control to coincide with a random node $i \in V$ of the graph, and we fix $U_i = 2$ (for the constant control) and $C = 1.5$ (for the feedback one).

Parameter used are summarized in Tab. 5.1. Our simulations in Fig. 5.11 allows for estimating the magnitude of the improvement given by the feedback control policy with respect to the constant control policy. We observe that, at the same cost (even not considering the energy wasted controlling nodes already occupied by the mutants), the diffusion time reduces in average by more than 56% (the level of significance of this improvement is guaranteed by a p-value $p << 0.001$). The comparison in Fig. 5.11 also shows that the outcomes of feedback control policy are variable than the ones of constant control policy. Hence, the feedback control policy we proposed seems to outperform the constant one, not only in average, but also considering worst case scenarios.

5.4 Conclusion

In this Chapter, inspired by a real-world problem concerning with the diffusion of a GMO in a geographic area, we have proposed a new formulation for evolutionary

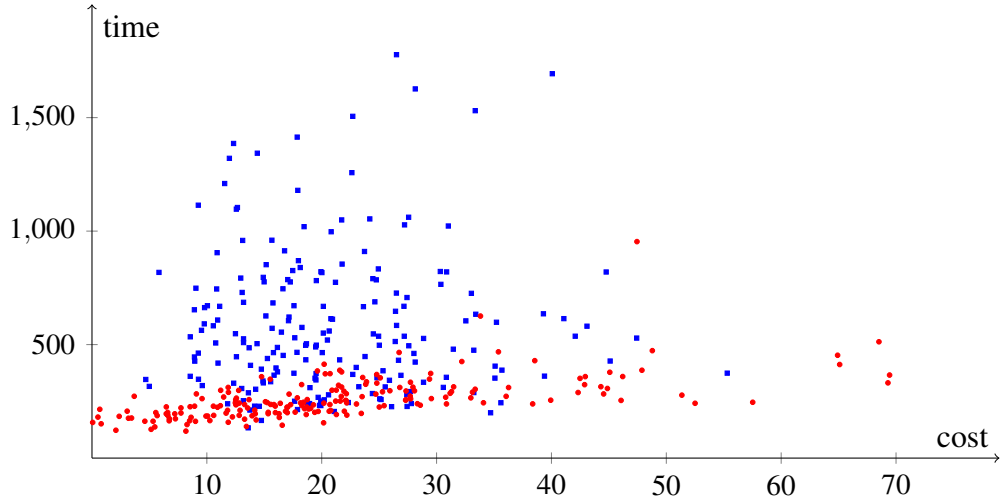

(a) Monte Carlo simulations

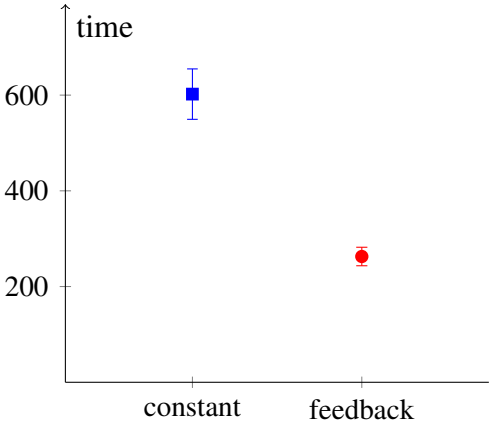

(b) Diffusion time

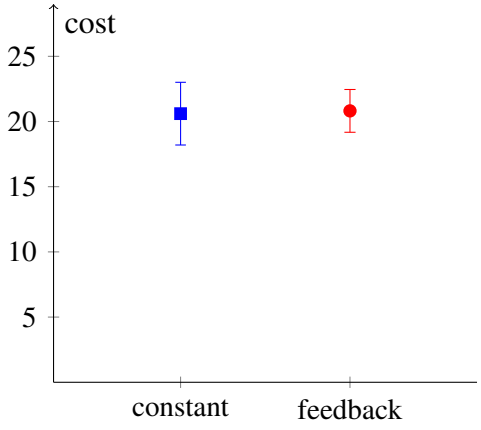

(c) Control cost

Fig. 5.11 Comparison of control policies for the Rwanda case study. In (a), 200 realizations of a CDS with their diffusion time and control cost. Monte Carlo estimation (200 simulations) of the expected diffusion time τ, in (b), and of the expected control cost, in (c), with 95% confidence intervals. Both for the constant (blue squares) and the feedback control policy (red circles).

dynamics that allows for an analytical treatment and incorporates an exogenous control input mechanism.

In Section 5.1, we have declined our mathematical framework for diffusion processes on networks into a link-based spreading process modeling controlled evolutionary dynamics including an exogenous, possibly time-varying control input. Then, we have analyzed the model obtained, providing some general results which allows for understanding how the time needed for the mutants to diffuse in a geographic region and the effort required to achieve this spread depend i) on the topological structure of the geographic region and ii) on the control policy adopted.

Specifically, we have identified three categories of network structures: i) the ones *easy to control*, for which a simple time-invariant control policy is sufficient to achieve fast diffusion (e.g., expander graphs); ii) the *hard to control* ones, for which we proved that no control policy is able to guarantee fast diffusion (e.g., ring graphs); and iii) those topologies for which fast diffusion can be achieved, but not adopting a simple time-invariant control policies, such as the case of barbell graphs.

In order to improve the performance for the latter class of topologies, in Section 5.3, we have finally designed an effective feedback control policy that, using few topological data and observables on the system, provides a dramatic improvement on the speed of the evolutionary process. The efficiency of our proposed feedback control policy have been proved both analytically (in Corollary 5.4) and through two relevant applications: i) on a synthetic network generated according to a stochastic block model and ii) on a case study inspired by real-world data from Zika outbreak in Rwanda.

We strongly believe that the generality of the results in this chapter as well as the effectiveness of the feedback control policy proposed in Section 5.3 could lead to the application of a similar approach also to other diffusion dynamics over networks such as epidemic models or opinion dynamics.

Chapter 6

Conclusion and Further Research

6.1 Conclusion

In this dissertation, we have proposed a general and flexible theory for diffusion processes on networked systems. Then, we have considered different real-world diffusion phenomena, and we have analyzed them using the results developed in our general theory. Specifically, we have studied an epidemic outbreak (in Chapter 3), the diffusion of a new smartphone application (in Chapter 4), and the competition between two species in a biological system (in Chapter 5),

In the first part of this theses, we have formalized diffusion processes in a unique, flexible theory, which, on the one hand, can be used to provide general results for this class of dynamics, and, on the other hand, can be tailored to suit the specificity of the various applications, giving novel insights on the various diffusion phenomena. Within this general framework, we have adapted and developed some useful techniques for the analysis of a diffusion process, as detailed in Chapter 2 and in Appendix A.

In the second part of the thesis, we have tailored our general theory to represent some specific scenarios. In Chapter 3, we have analyzed an SIS epidemic model, which study the diffusion of a disease in a connected community. Our main contributions are the followings.

- We have refined the results on the phase transition between the fast extinction regime and the one where the disease becomes endemic. Specifically, we

have proposed a novel bound on the tail probabilities of the time to extinction distribution, extending the results available in the literature, which are only concerned with its expected value. Using this bound, we have found conditions for the disease to become endemic with high probability, depending on the topology of the network of interactions and on the initial condition.

- We have applied our result to specific topologies, gaining new insights in the epidemic process and demonstrating the use of our theoretical result.
- We have developed a new analytically treatable theory to deal with epidemics on a heterogeneous time-varying network of interaction by shifting the ADN paradigm into our formulation of diffusion dynamics.
- Using this new theory, we have been able to estimate the number of infected individuals when the disease becomes endemic, and to predict the short- and medium-term evolution of the epidemic process using few empirical data sampled at the population level as the disease spreads.

In Chapter 4 we have dealt with a marketing problem: does a new smartphone application diffuse deeply in the population or will it sink into oblivion soon? To predict this, we have developed a new mathematical model, within our general theory. Our main results are the followings.

- We have developed a model within our general theory, which is capable of modeling the effect of positive externalities, as discussed in Section 4.1.
- We have analyzed the system under mean field hypotheses, proving the presence of three regimes: a regime where the diffusion fails and the product extinguish soon, a second regime where the diffusion succeeds and we guarantee a fraction of population to use the product for a long time, and, finally, an intermediate regime where the initial condition determines the outcome of the diffusion, depending on the model's parameters. The presence of the intermediate regime is the main novelty of this model.
- We have studied the model on a general network of interaction, identifying topological conditions for the existence of the three regimes described above.
- Using these results, we have detected a family of network topologies, characterized by a large expansivity, which exhibit the intermediate regime.

In Chapter 5, instead, we have focused on controlled evolutionary dynamics. Our work have been inspired by a hot topic in epidemics control: to create harmless genetically modified mosquitoes, which can be introduced in nature to substitute the dangerous mosquitoes responsible of transmitting infections and diseases, without modifying the environmental equilibria. Our main contributions are the followings.

- We have designed our model within the general theory developed in Chapter 2. The main novelty with respect to the models presented so far is in the presence of an external control.
- We have studied the system, understanding the effect of the topology and of the control policy adopted on the time needed for the mutants to spread in the whole network.
- Using these results, we have identified three classes of network structures: i) those *easy to control*, for which a simple control policy guarantees fast diffusion (e.g., expander graphs); ii) those *hard to control*, for which it is not possible to obtain fast diffusion (e.g., ring graphs); and, finally, iii) the ones *controllable with feedback control*, for which simple control strategies are not sufficient to achieve fast diffusion, but we have been able to propose a feedback control policy that yields fast diffusion.
- We have extensively analyzed the feedback control policy proposed demonstrating its high performances both on artificial networks and on a case study.

To sum up, in this dissertation we have proposed a flexible analytical theory to deal with diffusion processes on networks. Using this framework, we have been able to improve the analysis of a well established model, giving new insights into the diffusion phenomenon (Chapter 3), as well as include and study external control into a dynamical system (Chapter 5), or even develop a new mathematical model to study a realistic dynamics on a networked system (Chapter 4).

6.2 Current and Future Research

Besides the extension and the generalization of the various results found in the applications considered in this dissertation, which have been already extensively

discussed in the conclusion of the relative chapters, two main goals are envisaged for our current and future research. Specifically, i) we want to extended our general theory to non-binary cases, where nodes have more than two states; and ii) we aim to explore a further application of our theory, to study learning dynamics in the framework of population game on networks.

In this dissertation, for the sake of simplicity and in order to keep the notation as simple as possible, we have restricted our analysis to the binary case, where each node can have either state 0 or 1. However, to model more realistic phenomena, nodes can have more than two states. For example, in epidemics, different states can be used to model individuals that are exposed but not jet infectious, or those that are immunized and/or vaccinated; in opinion dynamics, more that two beliefs can be present among a population (e.g., elections in a multi-party system). On the one hand, the formal extension of our theory to non-binary systems comes naturally by introducing a set of mutation probabilities m_{ij} and copying probability p_{ij} for each possible pair of states. On the other hand, unfortunately, it is not trivial and it is still an open problem to understand how the results for the binary model can be generalized to multi-dimensional systems.

Some promising preliminary results, however, encourage us to tackle this problem. In [41], we have successfully extended our techniques to predict the evolution of the epidemic curve of an SIS model (see Section 3.3 for details), to a generic epidemic model, with an arbitrary number of health states and admissible transitions between them. Our goal is thus to extend also the results on the Markov process to more general dynamics, in order to successfully model and analyze realistic diffusion phenomena.

Second, imitation dynamics [85] in the framework of population game on networks are subject to our current and future research. In contrast to most of the other learning dynamics studied in the literature, such as best response and its noisy versions [86, 87] or logit learning [88], imitation dynamics require very little information about the game and its structure to be known by the players: each player only has to know his/her own current utility and to be able to observe the one of some of her/his fellow players. Then, players can exchange information through pairwise interactions and, in response to this information, they can update the strategy they play (that in general is wider than a binary choice) according to some stochastic

rules. Hence, they fit our general theory for diffusion processes and can be analyzed by means of the tecniques we have developed in this dissertation.

The main goal of our analysis consists in understanding the long-run behavior of the system, to find conditions under which the system converges close to some "good" Nash equilibria of the game. We have some preliminary results toward this objective: in [89] we have analyzed the deterministic approximation of an imitation dynamics, obtained using the techniques presented in Section 2.5, proving its convergence to the set of Nash equilibria. Then, we have extended our studies to the Markov jump process to gain more insights on the learning process. In [90], we have analyzed the system under a mean field assumption, proving convergence and long-lasting permanence close to the a desired subset of the Nash equilibria. Encouraged by these preliminary results, we are now planning to extend our results beyond the fully mixed case leveraging the techniques developed in this dissertation, to understand the effect of the communication networks on the evolution of the system.

References

[1] Thomas Milton Ligget. *Interacting particle systems*. Springer-Verlag, New York, NY, USA, 1985.

[2] Claudio Castellano, Santo Fortunato, and Vittorio Loreto. Statistical physics of social dynamics. *Reviews of Modern Physics*, 81(2):591–646, 2009.

[3] David Aldous. Interacting particle systems as stochastic social dynamics. *Bernoulli*, 19(4):1122–1149, 2013.

[4] Daron Acemoglu, Giacomo Como, Fabio Fagnani, and Asuman Ozdaglar. Opinion fluctuations and disagreement in social networks. *Mathematics of Operations Research*, 38(1):1–27, 2013.

[5] Uri Alon. *An Introduction to Systems Biology: Design Principles of Biological Circuits*. Chapman & Hall, London, U.K., 2006.

[6] Guy Karlebach and Ron Shamir. Modelling and analysis of gene regulatory networks. *Nature Reviews*, 9:770–780, 2008.

[7] Alessandro Chiuso, Fabio Fagnani, Luca Schenato, and Sandro Zampieri. Gossip algorithms for simultaneous distributed estimation and classification in sensor networks. *IEEE Journal of Selected Topics in Signal Processing*, 5(4):691–706, 2011.

[8] Fabio Fagnani, Sophie Fosson, and Chiara Ravazzi. A distributed classification/estimation algorithm for sensor networks. *SIAM Journal on Control and Optimization*, 52(1):189–218, 2014.

[9] Giacomo Como, Enrico Lovisari, and Ketan Savla. Convexity and robustness of dynamic traffic assignment and freeway network control. *Transportation Research: Part B*, 91:446–465, 2016.

[10] Ayalvadi Ganesh, Laurent Massoulié, and Don Towsley. The effect of network topology on the spread of epidemics. *Proceedings - IEEE INFOCOM*, 2:1455–1466, 2005.

[11] Moez Draief. Epidemic processes on complex networks: The effect of topology on the spread of epidemics. *Physica A: Statistical Mechanics and its Applications*, 363(1):120–131, 2006.

[12] Romualdo Pastor-Satorras, Claudio Castellano, Piet Van Mieghem, and Alessandro Vespignani. Epidemic processes in complex networks. *Reviews of Modern Physics*, 87(3):925–979, 2015.

[13] Fan Chung, Paul Horn, and Alexander Tsiatas. Distributing Antidote Using PageRank Vectors. *Internet Mathematics*, 6(2):237–254, 2009.

[14] Christian Borgs, Jennifer Chayes, Ayalvadi Ganesh, and Amin Saberi. How to distribute antidote to control epidemics. *Random Structures and Algorithms*, 37(2):204–222, 2010.

[15] Kimon Drakopoulos, Asuman Ozdaglar, and John N. Tsitsiklis. An efficient curing policy for epidemics on graphs. *IEEE Transactions on Network Science and Engineering*, 1(2):67–75, 2014.

[16] Stojan Trajanovski, Yezekael Hayel, Eitan Altman, Huijuan Wang, and Piet Van Mieghem. Decentralized Protection Strategies Against SIS Epidemics in Networks. *IEEE Transactions on Control of Network Systems*, 2(4):406–419, 2015.

[17] Cameron Nowzari, Victor M. Preciado, and George J. Pappas. Analysis and control of epidemics: a survey of spreading processes on complex networks. *IEEE Control Systems*, 36(1):26–46, 2016.

[18] Laurent Frachebourg and Pavel Krapivsky. Exact results for kinetics of catalytic reactions. *Physical Review E*, 53(4):R3009–R3012, 1996.

[19] Andrea Montanari and Amin Saberi. The spread of innovations in social networks. *Proceedings of the National Academy of Sciences*, 107(47):20196–20201, 2010.

[20] Hobart Peyton Young. The dynamics of social innovation. *Proceedings of the National Academy of Sciences*, 108(4):21285–21291, 2011.

[21] David Kempe, Jon Kleinberg, and Éva Tardos. Maximizing the spread of influence through a social network. In *Proceedings of the ninth ACM SIGKDD international conference on Knowledge discovery and data mining - KDD '03*, page 137, New York, New York, USA, 2003. ACM Press.

[22] Marcella Tambuscio, Giancarlo Ruffo, Alessandro Flammini, and Filippo Menczer. Fact-checking effect on viral hoaxes. In *Proceedings of the 24th International Conference on World Wide Web - WWW '15 Companion*, pages 977–982, New York, New York, USA, 2015. ACM Press.

[23] Thomas William Valente. *Network models of the diffusion of innovations*. Number 303.484 V3. 1995.

[24] Stephen Morris. Contagion. *Review of Economic Studies*, 67(1):57–78, 2000.

[25] William Ogilvy Kermack and Anderson Gray McKendrick. A contribution to the mathematical theory of epidemics. *Proceedings of the Royal Society of London A: Mathematical, Physical and Engineering Sciences*, 115(772):700–721, 1927.

[26] Norman Bailey. *The mathematical theory of infectious diseases and its applications. 2nd edition*. 1975.

[27] Erez Lieberman, Christoph Hauert, and Martin Andreas Nowak. Evolutionary dynamics on graphs. *Nature*, 433, 2005.

[28] Angela Felicity Harris, Derric Nimmo, Andrew McKemey, Nick Kelly, Sarah Scaife, Christl Ann Donnelly, Camilla Beech, William Petrie, and Luke Alphey. Field performance of engineered male mosquitoes. *Nature Biotechnology*, 29(11):1034–1037, 2011.

[29] Danilo O. Carvalho, Andrew R. McKemey, Luiza Garziera, Renaud Lacroix, Christl A. Donnelly, Luke Alphey, Aldo Malavasi, and Margareth L. Capurro. Suppression of a field population of Aedes aegypti in Brazil by sustained release of transgenic male mosquitoes. *PLoS Negl. Trop. Dis.*, 9(7):1–15, 2015.

[30] Paul Erdos and Alfréd Rényi. On random graphs I. *Publicationes Mathematicae*, 6, 1959.

[31] Réka Albert and Albert-László Barabási. Statistical mechanics of complex networks. *Statistical mechanics of complex networks*, 2002.

[32] Fan Chung, Linyuan Lu, and Van Vu. Spectra of random graphs with given expected degrees. *Proceedings of the National Academy of Sciences of the United States of America*, 100(11):6313–6318, 2003.

[33] J. R. Norris. *Markov Chains*. Cambridge Series in Statistical and Probabilistic Mathematics. Cambridge University Press, 1997.

[34] David A. Levin, Yuval Peres, and Elizabeth L. Wilmer. *Markov chains and mixing times*. American Mathematical Society, Providence, RI, USA, 2009.

[35] Daniel T. Gillespie. A general method for numerically simulating the stochastic time evolution of coupled chemical reactions. *J. Comput. Phys.*, 22:403–434, 1976.

[36] Patrick Alfred Pierce Moran. Random processes in genetics. *Mathematical Proceedings of the Cambridge Philosophical Society*, 54(01):60, 1958.

[37] Thomas G. Kurtz. Solutions of ordinary differential equations as limits of pure jump Markov processes. *Journal of Applied Probability*, 7(1):49–58, 1970.

[38] Thomas G. Kurtz. Limit theorems for sequences of jump Markov processes approximating ordinary differential processes. *Journal of Applied Probability*, 8(2):344–356, 1971.

[39] Fabio Fagnani and Lorenzo Zino. Time to extinction for the SIS epidemic model: new bounds on the tail probabilities. *IEEE Transactions on Network Science and Engineering*, 2017. Published online.

[40] Lorenzo Zino, Alessandro Rizzo, and Maurizio Porfiri. Continuous-Time Discrete-Distribution Theory for Activity-Driven Networks. *Physical Review Letters*, 117(22):228302, 2016.

[41] Lorenzo Zino, Alessandro Rizzo, and Maurizio Porfiri. An analytical framework for the study of epidemic models on activity driven networks. *Journal of Complex Networks*, 5(6):924–952, 2017.

[42] Fan Chung. Laplacians and the Cheeger inequality for directed graphs. *Annals of Combinatorics*, 9(1):1–19, 2005.

[43] Håkan Andersson and Boualem Djehiche. A threshold limit theorem for the stochastic logistic epidemic. *Journal of Applied Probability*, 35(3):662–670, 1998.

[44] Bela Bollobas. *Random Graphs*. 2001.

[45] Rick Durrett. *Random graph dynamics*. 2006.

[46] Eric Cator and Piet Van Mieghem. Susceptible-infected-susceptible epidemics on the complete graph and the star graph: Exact analysis. *Physical Review E - Statistical, Nonlinear, and Soft Matter Physics*, 87(1), 2013.

[47] Nicola Perra, Bruno Gonçalves, Romualdp Pastor-Satorras, and Alessandro Vespignani. Activity driven modeling of time varying networks. *Scientific reports*, 2(1):469, 2012.

[48] Alessandro Rizzo, Mattia Frasca, and Maurizio Porfiri. Effect of individual behavior on epidemic spreading in activity-driven networks. *Physical Review E - Statistical, Nonlinear, and Soft Matter Physics*, 90(4):1–8, 2014.

[49] Bruno Ribeiro, Nicola Perra, and Andrea Baronchelli. Quantifying the effect of temporal resolution on time-varying networks. *Scientific reports*, 3:3006, 2013.

[50] Hal L. Smith. *Monotone Dynamical Systems: An Introduction to the Theory of Competitive and Cooperative Systems*. Number 41. American Mathematical Society, Providence, RI, 2008.

[51] Jean Pierre Aubin and Arrigo Cellina. *Differential Inclusions: Set-Valued Maps and Viability Theory*. Grundlehren der mathematischen Wissenschaften. Springer Berlin Heidelberg, 2012.

[52] Zino Lorenzo, Rizzo Alessandro, and Porfiri Maurizio. Modeling memory effects in activity driven networks. *SIAM Journal on Applied Dynamical Systems*, 2018. *Accepted for Publication*.

[53] Christian Bongiorno, Lorenzo Zino, and Alessandro Rizzo. On unveiling the community structure of temporal networks. In *2018 IEEE 57th Annual Conference on Decision and Control (CDC)*, 2018. *Accepted for presentation*.

[54] David Easley and Jon. Kleinberg. *Networks, crowds, and markets : reasoning about a highly connected world*. Cambridge University Press, 2010.

[55] Fabio Fagnani and Lorenzo Zino. Diffusion of innovation in large scale graphs: a mean-field analysis. In *Proceedings of the 22nd International Symposium on Mathematical Theory of Networks and Systems*, page 8, 2016.

[56] Fabio Fagnani and Lorenzo Zino. Diffusion of innovation in large scale graphs. *IEEE Transactions on Network Science and Engineering*, 4(2):100–111, 2017.

[57] Nielsen. Global trust in advertising, 2015.

[58] Michael L. Katz and Carl Shapiro. Network Externalities, Competition, and Compatibility. *American Economic Review*, 1985.

[59] Thomas G. Kurtz. *Approximation of population processes*, volume 36. Philadelphia: SIAM, 1981.

[60] Hyoung Jun Ahn and Babak Hassibi. On the Mixing Time of the SIS Markov Chain Model for Epidemic Spread. *53rd IEEE Conference on Decision and Control*, pages 6221–6227, 2014.

[61] Jeff Cheeger. A Lower Bound for the Smallest Eigenvalue of the Laplacian. In *Problems in Analysis: A Symposium in Honor of Salomon Bochner*, volume 31, pages 195–200. 1970.

[62] Giacomo Como, Fabio Fagnani, and Sandro Zampieri. Distributed learning in potential games over large-scale networks. In *The 21st International Symposium on Mathematical Theory of Networks and Systems (MTNS 2014)*, 2014.

[63] Lothar Collatz and Ulrich Sinogowitz. Spektren endlicher Grafen. *Abhandlungen aus dem Mathematischen Seminar der Universität Hamburg*, 21(1):63–77, 1957.

[64] Vadim Georgievich Vizing. The Cartesian Product of Graphs. *Vyčisl. Sistemy*, 9:30–43, 1963.

[65] Mark Broom, Jan Rychtář, and Brian T. Stadler. Evolutionary dynamics on graphs - the effect of graph structure and initial placement on mutant spread. *Journal of Statistical Theory and Practice*, 5(3):369–381, 2011.

[66] Benjamin Allen, Gabor Lippner, Yu-Ting Chen, Babak Fotouhi, Naghmeh Momeni, Shing-Tung Yau, and Martin A. Nowak. Evolutionary dynamics on any population structure. *Nature*, 544(7649):227–230, 2017.

[67] Jan Rychtář and Brian Stadler. Evolutionary dynamics on small-world networks. *International Journal of Computational and Mathematical Sciences*, 2(1):1–4, 2008.

[68] Hisashi Ohtsuki and Martin A. Nowak. Evolutionary games on cycles. *Proceedings of the Royal Society B-Biological Sciences*, 273(1598):2249–2256, 2006.

[69] Josep Díaz, Leslie Ann Goldberg, David Richerby, and Maria Serna. Absorption time of the moran process. *Random Structures & Algorithms*, 49(1):137–159.

[70] Lorenzo Zino, Giacomo Como, and Fabio Fagnani. Fast Diffusion of a Mutant in Controlled Evolutionary Dynamics. *IFAC-PapersOnLine*, 50(1):11908–11913, 2017.

[71] Lorenzo Zino, Giacomo Como, and Fabio Fagnani. Controlling Evolutionary Dynamics in Networks: A Case Study. In *7th IFAC Workshop on Distributed Estimation and Control in Networked Systems (NecSys)*, 2018. *To appear*.

[72] Lorenzo Zino, Giacomo Como, and Fabio Fagnani. On Controlling Evolutionary Dynamics in Networked Systems. *Working paper*, 2018.

[73] Irene Ferreira. The probability of survival for the biased voter model in a random environment. *Stochastic Processes and their Applications*, 34(1):25–38, 1990.

[74] Piet Van Mieghem. The n-intertwined sis epidemic network model. *Computing*, 93(2):147–169, 2011.

[75] Duncan James Watts and Steven Henry Strogatz. Collective dynamics of'small-world' networks. *Nature*, 393(6684):440–442, 1998.

[76] Alexander Lubotzky, Ralph Phillips, and Peter Sarnak. Ramanujan graphs. *Combinatorica*, 8(3):261–277, 1988.

[77] Paul W. Holland, Kathryn Blackmond Laskey, and Samuel Leinhardt. Stochastic blockmodels: First steps. *Social Networks*, 5(2):109–137, 1983.

[78] Marc Barthélemy. Spatial networks. *Physics Reports*, 499(1-3):1–101, 2011.

[79] Santo Fortunato and Darko Hric. Community detection in networks: A user guide. *Physics Reports*, 659:1–44, 2016.

[80] Oliver Riordan and Alex Selby. The maximum degree of a random graph. *Comb. Probab. Comput.*, 9(6):549–572, 2000.

[81] CDC Centers for Disease Control and Prevention. Health Information for Travelers to Rwanda. https://wwwnc.cdc.gov/travel/destinations/traveler/none/rwanda. [Online; accessed 13-Sep-2018].

[82] National Imagery and Mapping Agency. 1621 locations in Rwanda. http://www.math.uwaterloo.ca/tsp/world/rw1621.tsp. [Online; accessed 13-Sep-2018].

[83] Mirta Sudarić Bogojević, Tomislav Hengl, and Enrih Merdić. Spatiotemporal monitoring of floodwater mosquito dispersal in Osijek, Croatia. *Journal of the American Mosquito Control Association*, 23(2):99–108, 2007.

[84] CDC Centers for Disease Control and Prevention. Mosquito Life-Cycle. https://www.cdc.gov/dengue/entomologyecology/m_lifecycle.html. [Online; accessed 13-Sep-2018].

[85] William H. Sandholm. *Population Games and Evolutionary Dynamics*, pages 153–164, 221–275. Cambridge University Press, 2010.

[86] Glenn Ellison and Drew Fudenberg. Rules of Thumb for Social Learning. *Journal of Political Economy*, 101(4):612–643, 1993.

[87] Drew Fudenberg and David Levine. *The Theory of Learning in Games*, volume 1. The MIT Press, 1 edition, 1998.

[88] Lawrence E. Blume. The Statistical Mechanics of Strategic Interaction. *Games and Economic Behavior*, 5(3):387–424, 1993.

[89] Lorenzo Zino, Giacomo Como, and Fabio Fagnani. On imitation dynamics in potential population games. In *2017 IEEE 56th Annual Conference on Decision and Control (CDC)*, pages 757–762, 2017.

[90] Lorenzo Zino, Giacomo Como, and Fabio Fagnani. On stochastic imitation dynamics in large-scale networks. In *2018 European Control Conference (ECC)*, 2018. *To appear*.

Appendix A

Technical Results on Birth-Death Markov Jump Processes

We present here the two technical lemmas on Markov birth-death jump processes along with their detailed proofs. Both lemmas deal with the computation of some bounds on the probability that a process takes "too many" steps "against the drift". Specifically, the first Lemma considers a scenario in which the increasing probability is greater than the decreasing one in an interval, and concludes that the probability that the process exits from this interval from below is exponentially small in the length of the interval. The second Lemma, instead, considers a scenario in which the increasing probability is less than the decreasing one in an interval close to the left-most extreme, which is an absorbing state, concluding that with probability exponentially large the process never exists from that interval, if it starts there.

Lemma A.1. *Let $Z(t)$ be a birth and death process on the state-space S_N with transitions rates, respectively, $\lambda^+(z)$ and $\lambda^-(z)$. Let $\mu := \max_z[\lambda^+(z)+\lambda^-(z)]$. Assume there exists an interval $(z_0-\varepsilon, z_0+\varepsilon) \subseteq (0,1)$, where $z_0 \in (0,1)$ and $\varepsilon > 0$, such that*

$$\lambda^+(z) \geq (1+\delta)\lambda^-(z), \quad \forall z \in S_N \cap (z_0-\varepsilon, z_0+\varepsilon) \tag{A.1}$$

for some $\delta > 0$. Then, for any $z > z_0$, there exists $C > 0$ only depending on δ such that

$$\mathbb{P}_z\Big(\exists t \in [0, e^{C\varepsilon N}] : Z(t) < z_0-\varepsilon\Big) < 10\mu^2 e^{-C\varepsilon N}, \tag{A.2}$$

where $C = \delta^2/24(1+\delta)(2+\delta)$ is a constant only depending on δ.

Proof. In order to simplify the notation, we consider the process $\tilde{Z}(t) = NZ(t)$. Let $\Lambda(t)$ be the number of jumps the process $\tilde{Z}(t)$ does in the time interval $[0,t]$. $\Lambda(t)$ is a time-varying Poisson process, whose rate is equal to the sum of the two transition rates of the process $\tilde{Z}(t)$. For this reason, $\Lambda(t)$ is dominated by a Poisson process with rate μ.

Let us denote by $\tilde{Z}^+(k)$ the state of the process $\tilde{Z}(t)$ immediately after its k-th jump and let us define

$$A(t) := \{k = 1, \ldots, \Lambda(t) \ : \ \tilde{Z}^+(k-1) \in N(z_0 - \varepsilon, z_0 + \varepsilon)\}. \tag{A.3}$$

Let ζ_k be the Bernoulli random variable that assumes value 1 if the k-th jump of $\tilde{Z}(t)$ increases $\tilde{Z}(t)$ by 1. If $\tilde{Z}^+(k-1) \in N(z_0 - \varepsilon, z_0 + \varepsilon)$, then

$$\mathbb{P}(\xi_k = 1) = \frac{\lambda^+(z)}{\lambda^+(z) + \lambda^-(z)} \geq \frac{1+\delta}{2+\delta} =: p. \tag{A.4}$$

Now, we bound the number of jumps of the process $\tilde{Z}(t)$ during a fixed time range T, with

$$\mathbb{P}(\Lambda(T) > K\mu T) \leq \sum_{k=\lceil K\mu T+1 \rceil}^{+\infty} e^{-\mu T} \frac{(\mu T)^k}{k!} \leq \frac{(\mu T)^{\lceil K\mu T \rceil}}{\lceil K\mu T \rceil !} \leq \left(\frac{e}{K}\right)^{\lceil K\mu T \rceil} \tag{A.5}$$

We notice that, for any $K > e$, (A.5) guarantees an exponential decay of the probability of having too many jumps during a time range T.

We now estimate the probability that $Z(t)$ goes below $z_0 - \varepsilon$ starting from above z_0, by conditioning on the number of jumps in the time range T, i.e., $\Lambda(T)$, and splitting the summation into two parts, where each one can be bounded using different techniques, as follows:

$$\begin{aligned}
\mathbb{P}\left(\inf_{t\in[0,T]} \tilde{Z}(t) \leq N(z_0 - \varepsilon)\right) &= \sum_{L\in\mathbb{N}} \mathbb{P}\left(\inf_{t\in[0,T]} \tilde{Z}(t) \leq N(z_0 - \varepsilon) \mid \Lambda(T) = L\right) \cdot \\
&\quad \cdot \mathbb{P}(\Lambda(T) = L) \\
&\leq \sum_{L=1}^{3\mu T} \mathbb{P}\left(\inf_{t\in[0,T]} \tilde{Z}(t) \leq N(z_0 - \varepsilon) \mid \Lambda(T) = L\right) \cdot \\
&\quad \cdot \mathbb{P}(\Lambda(T) = L) + \mathbb{P}(\Lambda(T) > 3\mu T).
\end{aligned} \tag{A.6}$$

We focus on the estimation of first term, since the second on can be easily bounded with (A.5). The estimation we carry on is based on the fact that for the process $\tilde{Z}(t)$ to reach $N(z_0-\varepsilon)$ there must exist a sequence of $l \geq \varepsilon N$ consecutive jumps while the process is in $N(z_0-\varepsilon, z_0+\varepsilon)$ for which the number of overall left transitions minus the number of overall right transitions in the sequence is above εN. Henceforth, using an union bound, we have

$$\mathbb{P}\left(\inf_{t\in[0,T]} \tilde{Z}(t) \leq N(z_0-\varepsilon) \mid \Lambda(T)=L\right) \leq \sum_{k=1}^{L} \sum_{l=\lceil \varepsilon N \rceil}^{L} \mathbb{P}(E_l), \tag{A.7}$$

where the event E_l is defined as

$$E_l := \bigcap_{i=0}^{l-1} \{k+i \in A(t)\} \bigcap \left\{ \sum_{i=0}^{l-1} \xi_{k+i} \leq \frac{l}{2} - \varepsilon \frac{N}{2} \right\}. \tag{A.8}$$

At this stage, we recall the Chernoff bound. Given a sequence of random Bernoulli variables ξ_i i.i.d. with success probability p, then

$$\mathbb{P}\left(\sum_{i=0}^{l-1} \xi_i \leq (1-\alpha)lp\right) = \sum_{h=0}^{(1-\alpha)lp} \binom{l}{h} p^h (1-p)^{l-h} \leq \exp\left\{-lp\frac{\alpha^2}{2}\right\}. \tag{A.9}$$

Using (A.4) and applying (A.9) with $\alpha = (2p-1)/2p$, we can estimate the probability of event E_l as

$$\mathbb{P}(E_l) = \sum_{h=0}^{\frac{l}{2}-\frac{\varepsilon N}{2}} \binom{l}{h} p^h (1-p)^{l-h} \leq \exp\left\{-lp\left(\frac{2p-1}{2p}\right)^2\right\} = \exp\left\{-\frac{(2p-1)^2 l}{8p}\right\}. \tag{A.10}$$

Then, by substituting the expression for p in (A.4), (A.10) reads

$$\mathbb{P}(E_l) \leq \exp\left\{-\frac{(2p-1)^2 l}{8p}\right\} = \exp\left\{-\frac{\delta^2 l}{8(1+\delta)(2+\delta)}\right\}. \tag{A.11}$$

Combining (A.7) and (A.11), we bound

$$\begin{aligned}\mathbb{P}\left(\inf_{t\in[0,T]}\tilde{Z}(t)\leq N(z_0-\varepsilon)\mid\Lambda(T)=L\right) &\leq \sum_{k=1}^{L}\sum_{l=\lceil\varepsilon N\rceil}^{L}\mathbb{P}(E_l)\\ &\leq \sum_{k=1}^{L}\sum_{l=\lceil\varepsilon N\rceil}^{L}\exp\left\{-\frac{\delta^2 l}{8(1+\delta)(2+\delta)}\right\}\\ &\leq L^2\exp\left\{-\varepsilon\frac{\delta^2}{8(1+\delta)(2+\delta)}N\right\},\end{aligned} \tag{A.12}$$

Finally, since the bound in (A.12) is monotonically increasing in L, we bound

$$\begin{aligned}&\sum_{L=1}^{3\mu T}\mathbb{P}\left(\inf_{t\in[0,T]}\tilde{Z}(t)\leq N(z_0-\varepsilon)\mid\Lambda(T)=L\right)\mathbb{P}(\Lambda(T)=L)\\ &\quad\leq\mathbb{P}\left(\inf_{t\in[0,T]}\tilde{Z}(t)\leq N(z_0-\varepsilon)\mid\Lambda(T)=3\mu T\right)\sum_{L=1}^{3\mu T}\mathbb{P}(\Lambda(T)=L)\\ &\quad\leq\mathbb{P}\left(\inf_{t\in[0,T]}\tilde{Z}(t)\leq N(z_0-\varepsilon)\mid\Lambda(T)=3\mu T\right)\\ &\quad\leq(3\mu T)^2\exp\left\{-\varepsilon\frac{\delta^2}{8(1+\delta)(2+\delta)}N\right\}.\end{aligned} \tag{A.13}$$

To conclude,we bound the second term of (A.6) using (A.5) with $K=3$, obtaining

$$\mathbb{P}\left(\inf_{t\in[0,T]}\tilde{Z}(t)\leq N(z_0-\varepsilon)\right)\leq(3\mu T)^2\exp\left\{-\varepsilon\frac{\delta^2}{8(1+\delta)(2+\delta)}N\right\}+\left(\frac{e}{3}\right)^{\lceil 3\mu T\rceil}. \tag{A.14}$$

Fix now $\varepsilon>0$ and put

$$T=\exp\left\{\frac{\delta^2}{24(1+\delta)(2+\delta)}\varepsilon N\right\}. \tag{A.15}$$

Using the fact that $(e/3)^x<x^{-2}$ for all $x>0$, we immediately obtain the thesis. □

Lemma A.2. *Let $Z(t)$ be a birth and death process on the state-space S_N with transitions rates, respectively, $\lambda^+(z)$ and $\lambda^-(z)$. Assume that $\lambda^+(0)=\lambda^-(0)=0$ and that there exists $\varepsilon>0$ such that*

$$\lambda^-(z)\geq(1+\delta)\lambda^+(z),\quad\forall z\in S_N\cap(0,2\varepsilon], \tag{A.16}$$

for some $\delta > 0$. Then, called $C = \ln(1+\delta)$, for any $z < \varepsilon$,

$$\mathbb{P}_z(\exists t \geq 0 : Z(t) > 2\varepsilon) < \varepsilon N \exp\{-C\varepsilon N\}. \tag{A.17}$$

Proof. First, for any $k \in \{0, \ldots, \lceil 2\delta N \rceil\}$, put $e_k = \mathbb{P}_{k/N}(\exists t \geq 0 : Z(t) \geq \lceil 2\varepsilon N \rceil / N)$. A straightforward argument based on conditioning on the transition at the first jump leads e_k to satisfy Laplace equation:

$$e_k = \frac{\lambda^+(k/N)e_{k+1} + \lambda^-(k/N)e_{k-1}}{\lambda^+(k/N) + \lambda^-(k/N)}. \tag{A.18}$$

This, along with the boundary condition $e_0 = 0$, gives

$$(e_{k+1} - e_k) = \prod_{j=1}^{k} \frac{\lambda^-(j/N)}{\lambda^+(j/N)} e_1. \tag{A.19}$$

We can bound $e_{\lceil \varepsilon N \rceil} \leq 1$, obtaining

$$e_1 \leq \left(\sum_{k=0}^{\lceil 2\varepsilon N \rceil - 1} \prod_{j=1}^{k} \frac{\lambda^-(\frac{j}{N})}{\lambda^+(\frac{j}{N})} \right)^{-1} \leq \left(\prod_{j=1}^{\lceil 2\varepsilon N \rceil - 1} \frac{\lambda^-(\frac{j}{N})}{\lambda^+(\frac{j}{N})} \right)^{-1} \tag{A.20}$$

Combining (A.19) and (A.20) we finally obtain

$$\begin{aligned} e_{\lfloor \varepsilon N \rfloor} = & \sum_{k=0}^{\lfloor \varepsilon N \rfloor - 1} \prod_{j=1}^{k} \frac{\lambda^-(j/N)}{\lambda^+(j/N)} e_1 \leq \lfloor \varepsilon N \rfloor \frac{\prod_{j=1}^{\lfloor \varepsilon N \rfloor - 1} \frac{\lambda^-(j/N)}{\lambda^+(j/N)}}{\prod_{j=1}^{\lceil 2\varepsilon N \rceil - 1} \frac{\lambda^-(\frac{j}{N})}{\lambda^+(\frac{j}{N})}} \\ \leq & \lfloor \varepsilon N \rfloor \prod_{j=\lfloor \varepsilon N \rfloor}^{\lfloor 2\varepsilon N \rfloor - 1} \frac{\lambda^+(j/N)}{\lambda^-(j/N)} \leq \lfloor \varepsilon N \rfloor (1+\delta)^{-\varepsilon N}, \end{aligned} \tag{A.21}$$

which yields the thesis. □

Appendix B

Second-Order Analysis of Linear Markov Jump Process

We present here the details of the second order analysis of a linear jump Markov process, straightening the convergence results known in the literature from the first-order analysis [10]. These stronger results coming from the second-order analysis will be used in Section 4.4, when analyzing the failure regime in the model for diffusion of innovation.

Consider the jump Markov process $Y(t)$ over $\Theta = \mathbb{N}^V$, with transition rates

$$\begin{cases} \bar{\lambda}_i^+ &= \mu \sum\limits_{j \in \mathcal{N}_i} y_j \\ \bar{\lambda}_i^- &= y_i, \end{cases} \tag{B.1}$$

where $\mu = \beta \bar{d}^{-1} \phi(1)$.

The analysis of $Z_Y(t)$ proceeds as follows. In Lemma B.1, we provide an upper bound for its first moment. Then, an analysis on its second moment and a bound on its variance is provided in Lemmas B.2 and B.3. Finally, we combine these results in Lemma B.4 that analyzes the asymptotic behavior of $Z_Y(t)$.

Lemma B.1. *Let $Z_Y(t) = z(Y(t))$ with $Y(t)$ that following* (B.1)*. Then it holds*

$$\mathbb{E}[Z_Y(t)] \leq \exp((\mu \rho_A - 1)t) Z(0)^{1/2}. \tag{B.2}$$

Proof. Let us denote the first moment of the process $Y(t)$ by $M^{(1)}(t) = \mathbb{E}(Y(t))$. The distribution $p(t) \in [0,1]^{\Theta}$ of $Y(t)$ satisfies the forward Kolmogorov equation $\dot{p} = -pL(\bar{\lambda})$ where $L(\bar{\lambda})$ is the Laplacian of the process (i.e. $L(\bar{\lambda})_{xy} = \sum_{y'} \bar{\lambda}_{xy'} - \bar{\lambda}_{xy}$, where $\bar{\lambda}_{xy}$ is the transition rate from state x to state y). Therefore, $M^{(1)}(t)$ satisfies the ODE

$$\dot{M}^{(1)} = (\mu A - I)M^{(1)}. \tag{B.3}$$

We can thus estimate

$$||M^{(1)}(t)|| \leq \exp((\mu\rho_A - 1)t)||Y(0)||, \tag{B.4}$$

where ρ_A is the spectral radius of A. This yields

$$\mathbb{E}[Z_Y(t)] \leq N^{-1}N^{1/2}\exp((\mu\rho_A - 1)t)||X(0)|| = \exp((\mu\rho_A - 1)t)Z(0)^{1/2}. \tag{B.5}$$

□

Remark B.1. *Since $\mu = \beta\bar{d}^{-1}\phi(1)$, it holds*

$$\mu\rho_A - 1 = \beta\bar{d}^{-1}\rho_A\phi(1) - 1. \tag{B.6}$$

Hence, $\beta < \bar{d}\rho_A^{-1}\phi(1)^{-1}$ implies $\mu\rho_A - 1 < 0$, yielding an exponential decay of $\mathbb{E}[Z(t)]$ to 0 . However, as already pointed out above, this is not yet sufficient to generalize item 1. of Theorem 4.1.

We now undertake a second order analysis of the process $Y(t)$. To this aim, put $M^{(2)} = \mathbb{E}(Y(t)Y(t)^*)$ and $\Omega = M^{(2)} - M^{(1)}M^{(1)*}$.

Lemma B.2. *Ω satisfies the ODE*

$$\dot{\Omega} = \mu(A\Omega + \Omega A) - 2\Omega + \mu\,\mathrm{diag}(AM^{(1)}) + \mathrm{diag}(M^{(1)}), \tag{B.7}$$

with $\Omega(0) = 0$.

Proof. Using the Kolmogorov equation it follows that

$$\begin{aligned}
\dot{M}^{(2)} &= \sum_{x\in\Theta} \dot{p}_x xx^* \\
&= \sum_{x\in\Theta} \mu \sum_{v\in V} p_{x-\delta_v}(A(x-\delta_v))_v xx^* + \sum_{x\in\Theta}\sum_{v\in V} p_{x+\delta_v}(x_v+1)xx^* + \\
&\quad - \sum_{x\in\Theta} \mu \sum_{v\in V} p_x(Ax)_v xx^* - \sum_{x\in\Theta}\sum_{v\in V} p_x x_v xx^*.
\end{aligned} \tag{B.8}$$

We rearrange the first two terms of (B.8) by adding and subtracting δ_v to both x and x^*, expanding the products and, finally, changing the indexes. We thus obtain

$$\begin{aligned}\sum_{x\in\Theta}\mu\sum_{v\in V}p_{x-\delta_v}(A(x-\delta_v))_v xx^* = \\ = \mu\sum_{v\in V}\sum_{x\in\Theta}p_x(Ax)_v xx^* + \mu(AM^{(2)}+M^{(2)}A)+\mu\,\mathrm{diag}(AM^{(1)}),\end{aligned} \tag{B.9}$$

and

$$\sum_{x\in\Theta}\sum_{v\in V}p_{x+\delta_v}(x_v+1)xx^* = \sum_{v\in V}\sum_{x\in\Theta}p_x x_v xx^* - 2M^{(2)} + \mathrm{diag}(M^{(1)}). \tag{B.10}$$

Substituting (B.9) and (B.10) into (B.8), we finally obtain

$$\dot{M}^{(2)} = \mu(AM^{(2)}+M^{(2)}A) - 2M^{(2)} + \mu\,\mathrm{diag}(AM^{(1)}) + \mathrm{diag}(M^{(1)}). \tag{B.11}$$

Thesis now follows by differentiating the expression $M^{(1)}M^{(1)*}$ with the use of (B.3) and then subtracting it from (B.11). □

We can now bound $\mathrm{Var}(Z_Y(t)) = N^{-2}\mathbb{1}^*\Omega\mathbb{1}$ through the following Lemma.

Lemma B.3. *Let $Z_Y(t) = z(Y(t))$ with $Y(t)$ following* (B.1)*. Then it holds*

$$\mathrm{Var}(Z_Y(t)) \le N^{-1/2}\frac{1+\mu\rho_A}{1-\mu\rho_A}e^{(\mu\rho_A-1)t}Z_Y(0)^{1/2}. \tag{B.12}$$

Proof. Let $\mathcal{S}(V)$ be the set of symmetric matrices over V and let $\mathcal{L}:\mathcal{S}(V)\to\mathcal{S}(V)$ be the linear operator given by $\mathcal{L}(M) = \mu(AM+MA)-2M$. Then, using (B.7), we can represent the centered second moment as

$$\Omega(t) = \int_0^t \exp((t-s)\mathcal{L})U(s)\,\mathrm{d}s, \tag{B.13}$$

where

$$U(t) = \mu\,\mathrm{diag}(AM^{(1)}(t)) + \mathrm{diag}(M^{(1)}(t)). \tag{B.14}$$

Hence,

$$\mathrm{Var}(Z_Y(t)) = N^{-2}\mathbb{1}^*\int_0^t \mathbb{1}^*[\exp((t-s)\mathcal{L})U(s)]\,\mathrm{d}s\,\mathbb{1}. \tag{B.15}$$

Using the representation

$$\exp(t\mathcal{L})M = \exp(t(\mu A - I))M\exp(t(\mu A - I)), \tag{B.16}$$

we can estimate the variance as follows:

$$\mathrm{Var}(Z_Y(t)) \leq N^{-2}N^{1/2}\int_0^t e^{(2(t-s)(\mu\rho_A-1)}||U(s)||\,\mathrm{d}s N^{1/2}, \tag{B.17}$$

where $||U(s)||$ is the induced 2-norm of $U(s)$. From (B.14), it can be estimated as

$$||U(s)|| \leq \mu \max_\nu |\delta_\nu^* A M^{(1)}| + \max_\nu |\delta_\nu^* M^{(1)}| \leq (\mu\rho_A + 1)\exp((\mu\rho_A - 1)s)||Y(0)||. \tag{B.18}$$

Combining this estimation with the previous inequality, we obtain the thesis. □

We are now ready to analyze the convergence behavior of the process $Z_Y(t)$ in the case when $\mu\rho_A < 1$.

Lemma B.4. *Let $Z_Y(t) = z(Y(t))$ with $Y(t)$ following* (B.1)*. Assume that $\mu\rho_A < 1$. For every $\varepsilon > 0$ there exists a time $T_\varepsilon > 0$ and a constant $K_\varepsilon > 0$ such that*

1. *if $Z_Y(0) \leq a^2$, it holds*

$$\mathbb{P}(\exists t \geq 0 : Z_Y(t) > a + \varepsilon) \leq K_\varepsilon N^{-1/2}; \tag{B.19}$$

2. *for every $Z_Y(0)$, it holds*

$$\mathbb{P}(\exists t \geq T_\varepsilon : Z_Y(t) > \varepsilon) \leq K_\varepsilon N^{-1/2}. \tag{B.20}$$

Moreover, for every $\varepsilon > 0$, the constants K_ε and T_ε only depend on the quantity $\mu\rho_A$ and are bounded when this quantity is bounded away from 1.

Proof. Consider the underlying discrete time Markov chain $\tilde{Y}(k)$ for $k = \{0, 1, \dots\}$ and the corresponding $Z_{\tilde{Y}}(k) = z(\tilde{Y}(k))$. The Poisson process $\Lambda(t)$ governing the jumps of $Y(t)$ has intensity $\nu = (\beta + 1)N$. Hence it holds

$$\mathrm{Var}(Z_Y(t)) = \sum_{k\geq 0} \mathrm{Var}(Z_{\tilde{Y}}(k))\mathbb{P}(\Lambda(t) = k) \geq \mathrm{Var}(Z_{\tilde{Y}}(\lfloor \nu t \rfloor))\mathbb{P}(\Lambda(t) = \lfloor \nu t \rfloor). \tag{B.21}$$

The last multiplicative term of (B.21) can be lower bounded using Stirling's approximation:

$$\mathbb{P}(\Lambda(t) = \lfloor \nu t \rfloor) = \frac{(\nu t)^{\lfloor \nu t \rfloor}}{\lfloor \nu t \rfloor !} e^{-\nu t} \geq \frac{(\nu t)^{\lfloor \nu t \rfloor}}{\lfloor \nu t \rfloor^{\lfloor \nu t \rfloor}} \frac{e^{\lfloor \nu t \rfloor}}{\sqrt{2\pi \lfloor \nu t \rfloor}} e^{-\nu t} \geq \frac{1}{9\lfloor \nu t \rfloor}. \tag{B.22}$$

From (B.21) and (B.22) we obtain that

$$\mathrm{Var}(Z_{\tilde{Y}}(k)) \leq 9k \mathrm{Var}(Z_Y(k/\nu)), \quad \forall k = \{0, 1, \dots\}. \tag{B.23}$$

Combining the assumption $Z_Y(0) \leq a^2$ with the estimation in Lemma B.1, we bound

$$\begin{aligned} \mathbb{P}(\exists t \geq 0 : Z_Y(t) > a + \varepsilon) &\leq \mathbb{P}(\exists k \geq 0 : Z_{\tilde{Y}}(k\lfloor \varepsilon N/2 \rfloor) > a + \frac{\varepsilon}{2}) \\ &\leq \sum_{k \geq 0} \mathbb{P}\left(|Z_Y(k\lfloor \varepsilon N/2 \rfloor) - \mathbb{E}(Z_Y(k\lfloor \varepsilon N/2 \rfloor))| \geq \frac{\varepsilon}{2} \right) \\ &\leq \frac{4}{\varepsilon^2} \sum_{k \geq 0} \mathrm{Var}(Z_{\tilde{Y}}(k\lfloor \varepsilon N/2 \rfloor)). \end{aligned} \tag{B.24}$$

Using now estimation (B.23) and Lemma B.3, we obtain item 1.

Item 2. can be proven in a similar fashion. First, we notice that Lemma B.1 implies that there exists $T_\varepsilon > 0$ such that $\mathbb{E}(Z_Y(t)) \leq \varepsilon/2$ for all $t \geq T_\varepsilon$. We then conclude using again the variance estimation in (B.3). □

Appendix C

Analysis of Controlled Diffusive Systems

In this Chapter, we gather all the technical proofs of the results on the Controlled Diffusive Systems, as well as a detailed analysis of the process. We start presenting the proof of Lemma 5.1.

Proof of Lemma 5.1. We first prove the lemma under assumption $\beta = \gamma$ and $X(0) < Y(0)$. We define the coupled process $Z(t) = (X(t), Y(t))$ as a bi-dimensional process on the state space $(\{0,1\}^n, \{0,1\}^n)$, with initial condition $Z(0) = (X(0), Y(0))$, associated with a (unique) geographical graph $\mathcal{G}$. The coupling mechanism is the following. Each link $\{i, j\}$ is equipped with an independent Poisson clock with rate W_{ij}. When the clock associate with the link $\{i, j\}$ clicks, then the spreading mechanism acts on that link for both $X(t)$ and $Y(t)$ as for a standard controlled diffusive systems, but for the fact that, if a conflict occur in both processes, then the outcome is the same. Each node i is given an inhomogeneous Poisson clock with rate $u_i(t)$, associated with the external control in node i. When the clock associated with node i clicks, then both X_i and Y_i turn to 1. We immediately deduce that the two marginals $X(t)$ and $Y(t)$ are controlled diffusive system $(\mathcal{G}, \beta, U(t))$ with the desired initial conditions.

We show now that, in this coupling, $Y(t) \geq X(t)$, for every $t \geq 0$. At $t = 0$ this is verified by assumption. Then, we show that, after each transition of the coupled process, the inequality is preserved. To this purpose, we suppose the process has a transition at time t, we name $Z(t) = (X(t), Y(t))$ the state of the process before the

transition, and $Z(t^+) = (X(t^+), Y(t^+))$ the state after the transition. If $X(t) = Y(t)$, then due to the coupling mechanism we have $X(t^+) = Y(t^+)$. If $Y(t) > X(t)$, we analyze the possible transitions:

- *Spreading mechanism*. Edge $\{i, j\}$ activates and a conflict occur. Then, being $Y(t) > X(t)$, the following configurations can occur:

  1. $X_i(t) = Y_i(t) = X_j(t) = 0$, $Y_j(t) = 1$ and mutants win. Then, $X_i(t^+) = X_j(t^+) = 0$, $Y_i(t^+) = Y_j(t^+) = 1 \implies Y(t^+) > X(t^+)$.
  2. $X_i(t) = Y_i(t) = X_j(t) = 0$, $Y_j(t) = 1$ and native species win. Then, $Y_i(t^+) = Y_j(t^+) = X_i(t^+) = X_j(t^+) = 0 \implies Y(t^+) \geq X(t^+)$.
  3. $X_i(t) = Y_i(t) = 0$, $X_j(t) = Y_j(t) = 1$ and mutants win. Then, $Y_i(t^+) = Y_j(t^+) = X_i(t^+) = X_j(t^+) = 1 \implies Y(t^+) > X(t^+)$.
  4. $X_i(t) = Y_i(t) = 0$, $X_j(t) = Y_j(t) = 1$ and native species win. Then, $Y_i(t^+) = Y_j(t^+) = X_i(t^+) = X_j(t^+) = 0 \implies Y(t^+) > X(t^+)$.
  5. $X_i(t) = 0$, $Y_i(t) = X_j(t) = Y_j(t) = 1$ and mutants win. Then, $Y_i(t^+) = Y_j(t^+) = X_i(t^+) = X_j(t^+) = 1 \implies Y(t^+) \geq X(t^+)$.
  6. $X_i(t) = 0$, $Y_i(t) = X_j(t) = Y_j(t) = 1$ and native species win. Then, $X_i(t^+) = X_j(t^+) = 0$, $Y_i(t^+) = Y_j(t^+) = 1 \implies Y(t^+) > X(t^+)$.

- *External control*. Mutants are introduced in node i, that is not occupied by mutants in both the processes. Then, being $Y(t) > X(t)$, the following configurations can occur:

  1. $X_i(t) = Y_i(t) = 0$ Then, $X_i(t^+) = Y_i(t^+) = 1 \implies Y(t^+) > X(t^+)$.
  2. $X_i(t) = 0$, $Y_i(t) = 1$ Then, $X_i(t^+) = Y_i(t^+) = 1 \implies Y(t^+) \geq X(t^+)$.

Therefore, we conclude that, after each transition of the process, the inequality $Y(t) \geq X(t)$ is preserved (possibly, a strict inequality can mutate into an equality).

The proof of the Lemma under the assumption $\beta < \gamma$ and $X(0) = Y(0)$, is performed using a similar argument. The coupled process $Z(t) = (X(t), Y(t))$ is a bi-dimensional process on the state space $(\{0,1\}^n, \{0,1\}^n)$, with initial condition $Z(0) = (X(0), Y(0))$, associated with a (unique) geographical graph $\mathcal{G}$. The coupling mechanism is the following. Each link $\{i, j\}$ is equipped with an independent Poisson clock with rate W_{ij}. When the clock associate with the link $\{i, j\}$ clicks, then the

spreading mechanism acts on that link for both $X(t)$ and $Y(t)$. If a conflict occur in only one of the two processes, then it is solved as in a standard controlled diffusive system with probability for the mutants to win the conflict equal to β and γ for the components $X(t)$ and $Y(t)$, respectively. If the conflict occurs in both processes, then with probability β mutants win in both components, with probability $\gamma-\beta$ mutants win only in component $Y(t)$, and with probability $1-\gamma$ mutants lose in both components. Each node i is given an inhomogeneous Poisson clock with rate $u_i(t)$, associated with the external control in node i. When the clock associated with node i clicks, then both X_i and Y_i turn to 1. We immediately deduce that the two marginals $X(t)$ and $Y(t)$ are controlled diffusive system $(\mathcal{G},\beta,U(t))$ and $(\mathcal{G},\gamma,U(t))$, respectively, with the same desired initial condition $X(0)=Y(0)$.

Similar to the proof of the lemma under the assumption $X(0)<Y(0)$, we have now to show that, in the coupling $Z(t)$, $Y(t)\geq X(t)$, $\forall t\geq 0$. At $t=0$ this is verified, being $X(0)=Y(0)$. Then, following the same procedure used above considering the state of the system after each transition, it is easy to show that both the spreading mechanism and the external control preserve the inequality. Finally, the case in which both $\beta<\gamma$ and $X(0)<Y(0)$ can be obtained by combining the two couplings described above.

To conclude the proof, the existence of the coupling $Z(t)=(X(t),Y(t))$ such that $Y(t)\geq X(t)$ for every $t\geq 0$, yields the stochastic domination $Y(t)\succeq X(t)$ [11]. The inequality $\tau_Y\leq\tau_X$ is a straightforward consequence of the stochastic domination and, being $U(t)\geq 0$ and $U(t)=0$ once the process is absorbed, we have

$$J_X=\int_0^{\tau_X}U(t)\mathrm{dt}=\int_0^{\tau_Y}U(t)\mathrm{dt}+\int_{\tau_Y}^{\tau_X}U(t)\mathrm{dt}\geq J_Y, \tag{C.1}$$

which completes the proof. □

Proof of Lemma 5.2. We define the coupled process $Z(t)=(X(t),Y(t))$ as a bi-dimensional process on the state space $(\{0,1\}^N,\{0,1\}^N)$, with initial condition $Z(0)=(X(0),Y(0))$, associated with a (unique) geographical graph $\mathcal{G}$. The coupling mechanism is the following. Each link $\{i,j\}$ is equipped with an independent Poisson clock with rate W_{ij}. When the clock associate with the link $\{i,j\}$ clicks, then the spreading mechanism acts on that link for both $X(t)$ and $Y(t)$, with $\beta=1$. Each node i is given an inhomogeneous Poisson clock with rate $u_i(t)$, associated with the external control in node i. When the clock associated with node i clicks, X_i turns to 1.

We immediately deduce that the two marginals $X(t)$ and $Y(t)$ are controlled diffusive system $(G,1,U(t))$ and $(G,1,0)$ with the desired initial conditions, respectively.

We show now that, under this coupling, $Y(t) \geq X(t)$, for every t. At $t=0$ this is verified by assumption. In the following, we show that, after each transition of the coupled process, the inequality is preserved.

- *Spreading mechanism.* Being $\beta = 1$, mutants always win. So only three transitions can occur when edge $\{i,j\}$ activates and a conflict occurs:

  1. $X_i(t) = Y_i(t) = X_j(t) = 0, Y_j(t) = 1$. Then, $X_i(t^+) = X_j(t^+) = 0, Y_i(t^+) = Y_j(t^+) = 1 \implies Y(t^+) > X(t^+)$.
  2. $X_i(t) = Y_i(t) = 0, X_j(t) = Y_j(t) = 1$. Then, $Y_i(t^+) = Y_j(t^+) = X_i(t^+) = X_j(t^+) = 1 \implies X(t^+) \geq Y(t^+)$.
  3. $X_i(t) = 0, Y_i(t) = Y_j(t) = X_j(t) = 1$. Then, $Y_i(t^+) = Y_j(t^+) = X_i(t^+) = X_j(t^+) = 1 \implies Y(t^+) \geq X(t^+)$.

- *External control.* We observe that i) mutants can be only introduced in the process $X(t)$ in nodes $i \in \mathcal{M}'$, for which $Y_i(0) = 1$, and ii) being $\beta = 1$, $Y_i(0) = 1 \implies Y_i(t) = 1$, for any $t \geq 0$. Hence, also external control preserves the inequality $Y(t) \geq X(t)$, which completes the proof.

Finally, Lemma 5.3 gives $J_X \geq |\mathcal{M}'|$. □

At this stage, we deepen our analysis of the Controlled Diffusive Systems. In order to perform this analysis, we focus on the process $\tilde{Z}(t)$. The dependency of the process $\tilde{Z}(t)$ on the control $U(t)$ restricts the possibility to analyze it directly using the techniques from Section 2.4. We tackle this issue defining an ancillary stochastic process $\bar{Z}(t)$, obtained by dropping the dependence on $C(t)$, whose transition rates now depend only on $\xi(t)$ in a linear way. $\bar{Z}(t)$ is a stochastic process with the following increasing and decreasing transition rates from state $\bar{Z}(t) = z$, conditioned to $\xi(t) = \xi$:

$$\begin{cases} \bar{\lambda}^+(z|\xi) = u_0 & \text{if } z = 0 \\ \bar{\lambda}^+(z|\xi) = \beta\xi & \text{if } z \in \{1,\dots,N-1\} \\ \bar{\lambda}^-(z|\xi) = (1-\beta)\xi & \text{if } z \in \{1,\dots,N-1\}, \end{cases} \tag{C.2}$$

where $u_0 := \inf_{t:X(t)=0\mathbb{1}} U(t)$. The assumption (5.2) guarantees $u_0 > 0$.

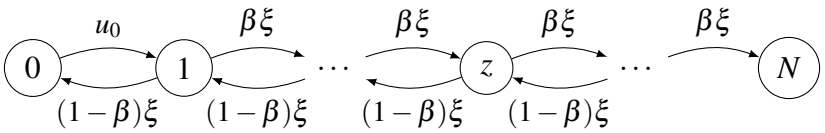

Fig. C.1 The transition graph of the continuous-time process $\bar{Z}(t)$, conditioned to $\xi(t) = \xi$.

Lemma C.1. *It holds* $\tilde{Z}(t) \succeq \bar{Z}(t)$.

Proof. In order to prove the stochastic domination, we exhibit a coupling $(\tilde{Z}(t), \bar{A}(t))$ in which $\tilde{Z}(t) \geq \bar{Z}(t)$. This coupling comes naturally since, as noticed above, $\lambda^+ \geq \bar{\lambda}^+$, while $\lambda^- = \bar{\lambda}^-$, similarly to [10]. □

The structure of the transitions of process $\bar{Z}(t)$ can be seen in Fig. C.1. We notice that $\bar{Z}(t)$ is still not Markovian, but all its transition rates depends on $X(t)$ only through $\xi(t)$, that will be very useful in our further analysis of the process.

At this stage, we prove a technical Lemma that will be used further on, combined with the stochastic domination from Lemma C.1, to compute our upper bound of τ.

Lemma C.2. *Let N_z be the random variable counting the number of times the process $\bar{Z}(t)$ enters in state z. Then it holds*

$$\mathbb{E}[N_0] \leq \frac{\beta}{2\beta - 1}, \tag{C.3}$$

and, $\forall z \in \{1, \ldots, N\}$, it holds

$$\mathbb{E}[N_z] \leq \frac{1}{2\beta - 1}. \tag{C.4}$$

Proof. Let $\{T_k\}$ be the set of random times at which the transitions of the process $\bar{Z}(t)$ occur. We can define the embedded discrete-time process $Y(k) = \bar{Z}(T_k)$, that evolves coupled with $\bar{Z}(t)$ and has a discrete time step for each transition of the continuous-time process. Differently form the continuous-time process, $Y(k)$ is a birth-death Markov chain, since in its transition probabilities we get rid of the dependence on the boundary $B(t)$. Notably, the non-zero increasing (decreasing)

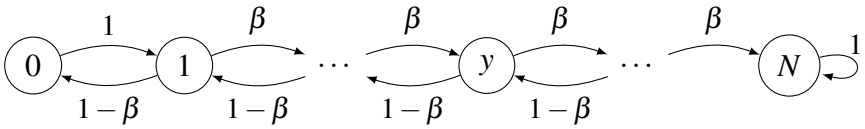

Fig. C.2 The transition graph of the embedded discrete-time process $Y(k) = \bar{Z}(T_k)$.

probabilities of $Y(k)$ are

$$\begin{cases} q^+(y) = 1 & \text{if } z = 0, \\ q^+(y) = \beta & \text{if } z \in \{1,\dots,N\}, \\ q^-(y) = 1-\beta & \text{if } z \in \{1,\dots,N\}. \end{cases} \tag{C.5}$$

Moreover, being N an absorbing state, a self-loop with probability 1 is added to it. The process $Y(k)$, whose structure is represented in Fig. C.2, is a well known birth-death Markov chain. In fact, between two consecutive entrances in 0, it acts as a Moran process [36]. Therefore, from the relative literature, we define the probability that, starting from a generic state z, the chain is absorbed in N before entering $z-1$, as

$$f_z = \frac{\dfrac{2\beta-1}{\beta}}{1-\left(\dfrac{1-\beta}{\beta}\right)^{N-z+1}} \geq \frac{2\beta-1}{\beta}. \tag{C.6}$$

Therefore, N_0 to be a geometrically distributed random variable with success probability $(2\beta-1)/\beta$, whose expected value is upper bounded by $\beta/(2\beta-1)$.

As the generic $\mathbb{E}[N_z]$ is considered, the process enters at least once in any state $z \in \{1,\dots,N-1\}$. Then, we bound the expected number of returns by conditioning on the first jump, as

$$\begin{aligned} R_z &= \beta(1-f_z)(R_z+1) + (1-\beta)(R_z+1) \\ &\leq \beta\frac{1-\beta}{\beta}(R_z+1) + (1-\beta)(R_z+1) \\ &\leq \frac{2-2\beta}{2\beta-1}, \end{aligned} \tag{C.7}$$

which yields the conclusion

$$\mathbb{E}[N_z] = 1 + R_z \leq 1 + \frac{2-2\beta}{2\beta-1} \leq \frac{1}{2\beta-1}. \tag{C.8}$$

□

We observe that the upper bounds provided in Lemma C.2 does not depend on the size of the network N. We are now ready to prove Theorems 5.2 and 5.3.

Proof of Theorem 5.2. Let N_z be the random variable counting the number of times the process $\tilde{Z}(t)$ enters in state z. Since $\tilde{Z}(0) = 0$ and the process is eventually absorbed in N, it holds $N_z \geq 1$. We bound

$$\mathbb{E}[T_z] = \mathbb{E}\left[\sum_{i=1}^{N_z} \mathbb{E}\left[S_z^i \,|\, N_z\right]\right] = \mathbb{E}\left[\sum_{i=1}^{N_z} \frac{1}{\xi(\bar{t}_i) + C(\bar{t}_i)}\right] \geq \frac{\mathbb{E}[N_z]}{g(z)} \geq \frac{1}{g(z)}. \tag{C.9}$$

Thus, the proof is concluded by summing up the time spent in each state. □

Proof of Theorem 5.3. Let N_z be the random variable counting the number of times the process $\tilde{Z}(t)$ enters in state z. Stochastic domination in Lemma C.1 ensures that $N_z \leq \tilde{N}_z$. Using the property of linearity of the expected value, τ can be expressed as the sum of the expected amounts of time the process $\tilde{Z}(t)$ spends in each one of the non-absorbing states. In formula $\tau = \sum_{z=0}^{N-1} \mathbb{E}[T_z]$, where T_z is the amount of time the process $\tilde{Z}(t)$ spends in state z. Let S_z^i be the i-th sojourn-time in state z (i.e. the time spent in z the i-th time it enters in it). S_z^i is an exponentially distributed random variable with parameter $\xi(t) + C(t)$. Finally, denote by $\bar{t}_i$ the time of the i-th entrance in state z of the process $\tilde{Z}(t)$. Using Lemma C.2 and the fact that N_z is independent from the various S_z^i's, we can now estimate, $\forall z \in \{1, \ldots, N-1\}$,

$$\mathbb{E}[T_z] = \mathbb{E}\left[\sum_{i=1}^{N_z} \mathbb{E}\left[S_z^i \,|\, N_z\right]\right] = \mathbb{E}\left[\sum_{i=1}^{N_z} \frac{1}{\xi(\bar{t}_i) + C(\bar{t}_i)}\right] \leq \frac{\mathbb{E}[N_z]}{f(z)} \leq \frac{1}{(2\beta - 1) f(a)}, \tag{C.10}$$

and, similarly,

$$\mathbb{E}[T_0] \leq \frac{\mathbb{E}[N_0]}{f(0)} \leq \frac{\beta}{(2\beta - 1) f(0)}. \tag{C.11}$$

Thus we complete the proof by bounding

$$\tau = \sum_{a=0}^{N-1} \mathbb{E}[T_z] \leq \frac{\beta}{(2\beta - 1) f(0)} + \frac{1}{2\beta - 1} \sum_{z=1}^{N-1} \frac{1}{f(z)}. \tag{C.12}$$

□